VACUUM REFINING COPPER MELTS

by

© David Danovitch

A Thesis Submitted to the Faculty of Graduate Studies and Research in Partial Fulfillment of the Requirements for the Degree of Master of Engineering in Metallurgical Engineering.

McGill University

Montréal

March 1982

To

Diane

ABSTRACT

Pilot plant scale experiments have investigated the removal of bismuth, antimony and arsenic from copper melts (doped copper, blister copper and white metal). The experiments were conducted in a 140 kg capacity, 150 kW induction furnace mounted inside a 3 m^3 vacuum chamber. Melt masses were in the range 20-35 kg, melt temperatures were in the range 1500-1790 K and chamber pressures were in the range 7-160 Pa.

It was found that 45 to 90 % of the initial bismuth, 50 to 60 % of the initial arsenic and nil to 60 % of the initial antimony were removed from molten copper in 1 hour by vacuum refining. Approximately 45 % of the initial bismuth was removed from molten white metal in 1 hour under vacuum.

Refining rate coefficients increased from 2×10^{-5} to 7×10^{-5} m s^{-1} when melt temperature was increased from 1500 to 1700 K. A similar increase (3×10^{-5} to 7×10^{-5} m s^{-1}) was seen when chamber pressure was decreased from 150 to 10 Pa. Refining rates also increased when initial solute concentration was increased in the range 0.01 to 0.1 weight %; the extent of this increase depended upon

the conditions of temperature and pressure. The presence of a slag layer on the copper melt lowered refining rates by approximately a factor of 10. Dissolved iron in the copper melt (≈ 1 %) lowered refining rate coefficients of antimony (2×10^{-5} to 0.1×10^{-5} m s^{-1}) but did not affect refining rates of bismuth or arsenic.

Elements which can exist as polyatomic gaseous species were found to evaporate predominantly in the monatomic form; that is, the volatility coefficients for As_2 and Bi_2 were approximately 1/500 and 1/3000 of that for As and Bi respectively.

A theoretical model to describe vacuum distillation was derived in terms of Machlin's expression for melt phase mass transfer, Hertz-Knudsen-Langmuir's expression for evaporation and an expression for gas phase mass transfer which includes diffusion and convection. Model predictions for bismuth and arsenic refining rates agreed with experimental results, while no agreement was obtained for the case of antimony.

Both theoretical predictions and experimental results indicate that vacuum refining copper to remove bismuth could become a viable industrial process. Slower refining

rates for antimony and arsenic indicate the need to use other processes such as oxidation and chlorination in conjunction with vacuum refining if these elements are to be efficiently removed on an industrial scale.

RESUME

Les expériences affectuées à l'échelle pilote ont étudié l'élimination de bismuth, antimoine et arsenic des bains de cuivre fondu (cuivre dopé, cuivre 'blister' et métal blanc). Ces expériences ont été dirigées dans un four de fusion à induction (d'une capacité de 140 kg et d'une puissance de 150 kW) monté dans une chambre sous vide. Les masses des charge étaient entre 20 et 35 kg, les températures des bains étaient entre 1500 et 1790 K et les pressions de chambre étaient entre 7 et 160 Pa.

Il fut découvert que 45 à 90 % du bismuth initial, 50 à 60 % de l'arsenic initial et zéro à 60 % de l'antimoine initial ont été éliminés du cuivre fondu en 1 heure d'affinage sous vide. A peu près 45 % du bismuth initial a été éliminé du métal blanc fondu en 1 heure sous vide.

Les coefficients du taux d'affinage ont augmenté de 2×10^{-5} à 7×10^{-5} m s^{-1} lorsque la température du bain fut augmentée de 1500 à 1700 K. Une augmentation similaire (de 3×10^{-5} à 7×10^{-5} m s^{-1}) a été observée lorsque la pression fut diminuée de 150 à 10 Pa. Les taux d'affinage ont aussi augmenté lorsque le contenu initial

en impuretés fut augmenté entre 0.01 et 0.1 % au poids; le degré de cette augmentation dépendait des conditions de température et pression. La présence d'une couche de scories sur le bain de cuivre a diminué les taux d'affinage par un facteur approximatif de 10. La présence de fer (≈ 1 %) dans le bain de cuivre a diminué les coefficients du taux d'affinage d'antimoine de 2×10^{-5} à 0.1×10^{-5} m s^{-1}, mais n'a produit aucun effet sur les taux d'affinage de bismuth ou arsenic.

Il fut découvert que les éléments qui peuvent exister comme espèce gazeuse polyatomique s'évaporent principalement dans la forme monatomique, c'est-à-dire que les coefficients de volatilité de As_2 et Bi_2 ont été approximativement 1/500 et 1/3000 de ceux de As et Bi respectivement.

Un modèle théorique pour décrire la distillation sous vide a été dérivé en fonction de l'expression de Machlin pour le transfert de masse en phase liquide, l'expression de Hertz-Knudsen-Langmuir pour l'évaporation et une expression pour le transfert de masse en phase gazeuse qui utilize la diffusion et la convection. Les prédictions du modèle pour les taux d'affinage de bismuth et arsenic sont en accord avec les résultats expérimentaux mais aucun accord a été obtenu dans le cas de l'antimoine.

Les prédictions théoriques et les résultats expérimentaux indiquent que l'affinage sous vide du cuivre pour éliminer le bismuth peut devenir un procédé industriel viable. Des taux d'affinage plus lents pour les cas de l'antimoine et de l'arsenic indiquent que l'affinage sous vide devra être utilisé conjointement avec d'autres procédés comme l'oxydation et la chloruration s'il est désiré d'éliminer ces éléments du cuivre à l'échelle industrielle.

ACKNOWLEDGEMENTS

The author gratefully thanks Professor Ralph Harris and Professor Bill Davenport for their sincere and patient guidance throughout this study.

I would also like to extend my appreciation to all members of the department of Metallurgical Engineering with whom I had the pleasure of working with.

The Horace Young Fellowship as well as funds from the National Research Council of Canada and McGill University enabled me to undertake this study.

TABLE OF CONTENTS

CHAPTER ONE

INTRODUCTION

SECTION 1.1 : GENERAL

The trend towards lower grade copper ores and the advent of continuous copper-making processes have resulted in certain impurity levels in anode copper which are unacceptably high for electrorefining; notably, bismuth, antimony and arsenic. A process which will maintain these impurity contents in anodes at a level agreeable to copper refineries is needed to complement existing copper-making practices.

It will be shown that vacuum refining molten copper, whereby volatile impurities are evaporated from a copper melt under vacuum, is one such process. The idea of using vacuum distillation technology to refine copper evolves from successes obtained in removing more volatile species from steel and lead melts.

This study investigates rates of removal of bismuth, antimony and arsenic from copper melts, as well as variables which affect these rates.

SECTION 1.2 : THE THESIS

Chapter Two of this thesis examines modern copper-making practices with particular reference to areas which are experiencing problems with high impurity levels. Possible solutions to this problem are reviewed, of which the most promising is concluded to be vacuum refining molten copper.

Chapter Three examines and summarizes previous studies of vacuum refining molten copper and a theoretical model for the said process is developed.

Chapter Four describes experiments which determine refining rates in several types of copper melts and the results of these experiments are tabulated, plotted and evaluated in Chapter Five.

Chapter Six discusses the effects of several variables on refining rates and compares experimentally determined rates to those predicted by the theoretical model.

Finally, future work is suggested and conclusions of this study are formed.

CHAPTER TWO

BACKROUND

SECTION 2.1 : EXTRACTIVE METALLURGY OF COPPER

The major processes involved in extracting copper from sulphide ore are illustrated in Figure 2.1. These pyrometallurgical processes which treat sulphide ores produce 90 % of the world's primary copper. Almost all of the remaining 10 % originate from oxide ores, and is treated by hydrometallurgical processes.

Before sulphide ores are smelted by one of the pyrometallurgical techniques, they are concentrated to produce a copper grade high enough to be economically smelted. Beneficiation is usually by froth flotation, in which the copper sulphide minerals are activated for extraction from a pulp of finely ground ore by the addition of reagents to the pulp.

Smelting consists of first heating and melting the concentrate at about 1200 ^{o}C in conjunction with a silica flux and air or oxygen enriched air. The result is two

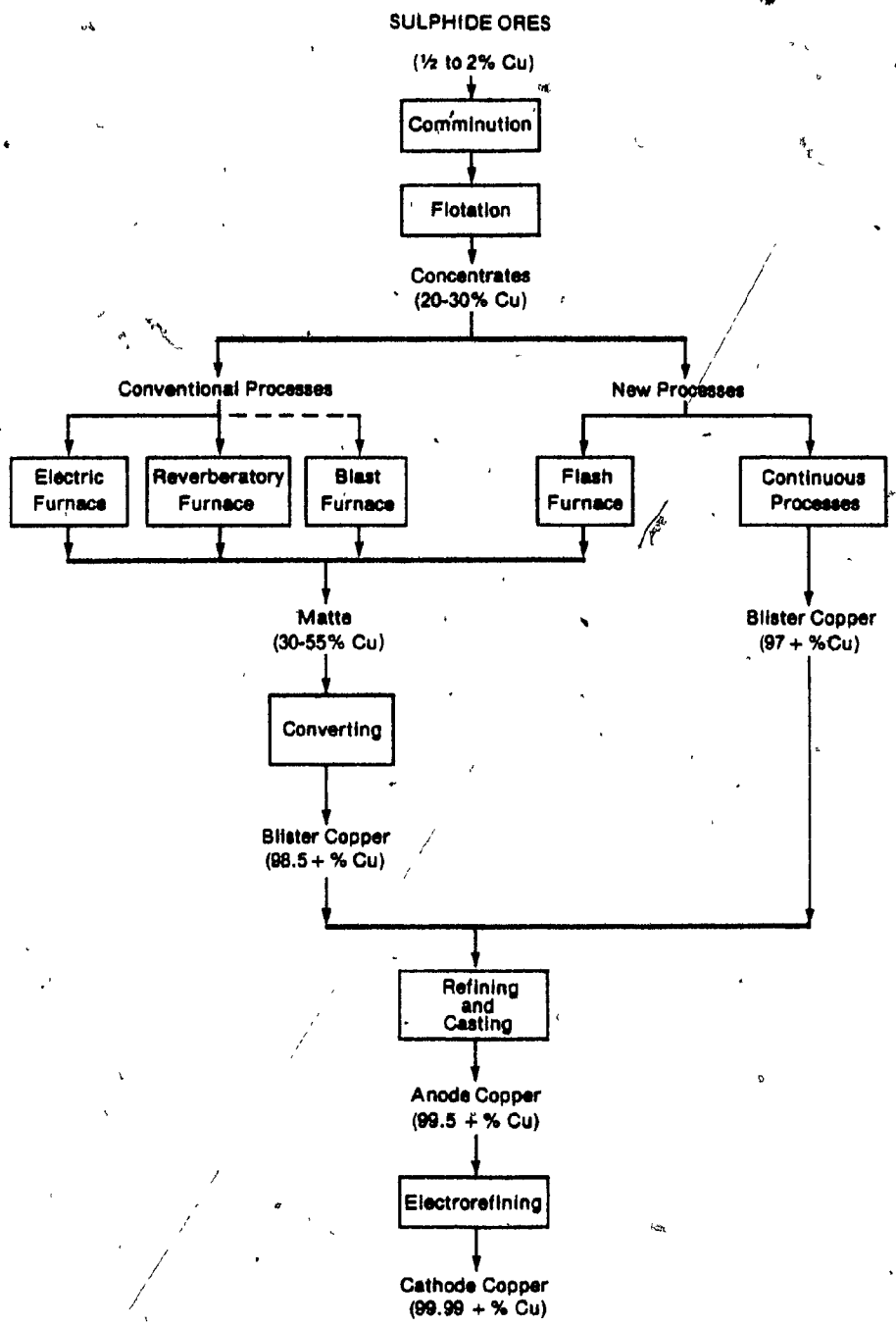

Figure 2.1 : Major Processes Involved in Extracting Copper from Sulphide Ores (----- Rare)[1a]

immiscible phases :

a) a copper rich liquid sulphide phase (matte) and

b) a liquid oxide phase (slag) virtually free of copper.

The matte phase is a mixture of Cu_2S and FeS, and is transferred to a second reaction vessel where it undergoes converting. In this two stage process, iron and sulphur are eliminated by oxidation with injected air. Iron is converted to FeO which enters a slag phase while sulphur is converted to SO_2 which is exhausted. When all of the iron has been eliminated, the only phase remaining is Cu_2S. Further oxidation by air eliminates the remaining sulphur as SO_2 gas and the copper which is produced is called blister copper. It is about 99 % pure, the main impurities being oxygen and sulphur.

Almost all blister copper produced today is fire-refined to prevent formation of sulphur dioxide 'blisters' during casting of copper anodes. In this process, sulphur is removed with air, then oxygen with hydrocarbon gas.

Next, copper anodes are electrorefined. An electrical potential is applied between the anode and a high

purity copper cathode, both of which are immersed in an electrolyte composed of H_2SO_4 and Cu_2SO_4. The copper from the anode dissolves in the electrolyte and subsequently plates onto the cathode. Many of the impurities from the anode are insoluble in the electrolyte and form 'slimes' at the bottom of the electrolytic cells. Others are partially soluble but do not plate at sufficiently low concentrations. The resulting copper cathodes are 99.99 % pure or better.

Innovation to these conventional copper-making processes has emerged in the past few years. It has been found that smelting and converting can be combined into a continuous process carried out in a single reactor because smelting and converting are both controlled oxidation processes. One advantage of this process is that the need to handle a matte phase between the smelting and converting stages is eliminated since the reactor produces blister copper from a copper concentrate feed.

SECTION 2.2 : THE TREND TOWARDS HIGHER IMPURITY LEVELS

There is a trend towards higher impurity contents in anode copper. The reason is twofold :

i) As the easily attainable high grade ores become depleted, the tendency is to exploit the easily attainable lower grade ores, resulting in a greater impurity content per unit of copper. To maintain a constant impurity level in the anode copper, the additional impurity content must be removed during smelting and converting. This may be achieved by further volatilization but, under normal smelting and converting conditions, will consume large amounts of time and energy.

ii) Impurities are more stable and less volatile in metallic copper than in copper sulphide. In one step copper production, blister copper is continuously present in the reactor and a large part of the impurity which would normally vaporize in the presence of matte alone will instead enter the metallic copper phase.

As a result of this trend, the impurity levels in anode copper are increasing. The next two sections point out that they are becoming too high for the electrorefining stage to handle safely and economically.

SECTION 2.3 : THE EFFECTS OF IMPURITIES IN PRODUCT COPPER

Typical levels of the most common impurities found in smelter matte and blister copper are shown in Table 2.1, while those for anode and cathode copper are shown in Table 2.2.

Maintaining extremely low levels of impurities in product copper is vital. All soluble impurities lower the the electrical and thermal conductivities of the metal. For example, 0.1 weight percent arsenic reduces the electrical conductivity by 23 % and the thermal conductivity by a similar amount. The offenders are Ag, As, Ni, S, Se, Te, Sb and Cd. Others form stable insoluble oxides which are precipitated in inert form, so that their effects are less.

Annealing properties are also adversely affected by impurity content. Almost all impurities induce a rise in the softening temperature of copper. For example, the presence of 0.05 weight percent arsenic raises the softening of copper by over 100 °C.

Element	Matte (range of %)	Blister Copper (range of %)
Cu	30-55	98.5-99.5
Fe	30-45	0.1
S	20-25	0.02-0.1
O	2-3	0.5-0.8
As	0-0.5	0-0.3
Bi	0-0.1	0-0.01
Pb	0-5	0-0.1
Sb	0-1	0-0.3
Zn	0-5	0-0.005
Au	$0\text{-}15 \times 10^{-4}$	$0\text{-}100 \times 10^{-4}$
Ag	0-0.1	0-0.1

Table 2.1 : Impurity Levels in Matte and Blister Copper (weight %) [1b]

Element	Anodes (range of %)	Cathodes (range of %)
Cu	99.4-99.8	99.99
O	0.1-0.3	n.i.
Ni	0-0.5	trace-0.0007
Pb	0-0.1	trace-0.0005
As	0-0.3	trace-0.0001
Sb	0-0.3	trace-0.0002
Se	0-0.02	trace-0.0001
Te	0-0.001	trace-0.0001
Fe	0.002-0.03	0.0002-0.0006
S	0.001-0.003	0.0004-0.0007
Bi	0-0.01	trace-0.0003
Ag	trace-0.1	0.0005-0.001
Au	0-0.005	0-0.00001

Table 2.2 : Impurity Levels in Anode and Cathode Copper (weight %) [1b]

SECTION 2.4 : THE EFFECT OF IMPURITIES IN THE ELECTROREFINING PROCESS

Electrorefining lowers impurity content to an acceptable level in the product copper. The amount of impurities that this stage can handle is limited. Consequently, a copper refinery sets a level of impurity content for copper anodes above which it will not accept. Higher impurity contents cause problems in the two areas where impurities accumulate : the anode slimes and the electrolyte.

Impurities found in the anode slimes are those that are insoluble or form insoluble compounds in the electrolyte. Table 2.3 lists these impurities and the compounds they form. Because the precious metals gold, silver and platinum are precipitated, the anode slimes are very valuable. Excessive levels of other impurities make it more difficult to extract these valuable metals.

Impurities found in the electrolyte are those that dissolve in the electrolyte but are less noble than copper and hence do not plate on the cathodes. They include three elements whose removal from copper are examined in this study (Bi, Sb and As) as well as Co, Fe and Ni. To prevent these impurities from contaminating the cathodes by

Element	Insoluble Compounds Formed
Au	none*
Pt	none
Ag	AgCl, Ag_2Se, Ag_2Te_4
Se	Ag_2Se, Cu_2Se
Te	Cu_2Te
Pb	$PbSO_4$
Sn	$Sn(OH)_2SO_4$
S	Cu_2S

* - although no compounds are formed, the element itself does not dissolve in the electrolyte and consequently precipitates into the anode slimes

Table 2.3 : Impurities Which are Found in the Anode Slimes and the Insoluble Compounds that they Form

electrolyte occlusion, they are regularly removed from the electrolyte in a purification section of the refinery by electrowinning them onto an impure copper cathode deposit. When higher impurity levels are present in the electrolyte, the purification process must be carried out for a longer period of time. This raises not only the expense of the process, but also the probability of dangerous arsine gas (AsH_3) evolving at the cathodes.

SECTION 2.5 : POSSIBLE PROCESSES FOR REDUCING THE IMPURITY CONTENT IN COPPER

Three potential solutions for eliminating impurities in copper have been proposed in previous studies : oxidation, chlorination and vacuum refining. Following is a brief description and general outlook for each of these possible solutions.

2.5.1 : OXIDATION

Oxidizing an impure copper melt to form a slag that is high in impurities is simply an extention of normal smelting and converting practices. In this process,

oxygen or air is fed into the molten bath, saturating the bath with oxygen as dissolved Cu_2O. Cu_2O reacts with impurities according to this general reversible reaction[2] :

$$Cu_2O_{(l)} + M_{(l)} = 2Cu_{(l)} + MO_{(l,s)} \quad .... 2.1$$

where M is the metallic impurity. The degree of oxidation and removal of an impurity depends upon the concentration of the impurity, the concentration of oxygen in the bath and the properties of the oxides formed such as volatility, specific gravity and rate of slagging (by combination with flux additions).

When a metallic impurity oxide neither dissolves in copper nor combines with other metallic oxides to give compounds soluble in copper, the content of that impurity in copper may be lowered by the above reaction to a minimum level determined by the following equilibrium equation :

$$K = \frac{a_{Cu}^2 \cdot a_{MO}}{a_{Cu_2O} \cdot a_M} \quad .... 2.2$$

where a is the activity. Typical values of K for some elements in copper are shown in Table 2.4.

The first group of elements, with very low values of K, will not be removed by oxidation and subsequent slagging. This is not a problem, since they are all valuable metals to be recovered in the electrorefining stage. The third group, with very high values of K, may easily be removed by oxidation.

Bismuth, antimony and arsenic fall in the second group and are problematical since they are neither desired nor easily eliminated. Bismuth, with the lowest value of K in this group, has been found to be very difficult to oxidize. Arsenic and antimony oxidize to volatile trioxides As_2O_3 and Sb_2O_3 which are easily removed with waste gases. However, these trioxides easily oxidize further to nonvolatile pentoxides which combine with other oxides to form arsenates and antimonates, many of which are soluble in molten copper. One way to avoid this is to find a flux which, when added, renders these compounds insoluble in the copper. In the case of arsenic, some success has been achieved using soda as the flux.

Element	K*
Au	1.2×10^{-7}
Ag	3.5×10^{-5}
Pt	5.2×10^{-5}
Pd	6.2×10^{-4}
Se	5.6×10^{-4}
Te	7.7×10^{-2}
Bi	0.64
Pb	3.8
Ni	25
Cd	31
Sb	50
As	50
Co	1.4×10^{2}
Sn	4.4×10^{2}
Fe	4.5×10^{3}
Zn	4.7×10^{4}
Na	1.1×10^{5}
Si	5.6×10^{8}

* - as defined in Equation 2.2

Table 2.4 : Values of the Oxidation Equilibrium Constant K for Some Elements in Copper[2]

2.5.2 : CHLORINATION

Removal of various impurities from liquid crude copper using various chlorides was studied thermodynamically and experimentally[3]. By taking into account the free energy of formation of chlorides and the activity coefficients of various impurities in molten copper, it was estimated that some impurities, including bismuth, could be volatilized by chlorination. However, experiments revealed that little or none of the bismuth was volatilized. Much of the arsenic and antimony was eliminated, but not by chlorination. It was concluded that the addition of calcium chloride probably caused the formation of calcium arsenate and calcium antimonate, as it was found that other chlorides were not effective in eliminating arsenic or antimony.

2.5.3 : VACUUM REFINING

Industrial applications of vacuum distillation to refining steel and lead have encouraged theoretical and experimental studies of vacuum refining molten copper. In this process, an impure copper melt is exposed to vacuum, which enhances evaporation of those species more volatile than copper in the melt, such as bismuth, antimony and

arsenic. In previous studies on vacuum refining copper, the results of bismuth removal have been promising, while antimony and arsenic have been removed to lesser extents. The vacuum levels required, approximately 10 to 100 Pa, are comparable to those required for refining steel, but less than those required for degassing steel.

2.5.4 : SUMMARY

This section has shown that oxidation and chlorination treatments for refining copper are unsuccessful in removing bismuth and partially successful in removing antimony and arsenic. Vacuum refining copper appears to be a more viable technical solution to the problem of eliminating antimony and arsenic. For the case of bismuth removal, it appears to be the only solution.

CHAPTER THREE

VACUUM DISTILLATION

SECTION 3.1 : PREVIOUS STUDIES

Previous studies on vacuum refining copper are summarized in Tables 3.1, 3.2 and 3.3 which show experimental conditions and results for elimination of bismuth, antimony and arsenic respectively from copper melts.

With one exception, experiments were carried out in crucibles made of either graphite, magnesia or alumina. The exception was a 'vacuum lift' method of refining[10], where a thin (0.04 m i.d.) vertical quartz tube was evacuated to lift and refine portions of a copper melt for 2 to 10 minutes and then repressurized with nitrogen gas to return the copper to the bulk of the melt; this 'lift and return' procedure was repeated between 5 and 30 times during one experimental run.

Previous small scale experiments were conducted using melt masses between 0.02 and 0.15 kg while prior pilot plant scale experiments used melt masses between 4 and 34 kg.

Source	Melt Mass (kg)	Melt Temperature (K)	Chamber Pressure (Pa)	Area Volume (m^{-1})	Initial Wt.% Bi	Processing Time (min)	% Elimination	K_{Bi} (10^{-5} m s^{-1})
Kameda[4]	0.03	1373	13	-	-	60	50-80	(20-45)/(A/V)
Kameda[4]	0.03	1473	13	-	-	60	+90	64/(A/V)
Ohno[5]	0.15	1473-1573	0.1-1	50-60	0.5	5-15	+95	8-27
Bryan[6]	0.02	1443	10	-	0.126	60	+99	128/(A/V)
Bryan[6]	4	1473-1573	1-150	15-20	0.02-0.3	50-60	80-95	1-8
Bryan[6]*	0.02	1443	10	-	0.32	60	80	50/(A/V)
Strel'tsov[7]	0.04	1473	0.01	55	0.9	25	90	2.8
Komorova[8]	0.03	1473	1	-	-	120	50-80	(10-22)/(A/V)
Golovko[9]	-	1473	13-67	-	-	5-15	93	443/(A/V)
Kametami[10]	0.6-6.0	1473	130-270	Vacuum Lift Refining	-	15-90	10	(2-12)/(A/V)
Taubenblat[11]	25	1423-1573	0.01	-	-	30	50	39/(A/V)
Ozberk[12]	34	1423-1623	8-40	6.7-10.2	0.02-0.04	120	40-80	1-3

* - the melt was Cu_2S

Table 3.1 : Summary of Results from Previous Vacuum Refining Studies Showing Bismuth Elimination from Molten Copper

Source	Melt Mass (kg)	Melt Temperature (K)	Chamber Pressure (Pa)	Area Volume (m^{-1})	Initial Wt.% Sb	Processing Time (min)	% Elimination	K_{Sb} (10^{-5} m s^{-1})
Kameda[4]	0.03	1373	13	-	-	60	50-55	20/(A/V)
Kameda[4]	0.03	1473	13	-	-	60	30-40	10/(A/V)
Komorova[8]	0.03	1473	1	-	-	120	50-75	(10-20)/(A/V)
Golovko[9]	-	1473	13-67	-	-	5-15	20	40/(A/V)
Kim[13]	-	-	-	-	-	-	40	-
Kametami[10]	0.6-6.0	1473	130-270	Vacuum Lift Refining	-	15-90	20	(4-25)/(A/V)
Ozberk[12]	34	1523	13	7.1	0.15-0.25	120	0	0

Table 3.2 : Summary of Results from Previous Vacuum Refining Studies showing Antimony Elimination from Molten Copper

Source	Melt Mass (kg)	Melt Temperature (K)	Chamber Pressure (Pa)	Area Volume (m^{-1})	Initial Wt.% As	Processing Time (min)	% Elimination	K_{As} (10^{-5} m s^{-1})
Kameda[4]	0.03	1373	13	-	-	60	10-30	(3-10)/(A/V)
Kameda[4]	0.03	1473	13	-	-	60	40-70	(15-30)/(A/V)
Komorova[8]	0.03	1473	1	-	-	120	50-80	(10-25)/(A/V)
Golovko[9]	-	1473	13-67	-	-	5-15	20	40/(A/V)
Kim[13]	-	-	-	-	-	-	30-50	-
Kametami[10]	0.6-6.0	1473	130-270	Vacuum Lift Refining	-	15-90	10-20	(2-25)/(A/V)
Ozberk[12]	34	1523	13	7.1	0.3-0.4	120	0	0

Table 3.3 : Summary of Results from Previous Vacuum Refining Studies Showing Arsenic Elimination from Molten Copper

Melt temperatures were generally between 1400 and 1500 K. Taubenblat[11], Ozberk[12], Ohno[5] and Bryan[6] conducted some experiments at 1600 K as well. A large range of pressures was investigated : low (0.01 Pa)[5,7,8,11], moderate (10-15 Pa)[4,6,9,12] and high (70-270 Pa)[6,9,10].

It can be seen that rates of antimony and arsenic removal were similar (30-60 % of initial content eliminated in 1 hour) while rates of bismuth eliminations were consistently higher (50-99 % of initial content eliminated in 1 hour). In the case of the 'vacuum lift' technique, the elimination rates of the three elements were about the same and low when compared to the other studies. On the whole, high elimination rates appear to have been promoted by high melt temperatures and high initial impurity contents.

It can also be seen that elimination rates were comparitively low for the pilot plant scale studies. Consequently, the goals of the present pilot plant scale study are to determine causes for these decreased elimination rates and how refining rates might be increased in practice.

SECTION 3.2 : GENERAL THEORY

Vacuum distillation as applied to liquid metals involves changing the composition of a melt through removal of volatile elements. In practice, two elements with distinctively different vapour pressures above a given melt are separated when exposed to a sufficiently low pressure, since the element with the higher vapour pressure will volatilize to a greater extent. This is the principle of vacuum refining, in which volatile impurities are distilled from a liquid metal.

The two predominant variables in the vacuum refining process are melt temperature and chamber pressure. They are adjusted to maximize distillation rate. A clean melt surface, a well stirred melt and a high surface area to volume ratio also enhance distillation.

The effects of these and other parameters on distillation rate may be determined by using mass transfer theory to develop a vacuum distillation model. It has been found[13,14,15] that three mass transfer mechanisms are required to describe the vacuum distillation process. They are :

a) transport of a solute atom through the melt to the melt surface,

b) evaporation of the atom at the melt surface and

c) transport of the evaporated atom away from the melt surface and through the bulk gas phase.

Under different conditions of vacuum distillation, each mechanism may be the rate controlling step.

In the sections that follow, these mechanisms are described and an overall mass transfer equation for vacuum distillation is derived. The equation is then applied to vacuum refining copper by incorporating the appropriate parameters.

SECTION 3.3 : MASS TRANSFER IN THE MELT TO THE MELT SURFACE

Machlin[16] developed a model for mass transfer in an inductively stirred melt. He assumed that unit volumes of melt which are adjacent to the melt-gas interface move as rigid bodies, that is, without shear gradients along the interface. Local convection currents within these unit volumes are assumed to be negligible. The rigid body motion

is from the center of the melt to the walls of the crucible.

Under these conditions of straight streamline flow, transport normal to the velocity of flow is independent of that velocity. Hence, Fick's second law of diffusion can be applied to each rigid body. When the rigid body is exposed to vacuum, the solute concentration at the melt-gas interface will decrease due to evaporation of solute atoms. This concentration gradient, illustrated in Figure 3.1, acts as the driving force for diffusion.

By incorporating the concentration gradient into Fick's law, Machlin obtained the following expression for the flux of solute atoms to the melt-gas interface :

$$N_i^m = \left(\frac{8\, D_i^m\, v}{\pi\, r} \right)^{\frac{1}{2}} (C_i^b - C_i^s) \qquad \ldots\ 3.1$$

or

$$N_i^m = K_i^m (C_i^b - C_i^s) \qquad \ldots\ 3.2$$

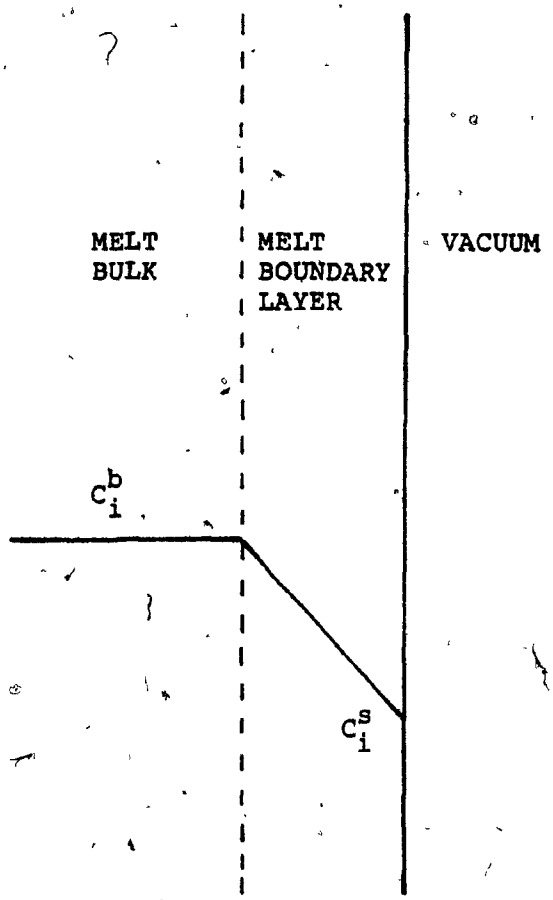

Figure 3.1 : Assumed Concentration Profile in the Melt

where

N_i^m = molar flux of solute atoms of species i through the melt to the melt-gas interface, kgmole m^{-2} s^{-1}

C_i = concentration of solute atoms of species i, kgmole m^{-3}

b,s = melt bulk and melt surface, respectively

D_i^m = coefficient of diffusion for solute species i through the liquid melt, m^2 s^{-1}

v = average melt surface velocity, m s^{-1}

r = melt radius, m

$$K_i^m = \left(\frac{8\ D_i^m\ v}{\pi\ r}\right)^{\frac{1}{2}},\ m\ s^{-1} \qquad \ldots\ 3.2a$$

Incorporation of this expression into the overall mass transfer model requires that values for C_i^b, D_i^m, v and r be known. The melt radius and bulk concentration are easily measured. The diffusion coefficient and surface velocity for the case of a copper melt will be discussed in a later section which deals with all parameters specific to the vacuum distillation of copper.

SECTION 3.4 : EVAPORATION AT THE MELT SURFACE UNDER PERFECT VACUUM

The rate of evaporation of species i from the melt into a perfect vacuum can be predicted by the Hertz-Knudsen-Langmuir equation[6,12,13,15,17] :

$$N_i^e = \varepsilon \left(\frac{1}{2 \pi M_i R T}\right)^{\frac{1}{2}} P_i^s \qquad \ldots. 3.3$$

or

$$N_i^e = K_i^e P_i^s \qquad \ldots. 3.4$$

where

N_i^e = molar flux of species i evaporating, kgmole m^{-2} s^{-1}

ε = coefficient of evaporation, usually assumed to be unity in liquid metal systems

M_i = molar mass of evaporating species i, kg $kgmole^{-1}$

R = gas constant 8314.34 J $kgmole^{-1}$ K^{-1}

T = melt temperature, K

P_i^s = equilibrium vapour pressure of species i at the melt surface, Pa

$$K_i^e = \varepsilon \left(\frac{1}{2 \pi M_i R T}\right)^{\frac{1}{2}} , \text{ kgmole s } m^{-1} \text{ kg} \quad \ldots. 3.4a$$

It is necessary to correlate surface vapour pressure and surface concentration in order to combine the mass transfer equations for the melt and evaporation. Surface vapour pressure is related to the mole fraction of species i at the surface, X_i^s, first by Henry's relation[18] :

$$P_i^s = P_i^o X_i^s \gamma_i \quad \ldots. 3.5$$

where

P_i^o = vapour pressure of pure species i, Pa

γ_i = Raoultian activity coefficient of species i in the melt

At low concentrations of the solute, it may be assumed that :

$$X_i = C_i \frac{M_b}{\rho_b} \quad \ldots. 3.6$$

where

M_b = molar mass of bulk material in the surface
≈ molar mass of bulk metal

ρ_b = density of bulk material in the surface
≈ density of bulk metal

It may be further assumed that the activity coefficient approaches the Raoultian activity coefficient in infinite dilution, γ_i^o. Equation 3.5 now becomes :

$$P_i^s = P_i^o \gamma_i \frac{M_b}{\rho_b} C_i^s \quad \ldots\ldots 3.7$$

Substituting Equation 3.7 into Equation 3.3 yields :

$$N_i^e = \varepsilon \left(\frac{1}{2 \pi M_i R T}\right)^{\frac{1}{2}} \left(P_i^o \gamma_i^o \frac{M_b}{\rho_b}\right) C_i^s \quad \ldots\ldots 3.8$$

or

$$N_i^e = K_i^e \phi_i C_i^s \quad \ldots\ldots 3.9$$

where

$$\phi_i = p_i^o \gamma_i^o \frac{M_b}{\rho_b} \quad \ldots\ldots 3.9a$$

and K_i^e is as previously defined.

SECTION 3.5 : EVAPORATION OF SPECIES WHICH CONTAIN MORE THAN ONE ATOM IN THE VAPOUR STATE

Bismuth, antimony and arsenic can form the following vapour molecules :

Bi, Bi_2

Sb, Sb_2, Sb_4

As, As_2, As_3, As_4

The model for evaporation as it is given in Equation 3.8 is limited to species which volatilize as monatomic vapour molecules, and must be modified to accomodate evaporation of polyatomic molecules of bismuth, antimony and arsenic. The modification is performed as follows.

The activity of species i in a melt is defined as[19] :

$$a_i = \left(\frac{P_{i_n}}{P^o_{i_n}}\right)^{1/n} \quad \ldots\ldots 3.10$$

where

a_i = activity of species i in the melt

P_{i_n} = equilibrium vapour pressure of polyatomic species i, Pa

$P^o_{i_n}$ = vapour pressure of polyatomic species i in its pure state, Pa

n = number of atoms in a molecule of species i in its vapour state

Rearranging Equation 3.10 and recalling that $a_i = \gamma_i^o C_i M_b/\rho_b$ for species i in dilute solution yields an expression to describe the equilibrium vapour pressure of polyatomic species i at the melt surface :

$$P^s_{i_n} = P^o_{i_n} \left(\gamma_i^o C_i^s \frac{M_b}{\rho_b}\right)^n \quad \ldots\ldots 3.11$$

This expression for $P^s_{i_n}$ may replace P^s_i in Equation 3.3, to give :

$$N^e_{i_n} = \varepsilon \left(\frac{1}{2 \pi M_{i_n} R T}\right)^{\frac{1}{2}} P^o_{i_n} \left(\gamma_i^o C_i^s \frac{M_b}{\rho_b}\right)^n \quad \ldots\ldots 3.12$$

or

$$N^{e}_{i_n} = K^{e}_{i_n} \cdot \phi_{i_n} \cdot (C^{s}_{i})^{n} \quad \ldots\ldots 3.13$$

where

$$K^{e}_{i_n} = \varepsilon \left(\frac{1}{2 \pi M_{i_n} R T}\right)^{\frac{1}{2}} \quad \ldots\ldots 3.13a$$

$$\phi_{i_n} = P^{o}_{i_n} \left(\gamma^{o}_{i} \frac{M_b}{b}\right)^{n} \quad \ldots\ldots 3.13b$$

SECTION 3.6 : EVAPORATION INTO AN IMPERFECT VACUUM

According to Krüger[34] , the gas space above a melt is said to behave like a perfect vacuum when the chamber pressure is below 0.1 Torr (13 Pa). This is attributed to the low probability of atom-atom collisions, which allows atoms to move in straight paths away from the melt surface until they collide with a bounding surface.

At higher pressures, frequent collisions between atoms occur, allowing a proportion of the evaporating species to

be back-scattered in the direction of the melt surface. Harris[15] refers to this phenomenom as back pressure of the evaporating species on the gas phase side of a 'Langmuir' plane just above the melt surface (see Figure 3.2 in the following section). The flux of atoms back into the melt due to the back pressure may be obtained by reapplying the Hertz-Knudsen-Langmuir expression :

$$N^{bp}_{i_n} = K^{e}_{i_n} \; p^{bp}_{i_n} \qquad \ldots\ldots 3.14$$

where

$N^{bp}_{i_n}$ = flux of atoms of species i back into the melt, kgmole m^{-2} s^{-1}

$p^{bp}_{i_n}$ = back pressure of species i in the gas space above the melt, Pa

Consequently, there exists a net flux of atoms away from the melt equal to the flux of evaporating species (Equation 3.13) less the flux of species back into the melt (Equation 3.14). This net flux is expressed as :

$$N^{e}_{i_n} = K^{e}_{i_n} \; \{\phi_{i_n} \cdot (C^{s}_{i})^{n} - p^{bp}_{i_n}\} \qquad \ldots\ldots 3.15$$

where all terms have the meanings previously defined. This equation represents the complete model of mass transfer due to the net evaporation of any monatomic or polyatomic species i.

SECTION 3.7 : MASS TRANSFER IN THE GAS PHASE

Mass transfer of evaporated species in the gas phase is a combination of convective flow and diffusion. Szekely and Themelis[20] developed a mass transfer equation for a binary gas system, A diffusing through B :

$$N^g_{A,x} = -c\, D_{A-B} \frac{dX_A}{dx} + X_A\, (N^g_{A,x} + N^g_{B,x}) \qquad \ldots\ 3.16$$

where

$N^g_{A(B),x}$ = molar flux of A (B) in the x direction in the gas space, kgmole m^{-2} s^{-1}

c = average molar density of the gas mixture, kgmole m^{-3}

D_{A-B} = diffusion coefficient of A in system A-B, m^2 s^{-1}

X_A = mole fraction of A in the gas mixture

By recognizing that $c = P_{ch}/(R\ T)$ by the universal gas law and that $N^g_{A,x} + N^g_{B,x} = \Sigma N^g_{i_n,x}$, Equation 3.16 may be re-written in a form which is applicable to a multi-component system :

$$N^g_{i_n,x} = - \frac{P_{ch}}{R\ T} D^g_{i_n} \frac{dX_{i_n}}{dx} + X_{i_n} \cdot \Sigma N^g_{i_n,x} \quad \ldots\ldots 3.17$$

where

$N^g_{i_n,x}$ = molar flux of species i_n in the x direction in the gas space, kgmole $m^{-2}\ s^{-1}$

P_{ch} = chamber pressure, Pa

$D^g_{i_n}$ = diffusion coefficient of species i_n in the gas mixture, $m^2\ s^{-1}$

X_{i_n} = mole fraction of species i_n in the gas mixture

The pressure profile (note that $X_{i_n} = P_{i_n}/P_{ch}$) in the gas space which is assumed in this study is illustrated in Figure 3.2. Using this pressure profile, Equation 3.17 and the assumption that the vapour pressure of species i in the gas bulk is much lower than the chamber pressure ($P^g_{i_n} << P_{ch}$, $X^g_i \simeq 0$), Persson[17] derived the following expression for gas phase mass transfer :

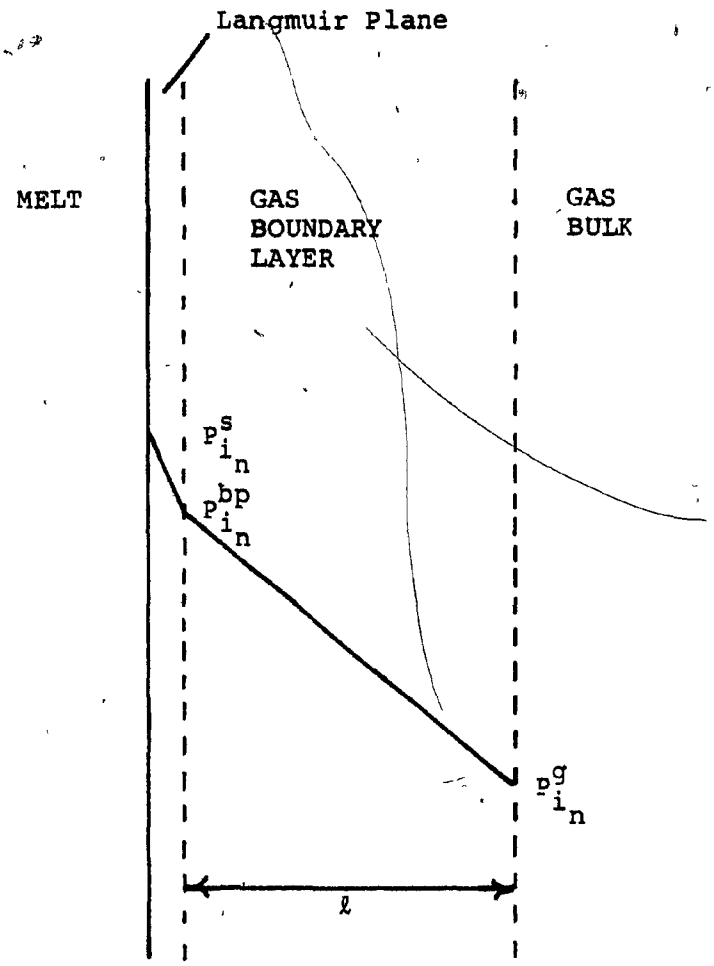

Figure 3.2 : Assumed Pressure Profile in the Gas Space

$$N^g_{i_n} = \frac{\Sigma N^g_{i_n}}{P_{ch}} \{1 - \exp(\frac{-\Sigma N^g_{i_n} R T \ell}{D^g_{i_n} P_{ch}})\}^{-1} p^{bp}_{i_n} \quad .... 3.18$$

or

$$N^g_{i_n} = K^g_{i_n} p^{bp}_{i_n} \quad .... 3.19$$

where

$$K^g_{i_n} = \frac{\Sigma N^g_{i_n}}{P_{ch}} \{1 - \exp(\frac{-\Sigma N^g_{i_n} R T \ell}{D^g_{i_n} P_{ch}})\}^{-1} \quad .... 3.19a$$

ℓ = thickness of gas phase boundary layer, m (see Figure 3.2)

This equation assumes that diffusion is one dimensional in the direction away from the melt.

SECTION 3.8 : COMBINED MASS TRANSFER EQUATION

The equations for the three mass transfer mechanisms which describe vacuum distillation are restated here :

a) melt phase mass transfer

$$N_i^m = K_i^m \ (C_i^b - C_i^s) \qquad \ldots\ 3.2$$

b) evaporation

$$N_{i_n}^e = K_{i_n}^e \ \{\phi_{i_n} \ (C_i^s)^n - p_{i_n}^{bp}\} \qquad \ldots\ 3.15$$

c) gas phase mass transfer

$$N_{i_n}^g = K_{i_n}^g \ p_{i_n}^{bp} \qquad \ldots\ 3.19$$

Because the accumulation of vapour in the gas space is negligible, it may be assumed that the flux of atoms by each mechanism is the same, that is :

$$N_i^m = n\, N_{i_n}^e = n\, N_{i_n}^g \qquad \ldots\ldots 3.20$$

where n is the number of atoms per molecule of polyatomic species i.

Equation 3.20 can now be used to combine Equations 3.2, 3.15 and 3.19, yielding an overall expression for the molar flux of species i from the melt in terms of its bulk concentration :

$$N_{i_n}\left(1 + \frac{K_{i_n}^e}{K_{i_n}^g}\right) = n\, K_{i_n}^e\, \phi_{i_n}\, \left(c_i^b - \frac{N_{i_n}}{K_i^m}\right)^n \qquad \ldots\ldots 3.21$$

where

$$K_i^m = \left(\frac{8\, D_i^m\, v}{\pi\, r}\right)^{\frac{1}{2}} \qquad \ldots\ldots 3.21a$$

$$K_{i_n}^e = \varepsilon \left(\frac{1}{2\, \pi\, M_{i_n}\, R\, T}\right)^{\frac{1}{2}} \qquad \ldots\ldots 3.21b$$

$$K^g_{i_n} = \frac{\Sigma N_{i_n}}{P_{ch}} \{1 - \exp(- \frac{\Sigma N_{i_n} \; R \; T \; \ell}{D^g_{i_n} \; P_{ch}})\}^{-1} \qquad \ldots\ldots 3.21c$$

$$\phi_{i_n} = P^o_{i_n} \; (\gamma^o_i \frac{M_b}{\rho_b})^n \qquad \ldots\ldots 3.21d$$

The molar flux term N_{i_n} on the right hand side of Equation 3.21 cannot be easily separated from the other terms unless the value for n is known. Consequently, this separation was performed for each of the two values for n which are encountered in this study. The resulting equations follow :

i) n = 1 : species i is monatomic in the gas phase

$$N_i = (\frac{1}{K^m_i} + \frac{1}{K^e_i \; \phi_i} + \frac{1}{K^g_i \; \phi_i})^{-1} \; C^b_i \qquad \ldots\ldots 3.22$$

ii) n = 2 : species i is diatomic in the gas phase

$$N_{i_2} = \frac{-b - (b^2 - 4 \; a \; c)^{\frac{1}{2}}}{2 \; a} \qquad \ldots\ldots 3.23$$

where

$$a = \frac{2}{(K_i^m)^2} \quad \ldots\ 3.23a$$

$$b = -\left(\frac{4\, C_i^b}{K_i^m} + \frac{1}{K_{i_2}^e\, \phi_{i_2}} + \frac{1}{K_{i_2}^g\, \phi_{i_2}}\right) \quad \ldots\ 3.23b$$

$$c = 2\, (C_i^b)^2 \quad \ldots\ 3.23c$$

SECTION 3.9 : PARAMETERS IN VACUUM REFINING COPPER

3.9.1 : DIFFUSION COEFFICIENT IN THE MELT PHASE, D_i^m

With the exception of Ozberk[12], previous studies did not publish any data on diffusivity of metallic impurity atoms in copper melts. For the case of steel, Machlin[16] assumed a value of 1×10^{-8} $m^2\ s^{-1}$ but pointed out that this value corresponds to a limiting value which would tend to maximize the melt mass transfer coefficient. Ozberk calculated the diffusion coefficient of bismuth and lead

in liquid copper using three different diffusivity equations : Wells and Upthegrove[21], Stokes and Einstein[21] and Sutherland[21]. At temperatures of 1523 and 1623 K, the values for each element were in the range of 2-3 x 10^{-9} m^2 s^{-1}. He also found that the diffusion coefficient of a given element at a given temperature differed by as much as 50 % when calculated by the different equations. Consequently, a constant value of 3 x 10^{-9} m^2 s^{-1} was chosen in this work for the diffusion coefficient of an impurity element in liquid copper in the temperature range of 1500-1750 K.

3.9.2 : AVERAGE MELT SURFACE VELOCITY, v

Machlin[16] observed the rate of motion of particles floating on top of melts, which ranged from 0.1 kg to 900 kg, and estimated that the surface velocity of a steel melt was 0.1 m s^{-1}, accurate to within an order of magnitude. Irons et al.[22] used the same method for 55 kg pig iron melts and obtained a value of 0.2 m s^{-1}. Szekely and Chang[23] timed the movement of dark streaks on the surface of large steel melts (≃ 14 tonnes). They found that the average melt surface velocity varied with power input. Values of 0.2 m s^{-1} at 500 kW and 0.4 m s^{-1} at 2000 kW

were obtained.

It is apparent that there is much variation in melt surface velocity. It was consequently decided to estimate the melt surface velocity under conditions of this study by observing the movement of dark streaks on the liquid copper surface. The value obtained was approximately 0.1 m s^{-1}.

3.9.3 : THERMODYNAMIC DATA

In order to model evaporation from a copper melt, three pieces of thermodynamic data are required :

a) density of molten copper melts

b) Raoultian activity coefficients in infinite dilution in copper melts,

and

c) vapour pressures of all species in their pure states

This data is listed in Appendix 1.

The data for arsenic is uncertain. In the most recent study by Lynch[19], the activity coefficient was found to be higher than in previous studies[2,24,25]. This latest

value is used in this work. Lynch also claimed that, although tetratomic arsenic is the predominant vapour species at low temperatures (300-800 K), considerable dissociation of this species to As, As_2 and As_3 will take place at higher temperatures (1373 K). It is difficult to determine the vapour pressures of these high temperature species. For the purpose of this study, the equations which Lynch used to describe equilibrium constants between two arsenic vapour species were extrapolated to the 1500-1700 K temperature range. Vapour pressures were then determined using these equilibrium constants and values for the vapour pressure of As_4 as given by Hultgren et al[26]. These calculations are described in detail in Appendix 2.

3.9.4 : DIFFUSION COEFFICIENT IN THE GAS PHASE, $D^g_{i_n}$

Szekely and Themelis[20] discuss several semi-empirical equations which describe the diffusivity of gases. Each equation differs slightly in form, but they all show that the diffusion coefficient is inversely proportional to total pressure of the system and directly proportional to the 1.5-1.8 power of the absolute temperature.

The equation used in this work was given by Bird

et al.[27] :

$$D_{A-B} = \frac{2}{3} \left(\frac{\kappa}{\pi}\right)^{3/2} \left(\frac{A^o}{2M_A} + \frac{A^o}{2M_B}\right)^{\frac{1}{2}} \frac{T^{3/2}}{P \left(\frac{d_A + d_B}{2}\right)^2} \quad .... \ 3.24$$

where

D_{A-B} = diffusion coefficient of species A in system A-B, $cm^2\ s^{-1}$

κ = Boltzmann's constant 1.38054×10^{-16} erg K^{-1} molecule^{-1}

A^o = Avogadro's number 6.022×10^{23} molecule gmole^{-1}

M_A, M_B = molecular weights of species A and B, g gmole^{-1}

T = temperature of system, K

P = pressure of system, dynes cm^{-2}

d_A, d_B = collision diameters for species A and B, cm

This expression is accurate to within an order of magnitude[27]. Collision diameters of all metal atoms are approximately 2.5×10^{-10} m. A difference in the diffusion coefficient of two species is consequently due only to their different molecular weights. In light of the claimed accuracy of the above expression, these differences can be assumed negligible, and a single expression for all species

is derived using an average molecular weight :

$$D_i^g = 1.82 \times 10^{-4} \frac{T^{1.5}}{P_{ch}} \quad \ldots\ldots 3.25$$

where D_i^g has the units $m^2\ s^{-1}$.

3.9.5 : THICKNESS OF GAS PHASE BOUNDARY LAYER, ℓ

The overall mass transfer equation (Equation 3.21) was applied to the work of Bryan[6] on vacuum refining copper to remove bismuth in order to determine the gas phase boundary layer thickness. Table 3.4 presents the values of chamber pressure, overall mass transfer coefficient, gas phase mass transfer coefficient and boundary layer thickness for three of Bryan's experimental runs. An example of the calculations is shown in Appendix 3. It can be seen that ℓ ranges between 0.02 and 0.2 m. An average value of 0.1 m was chosen for the present work. This value appears to be large for a gas boundary layer thickness. However, Bird et al.[27] state that diffusion will occur over a distance equal to several times the mean free path of the evaporating atoms. Ozberk[12] calculated the mean free paths

P_{ch} (Pa)	K_{Bi} ($m\ s^{-1}$)	K^g_{Bi} ($m\ s^{-1}$)	ℓ (m)
26.7	1.24×10^{-5}	1.72×10^{-7}	0.19
26.7	5.40×10^{-5}	1.35×10^{-6}	0.02
133.3	8.10×10^{-6}	1.08×10^{-7}	0.06

Table 3.4 : Experimental results of Bryan[6] on Vacuum Refining Copper to remove bismuth. Column 2 is the experimentally determined overall mass transfer coefficient. Columns 3 and 4 are calculated (Appendix 3) and present the gas phase mass transfer coefficient and the gas phase boundary layer thickness respectively.

of Bi, Sb, As, Pb and Cu under the conditions of vacuum refining, that is, pressures between 8 and 40 Pa and temperatures between 1423 and 1623 K. The resulting values varied between 0.001 and 0.01 m. The highest values were obtained when the pressure was low and the temperature high. These results imply that the gas boundary layer which is assumed in this study spans 10 to 100 mean free paths, which are reasonable lengths for diffusion.

SECTION 3.10 : THEORETICAL PREDICTIONS

3.10.1 : VOLATILITY COEFFICIENTS OF IMPURITIES IN COPPER

Estimation of refining rate require that the evaporation of bulk metal atoms be considered as well as the evaporation of solute atoms. This is achieved by applying the evaporation mass transfer model to the bulk metal in order to determine bulk metal losses. Equation 3.8, when applied to the case of the bulk metal and simplified by substituting $C_b M_b/\rho_b \simeq 1$ and $\gamma_b \simeq 1$, becomes :

$$N_b^e = \varepsilon \left(\frac{1}{2 \pi M_b R T}\right)^{\frac{1}{2}} p_b^o \qquad \ldots\ldots 3.26$$

Expected refining rates are reflected by the ratio between the solute evaporation rate (Equation 3.8) and solvent evaporation rate (Equation 3.26), that is :

$$\frac{N_{i_n}^e}{N_b^e} = \frac{P_{i_n}^o}{P_b^o} \left(\frac{M_b}{M_{i_n}}\right)^{\frac{1}{2}} \left(\gamma_i^o \frac{M_b}{\rho_b} C_i^s\right)^n \quad \ldots\ldots 3.27$$

or

$$\frac{N_{i_n}^e}{N_b^e} = \alpha_{i_n,b} X_i^s \quad \ldots\ldots 3.28$$

where

$$\alpha_{i_n,b} = \frac{P_{i_n}^o}{P_b^o} \left(\frac{M_b}{M_{i_n}}\right)^{\frac{1}{2}} (\gamma_i^o)^n (X_i^s)^{n-1} \quad \ldots\ldots 3.28a$$

The term $\alpha_{i_n,b}$ is called the volatility coefficient for species i in bulk metal b and was first used by Ollette[28]. When $\alpha_{i_n,b} > 1/n$, the ratio of moles of i evaporating to moles of b evaporating (N_i^e/N_b^e) is greater than the ratio of moles i to moles b in the melt (X_i) and refining of the

melt occurs. A larger value of $\alpha_{i_n,b}$ implies a greater difference between these two ratios and hence a greater refining rate, given that there is no mass transport resistance from other sources in the system.

The volatility coefficient was evaluated at different melt temperatures for bismuth, antimony and arsenic in their monatomic and diatomic states and selenium and tellurium in their monatomic states for the case of a copper melt, Table 3.5a. It was also calculated for Cu_2S melts at 1473 K for monatomic and diatomic bismuth, Table 3.5b.

There are three conclusions which can be drawn from these tables :

i) Refining rates for antimony will be very low since its volatility coefficient is close to one. Refining rates for bismuth, selenium, tellurium and arsenic will be considerably higher.

ii) Refining rates for a species as a diatomic molecule will be negligible when compared to those for the same species as a monatomic molecule. Refining rates for triatomic or quadratomic species will be still lower and hence were not considered.

(a)

Temperature (K)	$\alpha_{i_n,Cu}$							
	Bi	Bi_2*	Sb	Sb_2*	As	As_2*	Se	Te
1500	7106	3.2	3.0	1.4×10^{-3}	68	0.30	132	557
1600	2982	1.0	2.0	6.3×10^{-4}	100	0.23	80	265
1700	1384	0.38	1.3	3.1×10^{-4}	140	0.17	52	138

* - at 0.1 weight % Bi, Sb, As

(b)

Temperature (K)	α_{i_n,Cu_2S}	
	Bi	Bi_2*
1473	4384	5.1

* - at 0.1 weight % Bi

Table 3.5 : Volatility Coefficients for the Evaporation of Bi, Bi_2, Sb, Sb_2, As, As_2, Se and Te from Copper (a) and of Bi and Bi_2 from Cu_2S (b).

iii) With the exception of As*, volatility coefficients decrease with increasing temperature. This means that, per unit mass of solute evaporated, the loss of copper by evaporation will be greater.

3.10.2 : COMPUTER SIMULATION OF VACUUM REFINING COPPER

The overall mass transfer model (Equation 3.21) was used to simulate an experimental run for vacuum refining copper. Appendix 4 shows the interactive computer program which was written for this purpose. The method of simulation which this program used was similar to those of Harris[15] and Persson[17].

Values for all constant parameters which appear in Equations 3.21a to 3.21d and are described in Section 3.9 are stored in the program. All variable parameters were supplied by the operator each time the program was run. A brief description of the program follows.

A flux is first calculated for the initial conditions by assuming that there is a perfect vacuum above the melt.

---

* - the rate of increase of P^{o}_{As} for a given temperature increase is greater than the rate of increase of P^{o}_{Cu} for that same temperature increase.

This flux is used to calculate the gas phase mass transfer coefficient for Equation 3.21c. The program then recalculates a flux for the initial time interval and, using the melt area and the magnitude of the time interval, calculates the change in concentration through evaporation of each species in the melt. These values are used to evaluate the new volume and composition of the melt. The program then returns to the beginning of the loop and calculations are repeated for the next time interval. The total flux from the previous time interval is also used to calculate a new gas phase mass transfer coefficient.

This iterative method is accurate as long as the magnitudes of the fluxes do not change considerably from one time interval to the next. Harris[15] discovered that this condition may be satisfied by using time intervals of 10 seconds or less. This program also uses 10 second intervals.

Melt composition is outputted every 100 seconds of simulation. The program stops after a predetermined time representing the duration of the experimental run.

An example of the simulation is shown in Figure 3.3. The output is presented as a plot of the weight % of Bi in the melt as a function of time. The input variables are included in the figure.

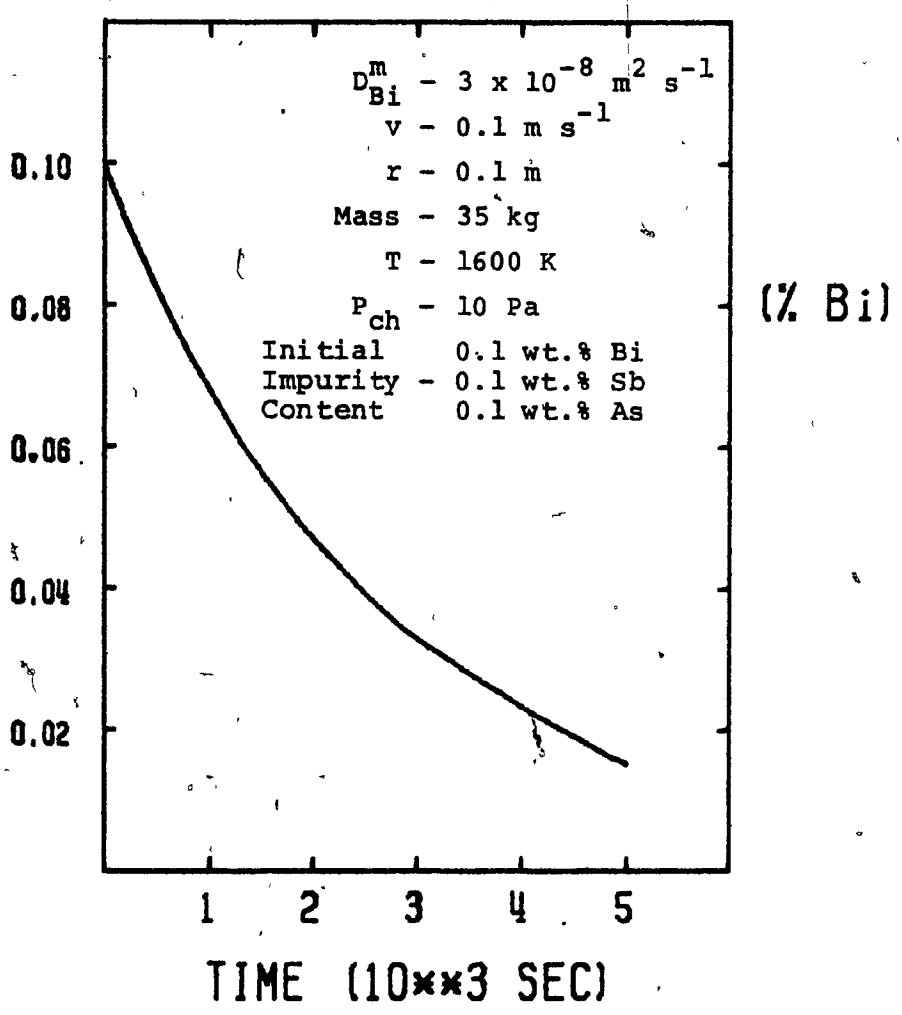

Figure 3.3 : Computer Simulation of Vacuum Refining Showing a Plot of % Bi against Time for the Conditions listed.

CHAPTER FOUR

EXPERIMENTAL

SECTION 4.1 : EXPERIMENTAL PROGRAM

The main objective of the experimental program was to determine rates of impurity elimination from copper melts by vacuum distillation. The element of principle concern was bismuth; subsequently, bismuth elimination was investigated in all 21 experiments. Other impurities studied were antimony (10 experiments), arsenic (3 experiments) and selenium and tellurium (1 experiment each).

The experimental program was separated into three parts according to the type of copper melt being used. In Part A, experiments were carried out using copper doped with impurities. Metallic bismuth, antimony and arsenic were added to the liquid copper (mostly cathode type but occasionally blister copper) without breaking vacuum. The Part A experiments, which made up the bulk of the experimental program, serve firstly as a preliminary investigation of impurity elimination rates and secondly as a study of the effect of some important parameters on those rates.

In Part B, two experiments were carried out using blister copper melts. Since no impurities were added, the initial impurity concentrations were those of the blister copper charge. These experiments acted as an important comparison between industrial type copper and that which was experimentally prepared. Furthermore, the removal of selenium and tellurium (two elements not investigated in Part A) were looked at in one of the experiments.

Part C consisted of two experiments using white metal (Cu_2S) doped with metallic bismuth. Bismuth elimination from this completely different type of melt was studied and compared to the bismuth elimination in the Part A experiments.

SECTION 4.2 : EXPERIMENTAL PARAMETERS

Several parameters were controlled and studied in the Part A experimental investigation. They are listed below, together with the ranges in which they were examined and why these ranges were chosen.

Melt Temperature

1500 K to 1790 K. The lower limit was fixed by the the melting points of the charge material. The upper limit was chosen by considering the rapid increases in copper vapour pressure and refractory wear which occur with increasing melt temperature.

Chamber Pressure

7 Pa to 160 Pa. The lower limit was set by the minimum pressure attainable by the vacuum pumps. The upper limit was chosen to be a pressure at which the refining rate was expected to be lower.

Melt Area to Volume Ratio (A/V)

6.8 m^{-1} to 10.4 m^{-1}. More than one experiment was conducted on the same melt with the result that each subsequent experiment had a smaller melt depth due to copper losses through sampling, splashing and evaporation and consequently a higher melt surface area to volume ratio.

Initial Impurity Concentration

0.002 % to 0.1 % by weight. This represented the range of impurity levels found in most industrial copper melts.

Presence of Slag Layer

A slag layer did not appear when melting pure cathode copper, but it was present when melting blister copper or previously oxidized copper. The slag layer was manually removed in all but two of the Part A experiments. In these specific cases, the slag layer was allowed to remain for the purpose of determining its effect on impurity elimination rates.

Other variables have been suggested[12-15,17] to affect refining rates. These variables and the reasons for omitting them from consideration are given below :

i) Pumping rate of the vacuum pumps is not expected to affect refining rate. It was consequently decided not to take the time or effort to change the pumping rate.

ii) Inert gas bubbling and jetting has been suggested[12,17] to increase mass transport kinetics in the melt and at the melt-gas interface. Due to the incapability of the present pumping system to handle larger volumes of gas, it was not possible to increase the gas load by either bubbling or jetting.

iii) Previous studies[12,15] have indicated that the distance from a condenser to the melt surface

would have to be extremely small (< 0.05 m) to imcrease refining rates. This poses a practical problem in that temperature measurement, sampling and visual observation would not be possible.

iv) A previous study[6] has indicated that the presence of oxygen and sulphur do not affect elimination rates of the metallic impurities from copper at levels normally found in the copper melts.

SECTION 4.3 : EXPERIMENTAL APPARATUS

The copper was melted in a 3000 Hz, 150 kW Tocco coreless induction furnace (see Appendix 5 for a list of all suppliers), with a coil diameter of 0.35 m and a steel melting capacity of 140 kg (Figure 4.1). A 3000 Hz, 150 kW, 800 V, 188 Amp Tocco Motor Generator was the power source.

The induction furnace was mounted inside a 3 m^3 (1.8 m diameter x 1.6 m long) vacuum chamber (Figure 4.2) and incorporated tilting capabilities for casting and deslagging. This chamber was provided with portholes (complete with vacuum-tight valves) at the top for measuring temperature, making additions to the melt and taking samples (Figure 4.3). Vacuum-tight windows in four locations

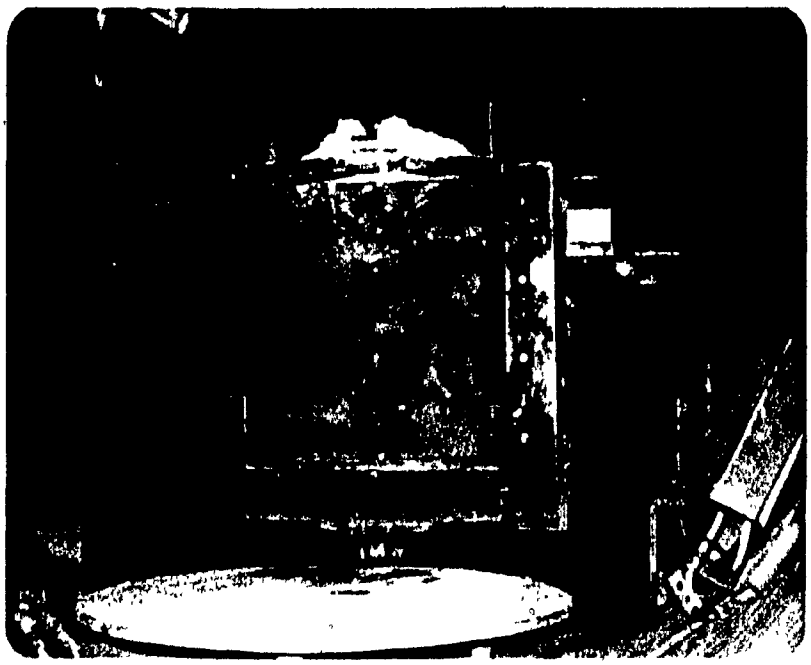

Figure 4.1 : Induction Furnace. The cable for the tilting mechanism can be seen in the top, center portion of the photograph. The vacuum outlet is seen in the top right portion.

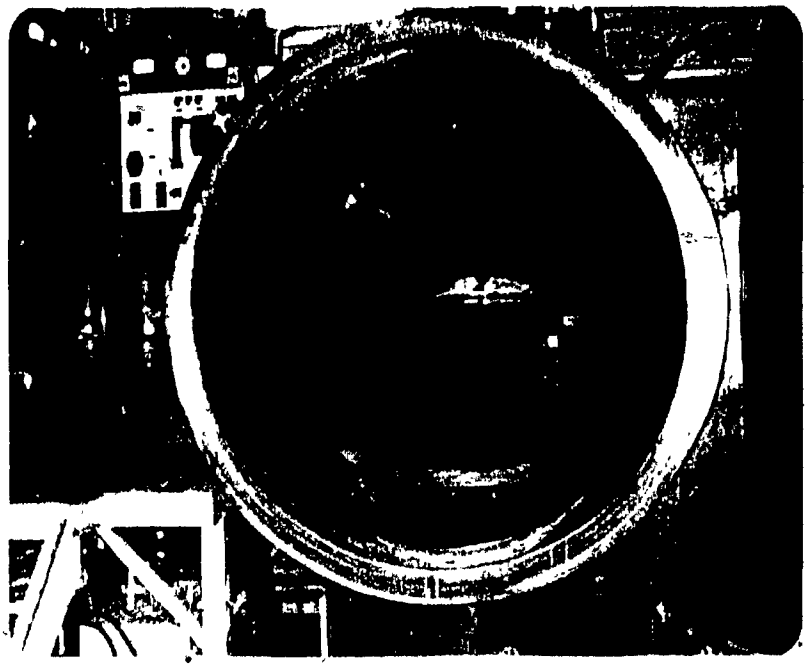

Figure 4.2 : Vacuum Chamber showing the induction furnace mounted inside. At the right of the chamber can be seen the control panels for the chamber and furnace.

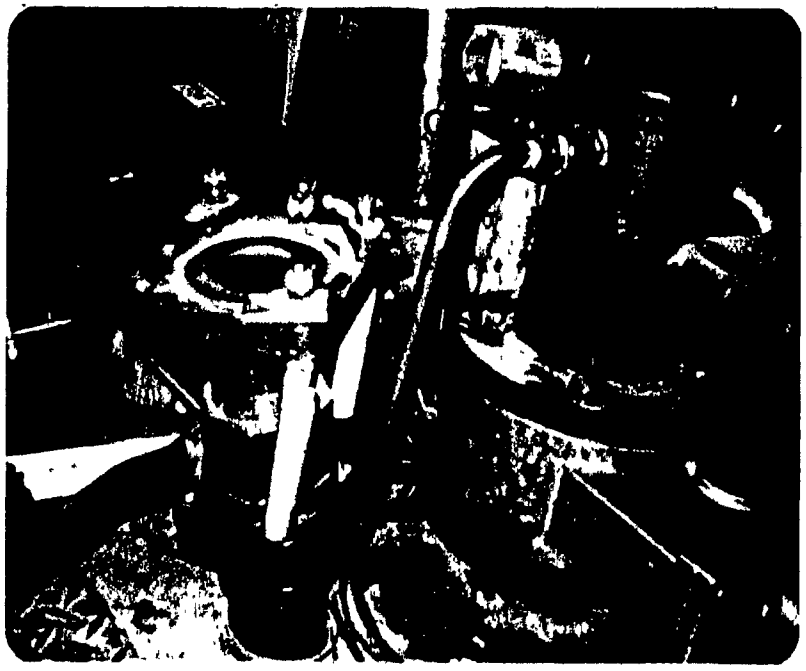

Figure 4.3 : Vacuum-tight Valves for temperature measuring (A), sample taking (B) and gas injecting (C). The latter was not used in the present study.

permitted observation and photography of both the melt surface and the gas space above the melt.

The vacuum chamber pumping system consisted of two stages : a Stokes mechanical pump of nominal capacity 0.142 $m^3\ s^{-1}$ and a Roots blower of nominal capacity 0.614 $m^3\ s^{-1}$ (Figure 4.4a and b).

Two types of crucibles were used to contain the liquid melts. For Part A and Part B experiments, 'Hycor' alumina crucibles of 0.195 m inside diameter and 0.17 m inside height were used (Figure 4.5a). For Part C experiments, due to the noninductive characteristics of Cu_2S, 'Tercod' crucibles made of graphite and carbon bonded silicon carbide were used (Figure 4.5b). The dimensions were 0.15 m top inside diameter and 0.22 m inside height.

As mentioned in the experimental program, three types of copper melts were used : doped copper, blister copper and white metal (Cu_2S) for Part A, Part B and Part C experiments respectively. Additions to the melts consisted of pure metallic bismuth, antimony and arsenic; the bismuth was in thin bar form, the antimony and arsenic in lump form.

(a)

(b)

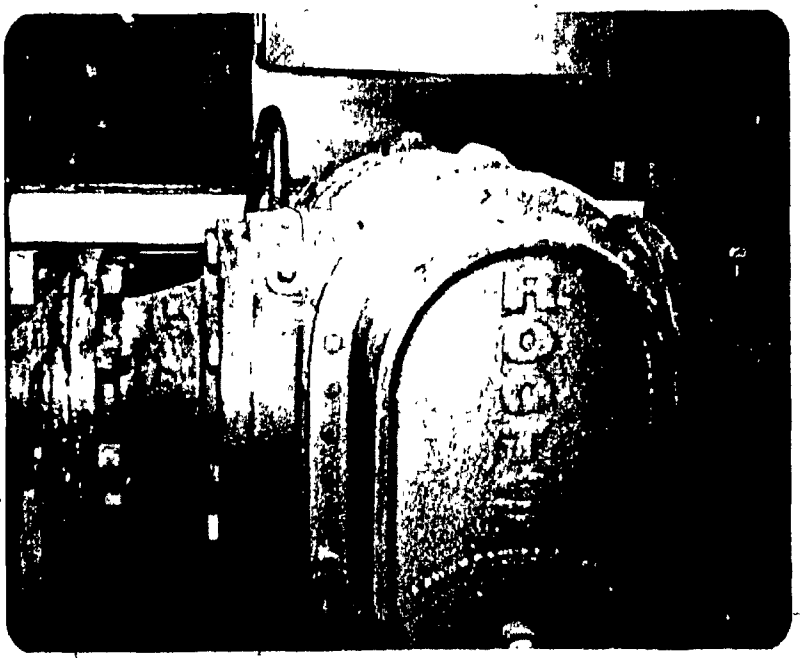

Figure 4.4 : Vacuum Chamber Pumping System showing (a) the Stokes Mechanical Pump and (b) the Roots Blower

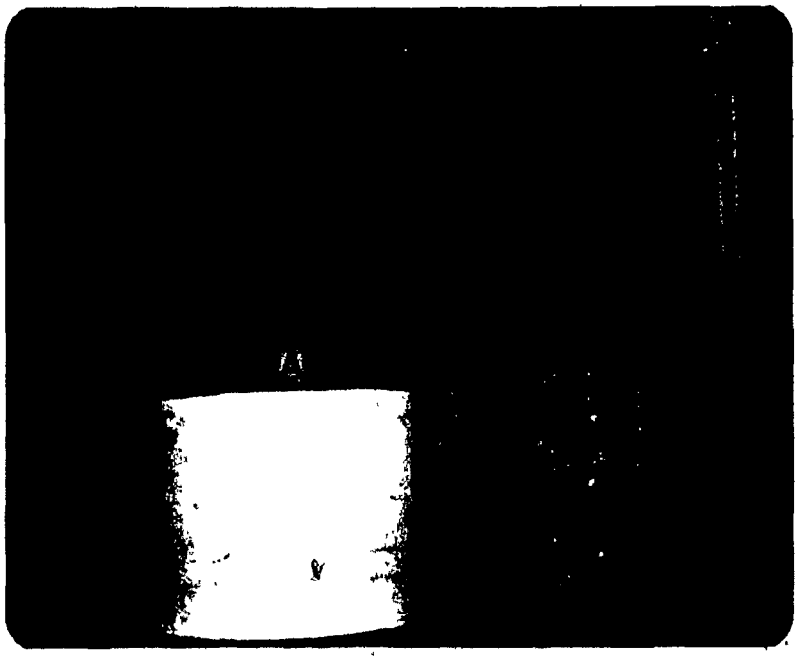

Figure 4.5 : Crucibles used in the experiments. The 'Hycor' alumina crucibles (A) were used for cathode and blister copper. The 'Tercod' graphite crucibles (B) were used for white metal (Cu_2S).

A tilting type McLeod vacuum gauge (Figure 4.6) was used to measure pressure in all experiments. The quoted accuracy of the gauge is ± 10 % at pressures below 300 Pa.

Melt temperature was taken using Norton type 'R' 'DIP TIP' disposable thermocouple assemblies mounted on a steel temperature probe (Figure 4.7) which fitted onto one of the portholes on top of the chamber. The probe was connected to a Fluke 8030A digital potentiometer that measured the thermocouple EMF. Melt samples were taken using sample cups (Figure 4.8) attached to a sampling probe. At first, graphite cups were chosen for the ease with which they could be separated from the solidified copper samples. However, these cups frequently snapped from their graphite stems while the sample was being taken and the use of black galvanized steel cups was adopted. It is recommended that, for future work, a graphite cup with a steel stem be used for sampling.

Samples were prepared for analysis by dissolving them in concentrated nitric acid. A lanthanum extraction step[35] was added for the samples with very low impurity levels.

Figure 4.6 : Tilting type McLeod Gauge

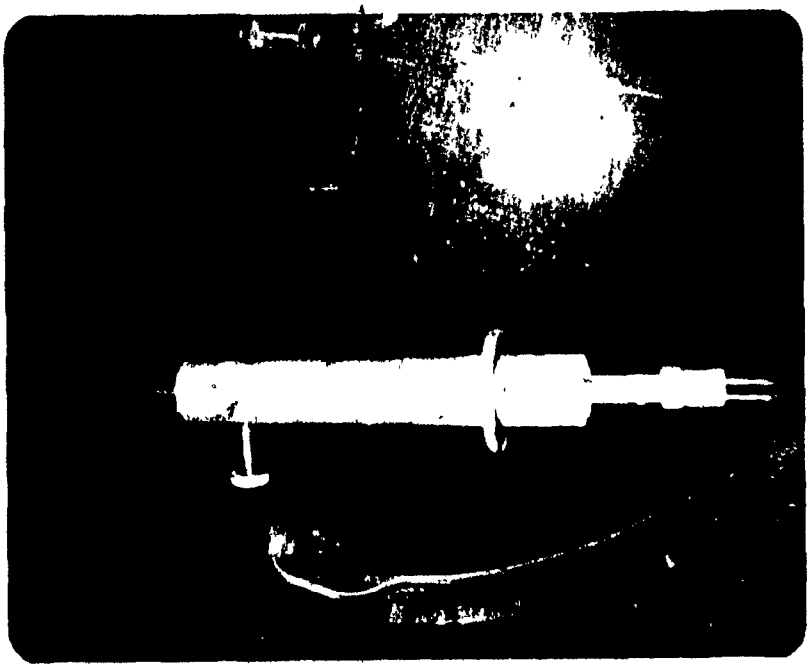

Figure 4.7 : Steel Temperature Probe showing 'DIP TIP' assembly attached at the right hand side in the photograph.

Figure 4.8 : Black Galvanized Steel Sample Cup with threaded steel stem.

Bismuth analyses of the samples were done on a Pye Unicam S.P. 190 atomic absorption spectrometer. Analyses for antimony and arsenic were done at the Noranda Research Center on a Perkin Elmer Model 306 Atomic Absorption Spectrometer.

SECTION 4.4 : PROCEDURE

4.4.1 : EXPERIMENTAL PREPARATION

The inside heights of the 'Hycor' alumina crucibles were reduced from 0.35 m to about 0.17 m by cutting with a diamond saw. This was done so that an easily handled 35 kg copper melt almost filled the crucible. The 'Tercod' crucibles required about 20 kg of white metal for filling.

The crucibles were placed in the furnace coils so that all but the top 0.01 m of the crucible was encircled by the coils. Refractory sand was tightly packed between the crucible and the furnace walls. The refractory sand was kept free from contamination by metal, dirt or refractory cement. This was especially important for the high temperature experiments, since contamination of the sand lowered its melting point. Nevertheless, some sintering

of the sand did occur when high temperatures were maintained for several hours. After packing was completed, refractory cement was placed on top of the sand to hold it in place.

The cathode copper was received in thin slabs measuring 0.015-0.025 m in thickness, 0.15 m wide and 0.45 m long. These slabs were cut into smaller pieces to facilitate packing into the crucible. This ensured that all of the copper being melted was inside the crucible and therefore directly affected by the induction field. Blister copper and white metal were in small enough pieces to charge as received. In all cases, the charge was not packed too tightly in order to avoid metal hold-up during melting. In experiments where the crucible could not accomodate the entire unmelted charge, material was kept aside for charging after initial melting was achieved.

With the crucible and initial charge in place, the chamber was sealed with vacuum grease at all locations, that is, chamber door, observation windows and porthole valves. The chamber was then evacuated to about 10 Pa by means of the mechanical pump and the blower. This lowered the oxygen potential to about 2 Pa. Commercial grade argon was introduced very slowly with the pump and blower

still on to further decrease the oxygen potential by flushing out residual oxygen for a few seconds. The pumps were then turned off and argon was admitted rapidly until the chamber pressure reached approximately one atmosphere. This procedure almost completely eliminated surface oxidation of the copper during melt down.

4.4.2 : MELT DOWN

Melting of the cathode copper and blister copper required between two and three hours. The white metal, placed inside the highly inductive 'Tercod' crucible, melted in about 30 minutes. Once the initial charge was molten, any remaining charge was added.

Some slag occurred on blister copper or oxidized copper melts. On the white metal melts, it was observed that silicon carbide from the 'Tercod' crucible formed a considerable slag. Any slag was removed manually at that point in time in all but two cases.

The furnace controls were manually adjusted until the desired temperature was attained. This was usually accomplished in less than 30 minutes.

4.4.3 : EVACUATION

The Stokes mechanical pump was restarted to evacuate the chamber to about 1500 Pa, at which time the Roots blower was also restarted. Pressure fell rapidly to about 150 Pa. When the melts were not doped, an initial sample was taken at that time to begin the experiment. Further reduction of pressure to a steady value in the range of 7-30 Pa required an additional 15 minutes. The final steady value depended upon how much air leaked through minor leaks in the system as well as the melt temperature. High melt temperatures tended to increase the final steady value of pressure. This was probably due to the larger amounts of vapour present at the higher temperatures. Some of this vapour might have entered the vacuum pumps instead of condensing beforehand, thus creating a greater load on the pumps.

Temperatures taken when the steady value of pressure was attained were found to be higher than before the pumps were turned on. Minor adjustments of the furnace controls corrected this increase within 10 minutes.

4.4.4 : ADDITIONS, SAMPLES AND CONTROL

The impurity or impurities were added (Figure 4.9) to the melts which required doping and an initial sample was taken. This marked the beginning of an experimental run. Samples were taken (Figure 4.10) without breaking vacuum. Splashing occurred when the sample cup was initially inserted into the melt. This was due to :

a) the presence of adsorbed gases on the sample cup and

b) the temperature difference between cup and melt.

Consequently, the cup was inserted into the melt three times before being removed from the chamber so that thermal and chemical equilibriums were reached between the cup and sample.

The time interval between samples was made progressively larger from 5 or 10 minutes at the beginning of the experiment to as much as 30 minutes at the end. Temperature and pressure readings were taken at the time of each sample. When the time interval between samples became greater than 10 minutes, readings were taken every 10 minutes.

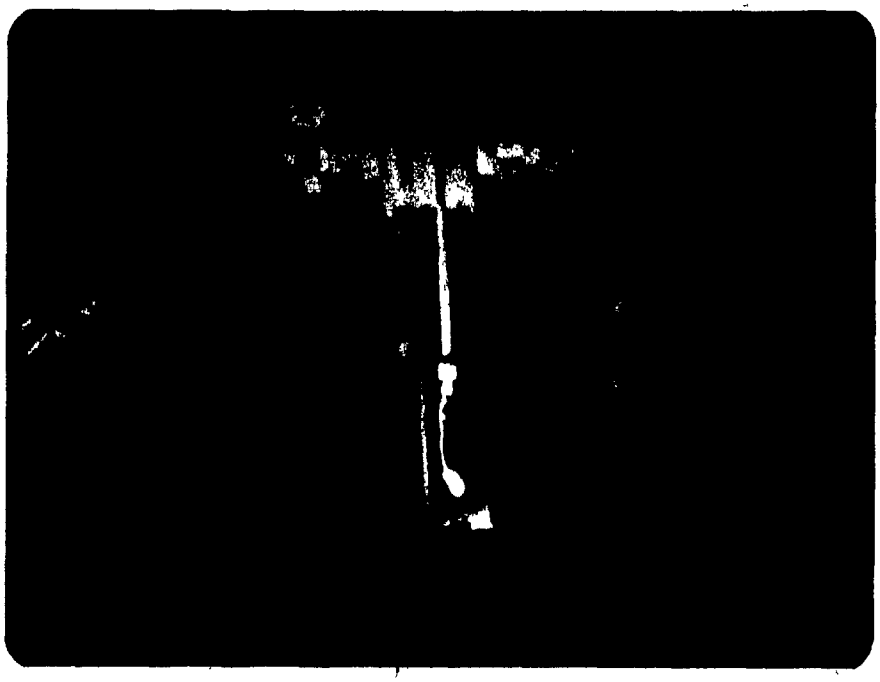

Figure 4.9 : Adding an impurity to the melt under vacuum

Figure 4.10 : Taking a sample of the melt under vacuum. Note the splashing of the melt for this, the initial insertion of the sample cup.

For temperature measurement, the 'DIP TIP' thermocouple was attached to a steel probe which was inserted into the chamber through the temperature port without breaking vacuum. The EMF rose to a steady value when the thermocouple junction entered the melt. The assembly was then immediately removed from the melt, thus preventing overheating of the cold junction located 0.05 m above the thermocouple bead. At least 5 minutes were required between temperature readings to allow the assembly to cool. The pressure reading was always taken before the temperature reading or sample, since the seals on the probes allowed some air to leak into the system.

4.4.5 : POST-EXPERIMENTAL PROCEDURE

The melt was allowed to cool in the crucible at the end of a day's experimentation and the remaining charge was weighed to estimate the weight loss due to evaporation, splashing and sampling. The average melt mass in each run was then estimated. This mass was converted to volume using the melt density, and a melt area to volume ratio was calculated. Finally, samples of the condensate at different locations in the chamber were scraped off and retained for analysis.

SECTION 4.5 : DISCUSSION OF EXPERIMENTAL TECHNIQUE AND PRECISION

The melt surface was kept extremely clean during all experiments except for two runs when a slag layer was desired and one when slag appeared after the chamber was evacuated despite manual slag cleaning prior to evacuation.

Splashing was negligible in all experiments in which cathode or blister copper was used for charge material, except for minor amounts which occurred when samples were taken. In experiments using white metal, sulphur dioxide bubbling caused excessive splashing. The splashing was reduced to a low level by keeping the temperature low and the pressure high.

Condensate refluxing was kept to a minimum by ensuring that the melt almost entirely filled the crucible. This prevented the phenomenom of evaporating species condensing on the crucible free wall, then being washed back into the melt by melt splashing.

Chamber pressure was controlled to ± 10 % during any low pressure experiment and to ± 20 % during the high pressure experiments.

Melt temperature was controlled within 1-2 %. Best temperature control was attained after experimentation had proceeded for at least one hour.

Good visual observation through the several chamber windows helped to ensure good sampling and temperature measurement techniques, as well as providing a good visual understanding of evaporation under vacuum.

The precision of the chemical analysis techniques were very good. Preparation techniques (i.e. dissolution and dilution) were reproducible within 10 %, while precision of atomic absorption analysis was within 5 %.

SECTION 4.6 : SUMMARY

In summary, the experiments were aimed at measuring elimination rates of bismuth, antimony and arsenic in doped copper, blister copper and white metal. The effects of melt temperature, chamber pressure, area to volume ratio, initial impurity content and the presence of a slag layer were examined. These variables were well controlled.

CHAPTER FIVE

RESULTS

SECTION 5.1 : CONDITIONS

The parameters which were controlled and measured were :

a) melt mass

b) melt temperature

c) chamber pressure

d) area to volume ratio (A/V)

and

e) elements investigated

These conditions are summarized for each experiment in Tables 5.1 to 5.3 which tabulate this data for Part A (doped copper), Part B (blister copper) and Part C (white metal) experiments, respectively.

TABLE 5.1 : Summary of Conditions for Doped Copper Experiments; A-1 to A-17

Test #	Melt Mass (kg)	Temperature (K)	Pressure (Pa)	A/V (1/m)	Duration of Test (min)	Elements Tested
A-1	35.0	1600-1650	10-12	6.8	38	Bi
A-2	30.4	1625-1640	10-12	7.8	33	Bi
A-3	27.4	1625-1645	11-12	8.6	21	Bi
A-4	29.0	1590-1600	12-16	8.2	74	Bi
A-5	24.4	1605-1610	9-11	9.7	72	Bi,Sb
A-6	35.0	1510-1550	12-16	6.8	72	Bi
A-7	29.0	1500-1510	11	8.3	51	Bi,Sb
A-8	22.9	1500	7	10.4	33	Bi,Sb
A-9	35.0	1650-1730	31-34	6.7	69	Bi
A-10*	28.9	1740	32-34	8.1	33	Bi,Sb
A-11*	25.9	1740-1745	27-30	9.0	44	Bi,Sb,As
A-12*	22.9	1740-1745	31-39	10.2	30	Bi,Sb,As
A-13	34.0	1620-1670	88-163	6.9	85	Bi
A-14	29.6	1600-1615	82-109	8.0	80	Bi,Sb
A-15	25.1	1615-1635	95-122	9.4	50	Bi,Sb
A-16**	34.1	1730-1790	13-15	6.9	51	Bi
A-17**	31.2	1710-1770	16-20	7.5	40	Bi,Sb

* - the melts in these experiments contained approximately 1 % Fe. This was caused by a steel sample cup which fell into the melt

** - a slag layer was maintained in these experiments

TABLE 5.2 : Summary of Conditions for Blister Copper Experiments; B-1 & B-2

Test #	Melt Mass (kg)	Temperature (K)	Pressure (Pa)	A/V (1/m)	Duration of Test (min)	Elements Tested
B-1	35.0	1615-1670	9-13	6.8	77	Bi
B-2*	35.0	1685-1775	20-28	6.7	50	Bi,Sb,As Se,Te

* - some slag (covering approximately one third of the melt surface area) was present

TABLE 5.3 : Summary of Conditions for White Metal (Cu_2S) Experiments; C-1 & C-2

Test #	Melt Mass (kg)	Temperature (K)	Pressure (Pa)	A/V (1/m)	Duration of Test (min)	Elements Tested
C-1	20.0	1510-1545	107-267	6.4	90	Bi
C-2	19.0	1540-1550	93-147	6.7	70	Bi

SECTION 5.2 : RESULTS

The results of this study are the changes in impurity content with time. This was evaluated by determining :

i) percent of initial content eliminated in 1 hour*

and

ii) overall refining rate coefficient K**

Tables 5.4 to 5.6 tabulate this data for bismuth, antimony and arsenic in Part A experiments. Table 5.7 tabulates data for impurities in Part B experiments. Table 5.8 tabulates data for bismuth in Part C experiments.

---

* - when experimental runs were less than 1 hour, this value was determined by extrapolation.

** - $K = \frac{1}{A/V\ t} \ln\left(\frac{\text{weight \% initial}}{\text{weight \% final}}\right)$ when only initial and final analyses were determined

or

$K = -\frac{2.303}{A/V} \cdot$ slope of 'log % i versus time' plot

The correlation coefficients of these slopes were :

≈ 0.99 when initial impurity concentration was about 0.1 weight %

≈ 0.96 when initial impurity concentration was about 0.01 weight %

≈ 0.89 when initial impurity concentration was about 0.002 weight %

TABLE 5.4 : Summary of Results for Bismuth Removal from Doped Copper

Test #	Initial Wt.% Bi	Final Wt.% Bi	Overall K_{Bi} (10^{-5} m s^{-1})	% of Initial Content Refined in One Hour
A-1	0.072	0.022	7.6	84.3
A-2	0.072	0.018	8.8	90.5
A-3	0.088	0.045	6.2	85.7
A-4	0.086	0.017	4.4	75.4
A-5	0.012	0.004	2.2	56.1
A-6	0.098	0.033	3.9	62.4
A-7	0.014	0.008	2.0	48.8
A-8	0.078	0.054	1.6	48.4
A-9	0.057	0.007	7.4	82.2
A-10	0.003	0.001	5.0	77.3
A-11	0.002	0.0005	6.1	87.7
A-12	0.063	0.019	6.4	90.9
A-13	0.046	0.021	1.9	46.6
A-14	0.012	0.006	3.0	57.5
A-15	0.055	0.023	3.2	66.5
A-16	0.124	0.055	0.6	13.0
A-17	0.052	0.047	0.6	14.1

TABLE 5.5 : Summary of Results for Antimony Removal from Doped Copper

Test #	Initial Wt.% Sb	Final Wt.% Sb	Overall K_{Sb} (10^{-5} m s^{-1})	% of Initial Content Refined in One Hour
A-5	0.066	0.027	2.4	59.6
A-7	0.093	0.076	0.8	21.0
A-8	0.076	0.045	2.6	61.5
A-10	0.050	0.082	-	--
A-11	0.078	0.074	0.2	6.9
A-12	0.068	0.069	-	--
A-14	0.058	0.054	0.3	6.9
A-15	0.047	0.044	0.2	7.8
A-17	0.089	0.084	0.3	8.5

TABLE 5.6 : Summary of Results for Arsenic Removal from Doped Copper

Test #	Initial Wt.% As	Final Wt.% As	Overall K_{As} (10^{-5} m s^{-1})	% of Initial Content Refined in One Hour
A-11	0.089	0.039	3.5	67.5
A-12	0.036	0.025	2.0	51.7

TABLE 5.7 : Summary of Results for Impurity Removal from Blister Copper

Test #	Element	Initial Wt. %	Final Wt. %	Overall K (10^{-5} m s^{-1})	% of Initial Content Refined in One Hour
B-1	Bi	0.0026	0.0011	3.5	54.4
B-2	Bi	0.0028	0.0017	2.2	41.5
B-2	Sb	<0.001	<0.001	-	--
B-2	As	<0.002	<0.002	-	--
B-2	Se	0.035	0.035	0	0
B-2	Te	0.0064	0.0064	0	0

TABLE 5.8 : Summary of Results for Bismuth Removal from White Metal (Cu_2S)

Test #	Initial Wt.% Bi	Final Wt.% Bi	Overall K_{Bi} (10^{-5} m s^{-1})	% of Initial Content Refined in One Hour
C-1	0.081	0.034	2.6	45.0
C-2	0.106	0.056	2.7	47.9

Each experiment is described in detail in the figures that follow. Included in each figure are :

a) experimental conditions

b) table of impurity content as a function of vacuum exposure time

c) plot of log(wt.% impurity) versus vacuum exposure time

d) overall refining rate coefficient, K

and

e) percent of initial content refined in 1 hour.

TEST NUMBER	:	A-1
TYPE OF MELT	:	Doped Cathode Copper
MELT TEMPERATURE	:	1625 ± 25 K
CHAMBER PRESSURE	:	11.0 ± 1.0 Pa
AREA TO VOLUME	:	6.8 ± 0.4 m^{-1}
ELEMENT TESTED	:	Bi

TIME (SEC)	Wt.% Bi
0	0.072
600	0.052
1140	0.040
1560	0.034
2280	0.022

		Bi
K (10^{-5} m s^{-1})	:	7.6
% of initial content refined in 1 hour.	:	84.3

Figure 5.1 : Experimental Conditions and Results of Bismuth Removal in Test A-1

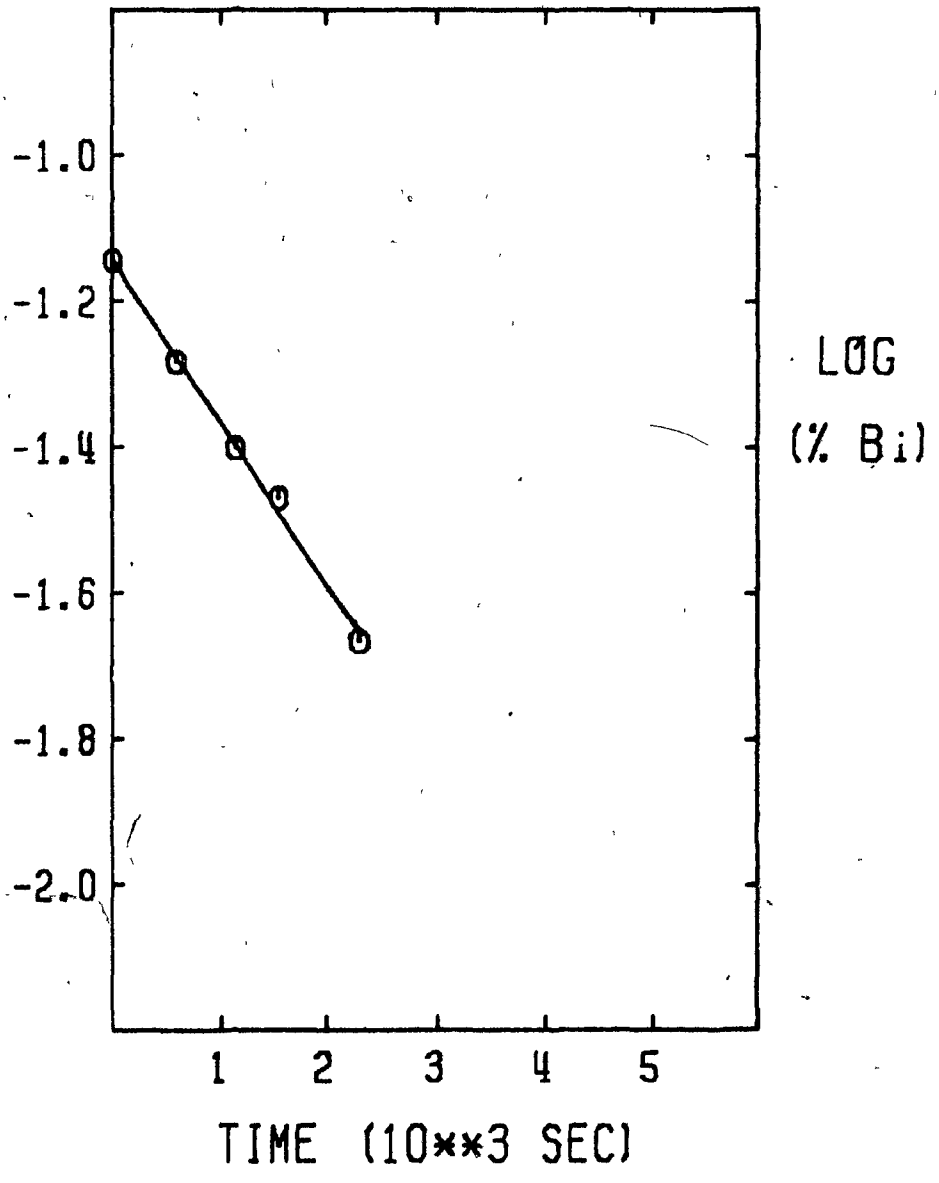

Figure 5.1a : Plot of Bismuth Removal in Test A-1

TEST NUMBER	:	A-2
TYPE OF MELT	:	Doped Cathode Copper
MELT TEMPERATURE	:	1633 ± 8 K
CHAMBER PRESSURE	:	11.0 ± 1.0 Pa
AREA TO VOLUME	:	7.8 ± 0.4 m^{-1}
ELEMENT TESTED	:	Bi

TIME (SEC)	Wt.% Bi
0	0.072
240	0.066
540	0.060
960	0.047
1260	0.040
1980	0.018

		Bi
K (10^{-5} m s^{-1})	:	8.8
% of initial content refined in 1 hour	:	90.5

Figure 5.2 : Experimental Conditions and Results of Bismuth Removal in Test A-2

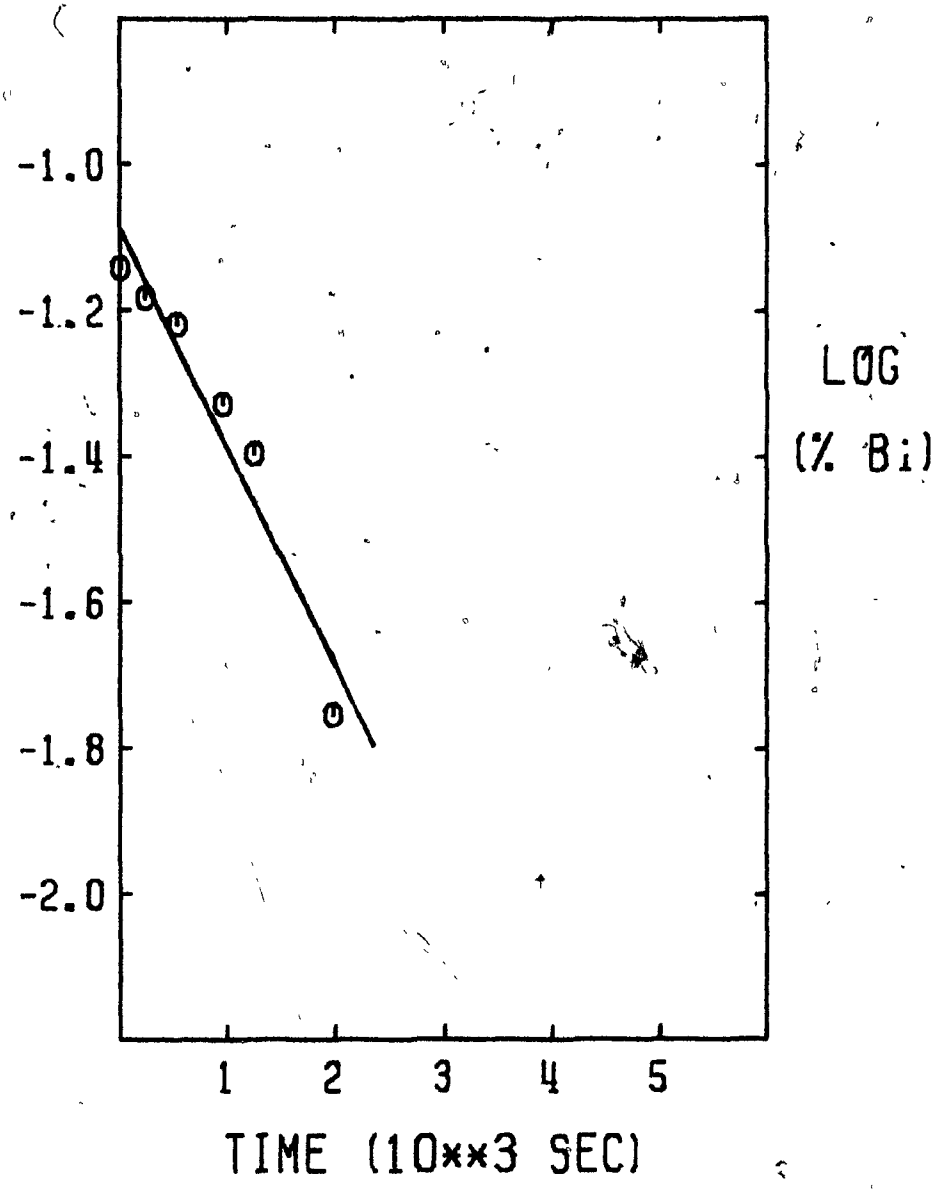

Figure 5.2a : Plot of Bismuth Removal in Test A-2

TEST NUMBER	:	A-3
TYPE OF MELT	:	Doped Cathode Copper
MELT TEMPERATURE	:	1635 ± 10 K
CHAMBER PRESSURE	:	11.5 ± 0.5 Pa
AREA TO VOLUME	:	8.6 ± 0.4 m^{-1}
ELEMENT TESTED	:	Bi

TIME (SEC)	Wt.% Bi
0	0.088
420	0.068
1260	0.045

		Bi
K (10^{-5} m s^{-1})	:	6.2
% of initial content refined in 1 hour	:	85.7

Figure 5.3 : Experimental Conditions and Results of Bismuth Removal in Test A-3

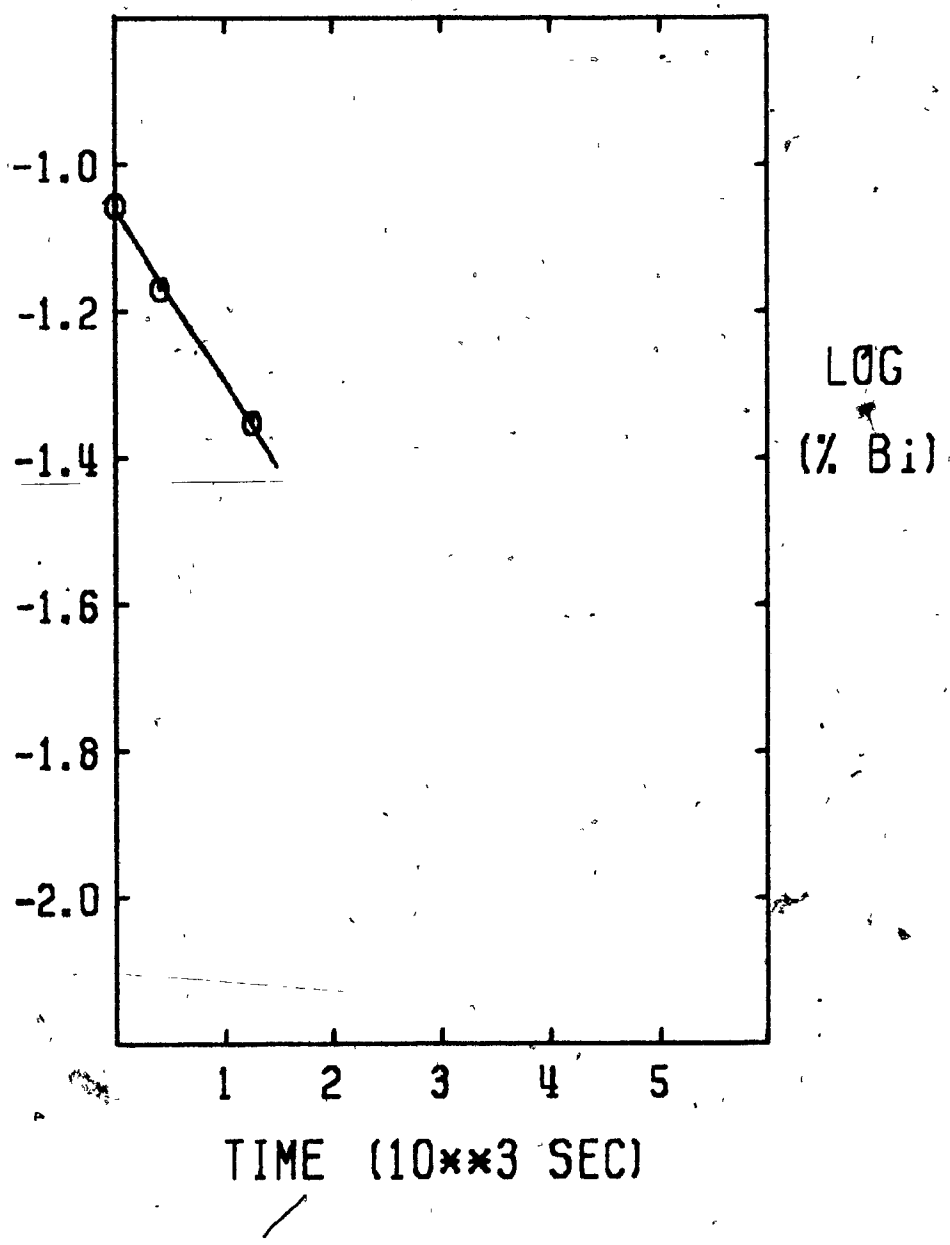

Figure 5.3a : Plot of Bismuth Removal in Test A-3

TEST NUMBER	:	A-4
TYPE OF MELT	:	Doped Blister Copper
MELT TEMPERATURE	:	1595 ± 5 K
CHAMBER PRESSURE	:	14.0 ± 2.0 Pa
AREA TO VOLUME	:	8.2 ± 0.4 m^{-1}
ELEMENT TESTED	:	Bi

TIME (SEC)	Wt.% Bi
0	0.086
180	0.075
480	0.060
1740	0.039
2640	0.028
4440	0.017

		Bi
K (10^{-5} m s^{-1})	:	4.4
% of initial content refined in 1 hour	:	75.4

Figure 5.4 : Experimental Conditions and Results of Bismuth Removal in Test A-4

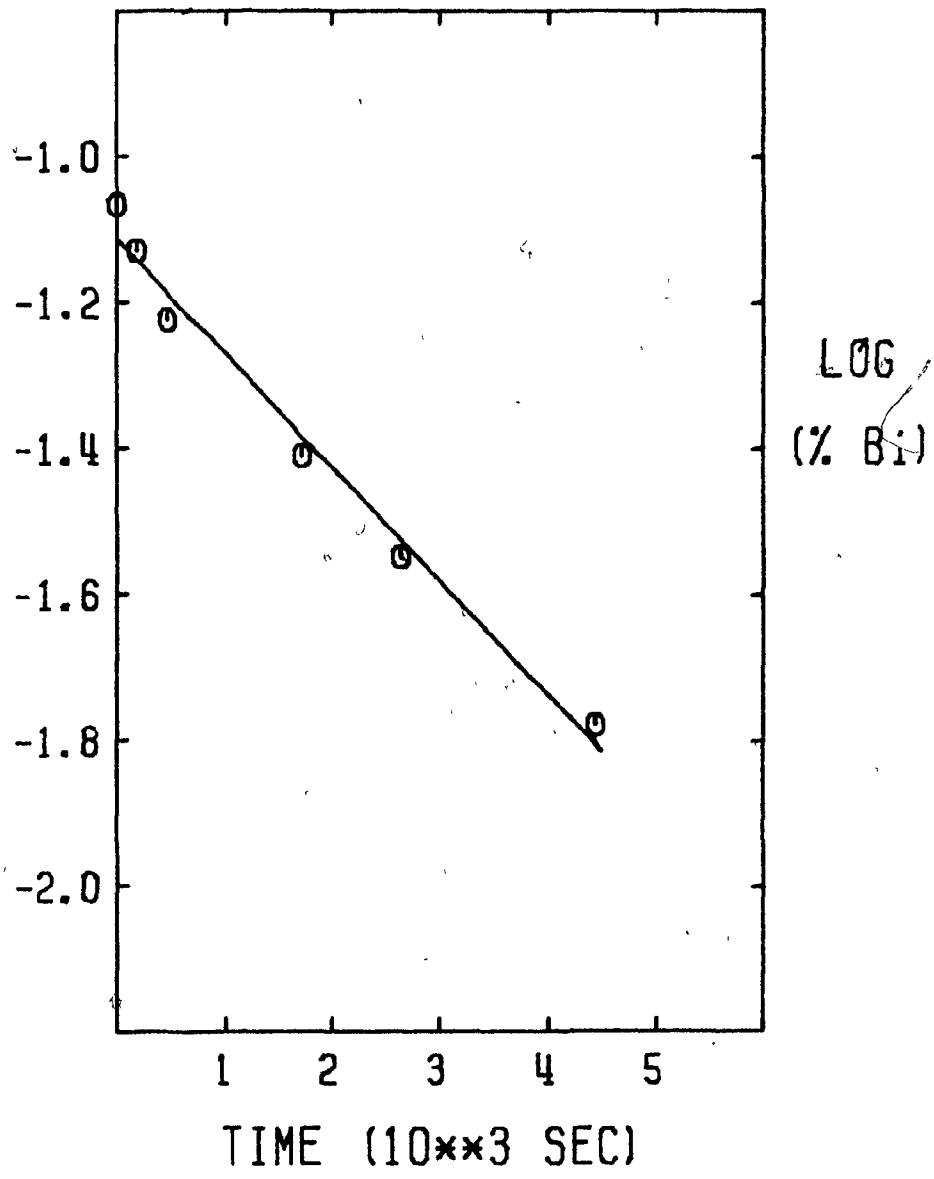

Figure 5.4a : Plot of Bismuth Removal in Test A-4

TEST NUMBER	:	A-5
TYPE OF MELT	:	Doped Blister Copper
MELT TEMPERATURE	:	1608 ± 5 K
CHAMBER PRESSURE	:	10.0 ± 1.0 Pa
AREA TO VOLUME	:	9.7 ± 0.4 m^{-1}
ELEMENTS TESTED	:	Bi Sb

TIME (SEC)	Wt.% Bi	Wt.% Sb
0	0.012	0.066
480	0.010	0.058
1860	0.007	0.034
3120	0.007	0.026
4320	0.004	0.027

		Bi	Sb
K (10^{-5} m s^{-1})	:	2.2	2.4
% of initial content refined in 1 hour	:	56.1	59.6

Figure 5.5 : Experimental Conditions and Results of Bismuth and Antimony Removal in Test A-5

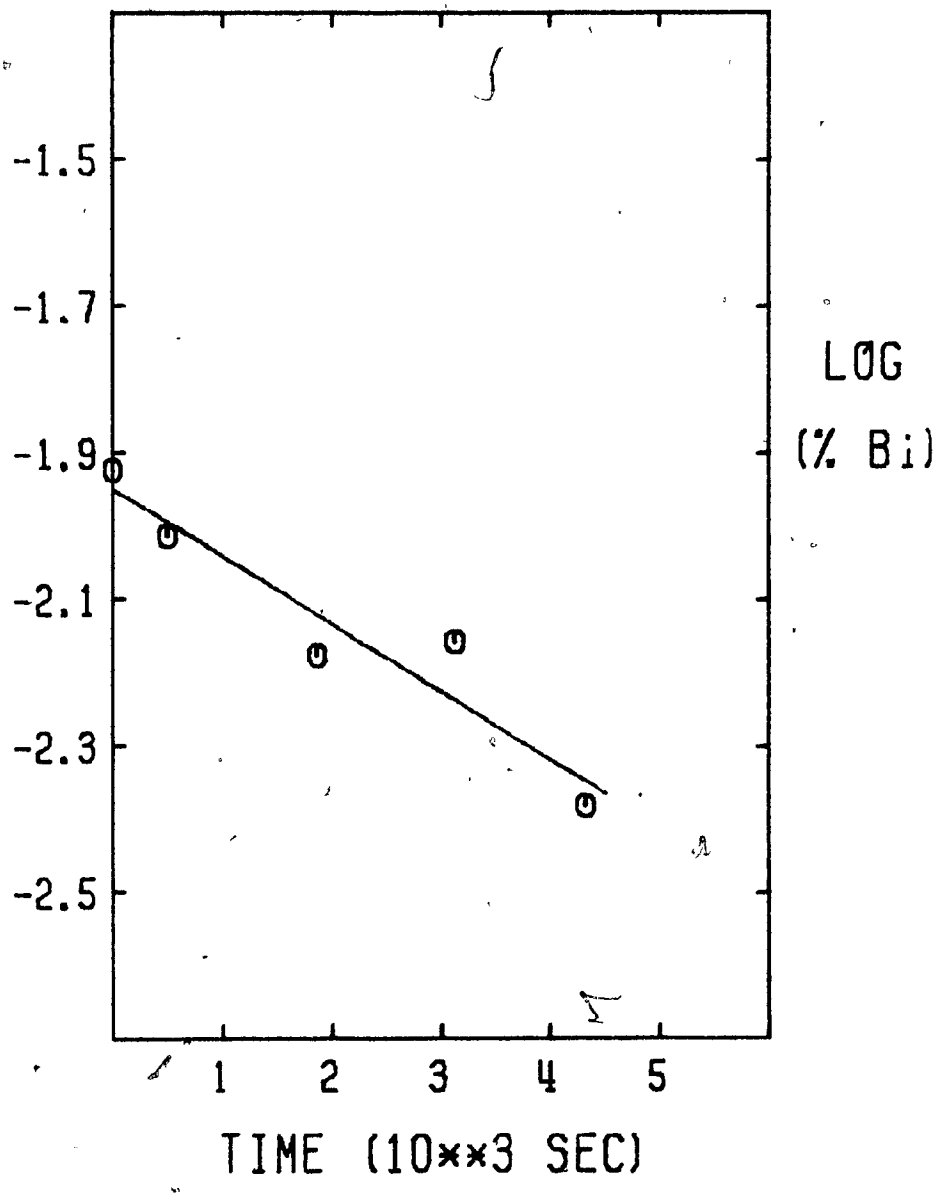

Figure 5.5a : Plot of Bismuth Removal in Test A-5

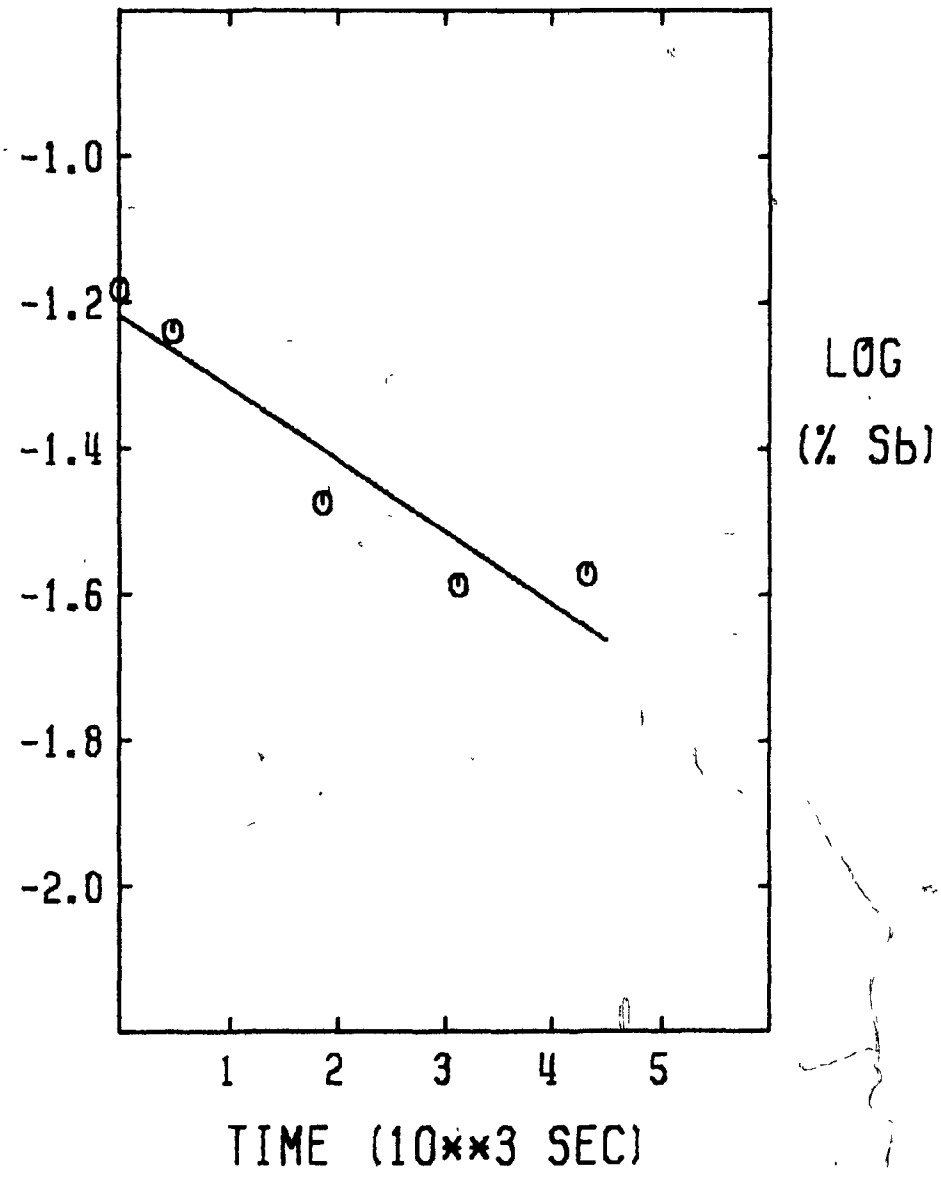

Figure 5.5b : Plot of Antimony Removal in Test A-5

TEST NUMBER	:	A-6
TYPE OF MELT	:	Doped Cathode Copper
MELT TEMPERATURE	:	1530 ± 20 K
CHAMBER PRESSURE	:	14.0 ± 2.0 Pa
AREA TO VOLUME	:	6.8 ± 0.4 m^{-1}
ELEMENT TESTED	:	Bi

TIME (SEC)	Wt.% Bi
0	0.098
720	0.079
1500	0.065
2760	0.039
4320	0.033

		Bi
K (10^{-5} m s^{-1})	:	3.9
% of initial content refined in 1 hour	:	62.4

Figure 5.6 : Experimental Conditions and Results of Bismuth Removal in Test A-6

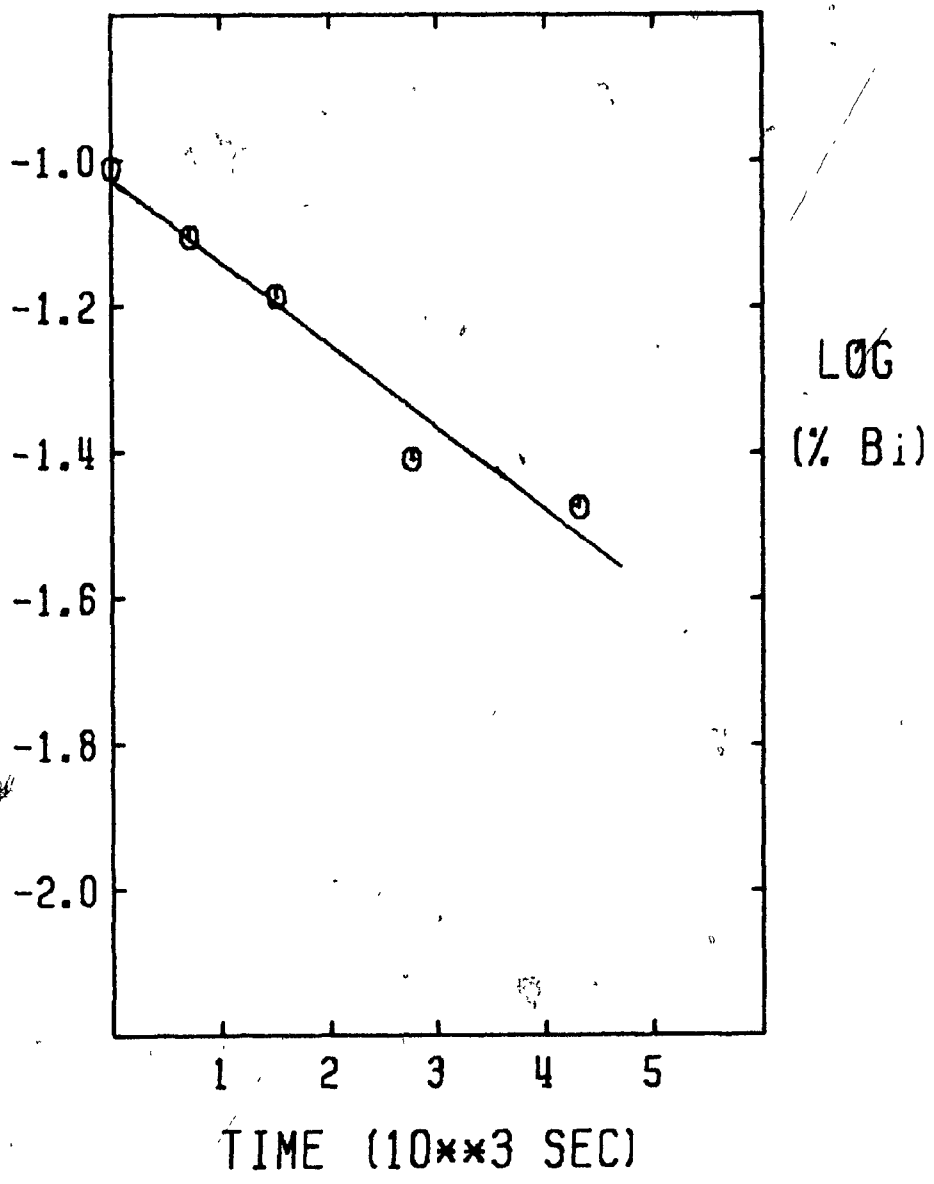

Figure 5.6a : Plot of Bismuth Removal in Test A-6

TEST NUMBER	:	A-7
TYPE OF MELT	:	Doped Cathode Copper
MELT TEMPERATURE	:	1505 ± 5 K
CHAMBER PRESSURE	:	11.0 ± 0.5 Pa
AREA TO VOLUME	:	8.3 ± 0.4 m^{-1}
ELEMENT TESTED	:	Bi Sb

TIME (SEC)	Wt.% Bi	Wt.% Sb
0	0.014	0.093
600	0.011	-
1860	0.010	-
3060	0.008	0.076

		Bi	Sb
K (10^{-5} m s^{-1})	:	2.0	0.8
% of initial content refined in 1 hour	:	48.8	21.0

Figure 5.7 : Experimental Conditions and Results of Bismuth and Antimony Removal in Test A-7

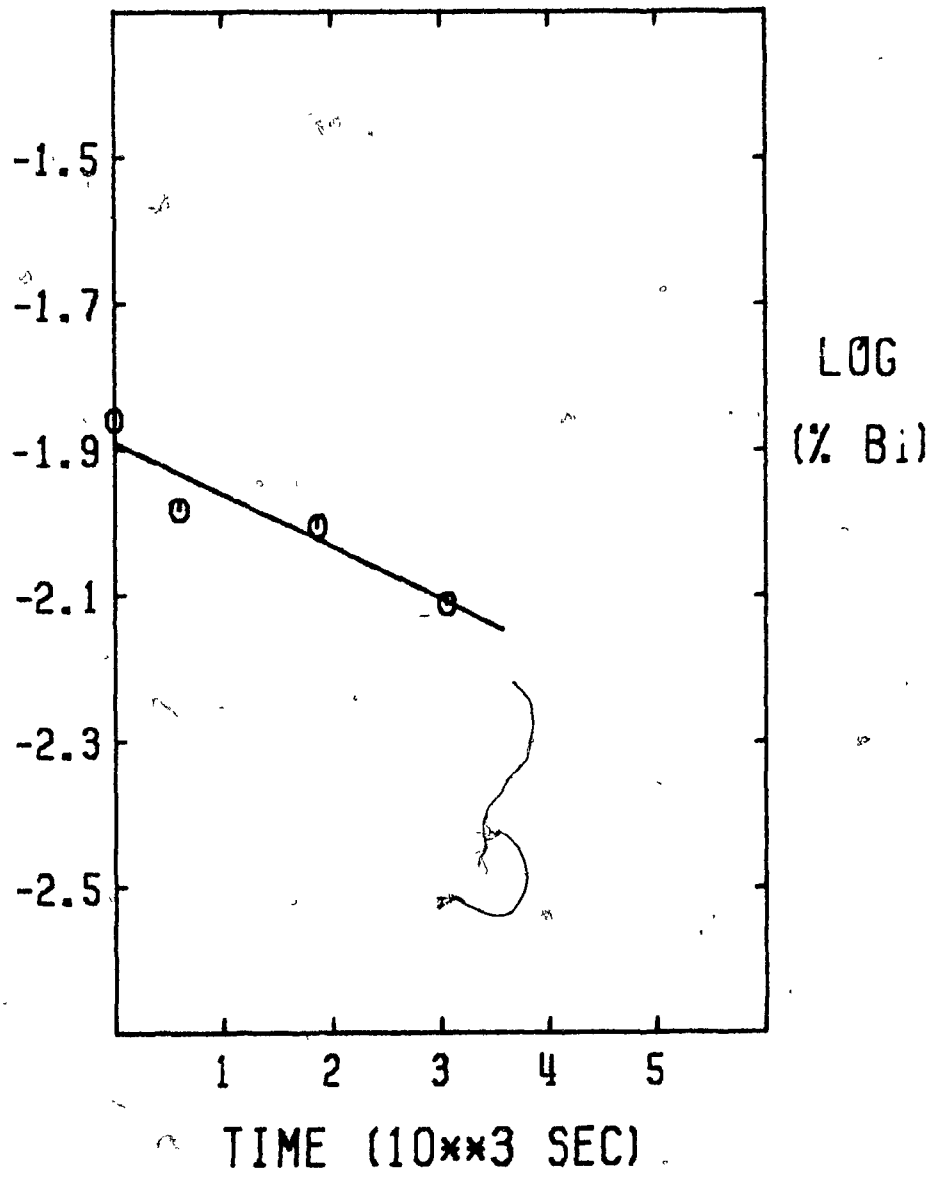

Figure 5.7a : Plot of Bismuth Removal in Test A-7

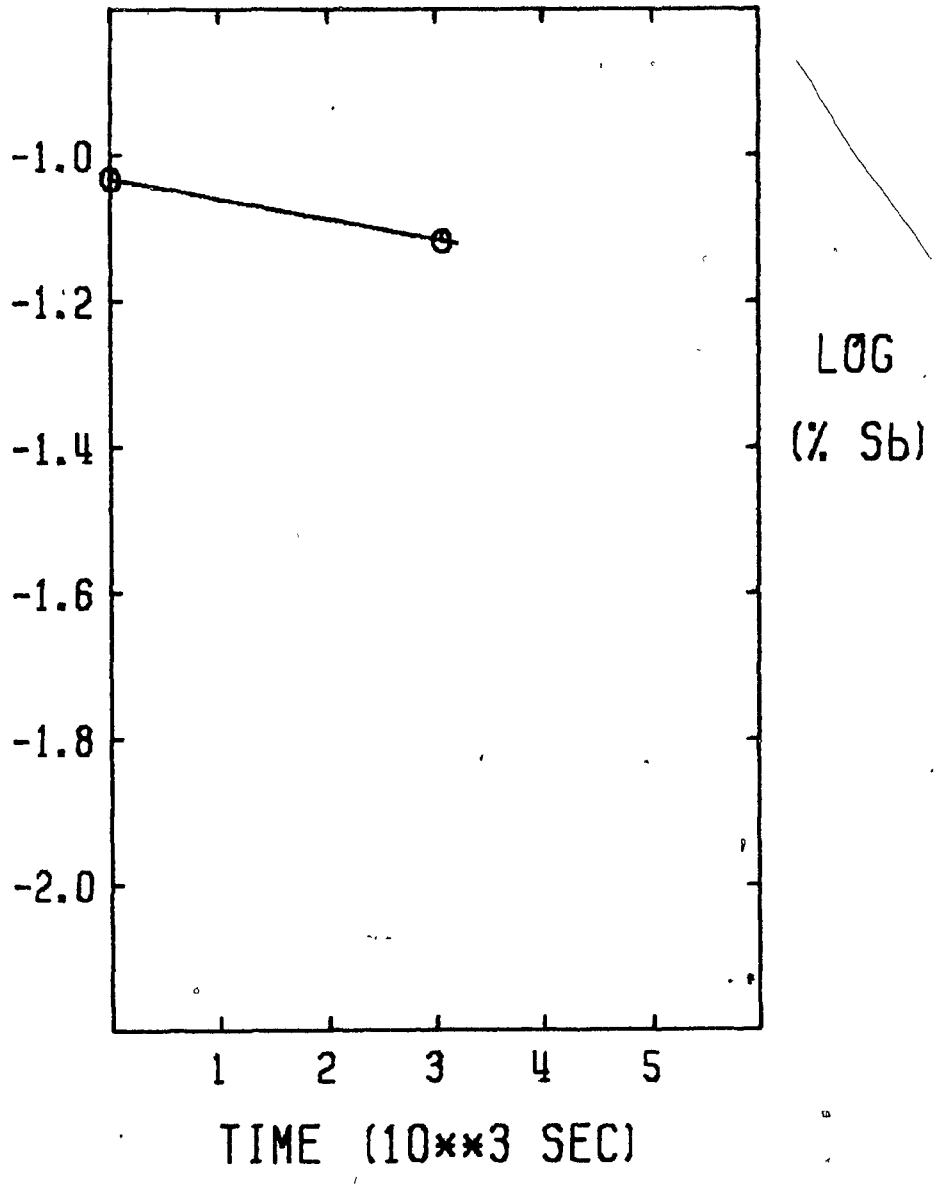

Figure 5.7b : Plot of Antimony Removal in Test A-7

TEST NUMBER	:	A-8
TYPE OF MELT	:	Doped Cathode Copper
MELT TEMPERATURE	:	1500 ± 5 K
CHAMBER PRESSURE	:	7.0 ± 0.5 Pa
AREA TO VOLUME	:	10.4 ± 0.4 m^{-1}
ELEMENTS TESTED	:	Bi Sb

TIME (SEC)	Wt.% Bi	Wt.% Sb
0	0.078	0.076
600	0.061	-
1980	0.054	0.045

		Bi	Sb
K (10^{-5} m s^{-1})	:	1.6	2.6
% of initial content refined in 1 hour	:	48.4	61.5

Figure 5.8 : Experimental Conditions and Results of Bismuth and Antimony Removal in Test A-8

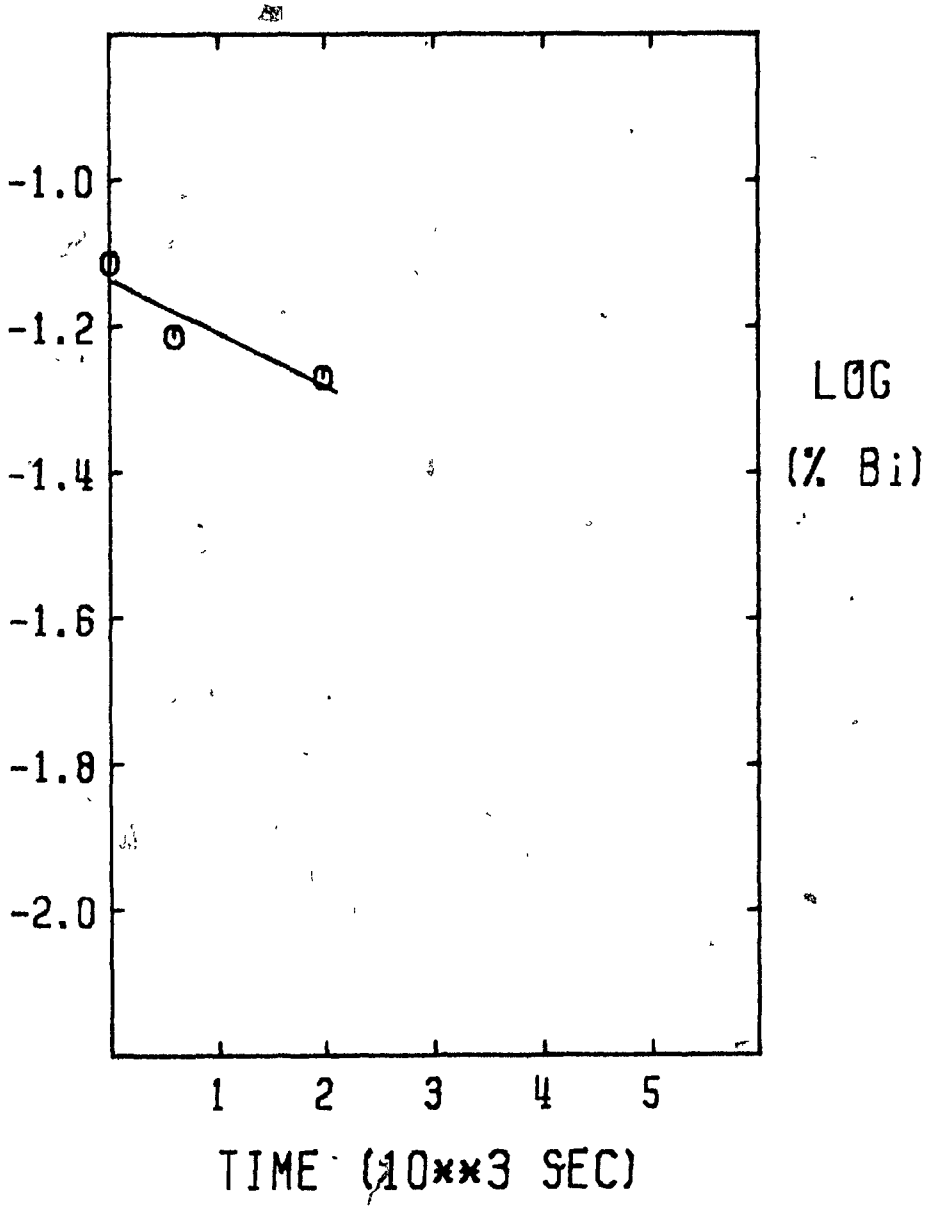

Figure 5.8a : Plot of Bismuth Removal in Test A-8

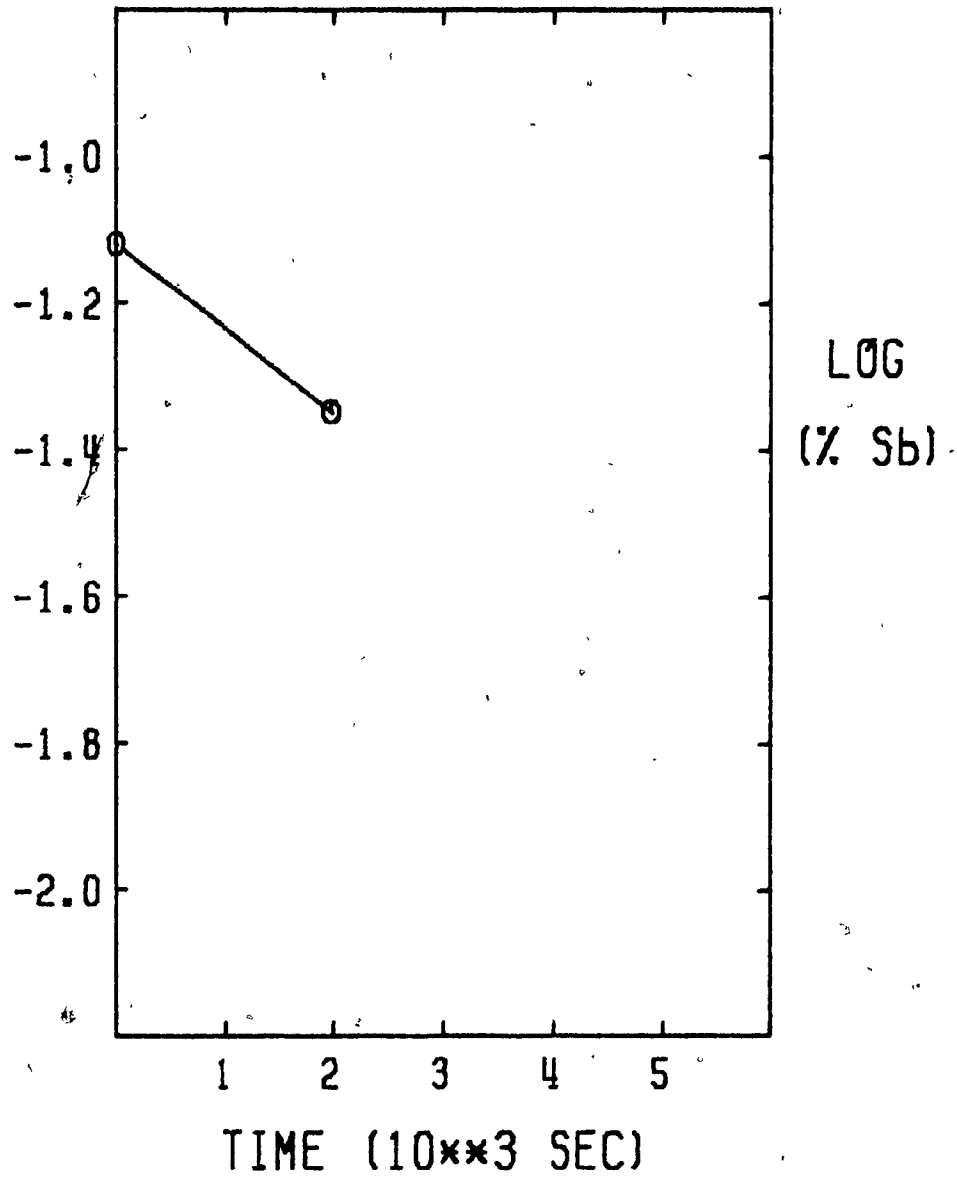

Figure 5.8b : Plot of Antimony Removal in Test A-8

TEST NUMBER	:	A-9
TYPE OF MELT	:	Doped Cathode Copper
MELT TEMPERATURE	:	1690 ± 40 K
CHAMBER PRESSURE	:	32.5 ± 1.5 Pa
AREA TO VOLUME	:	6.7 ± 0.4 m^{-1}
ELEMENT TESTED	:	Bi

TIME (SEC)	Wt.% Bi
0	0.057
480	0.046
1500	0.031
2400	0.021
4140	0.007

		Bi
K (10^{-5} m s^{-1})	:	7.4
% of initial content refined in 1 hour	:	82.2

Figure 5.9 : Experimental Conditions and Results of Bismuth Removal in Test A-9

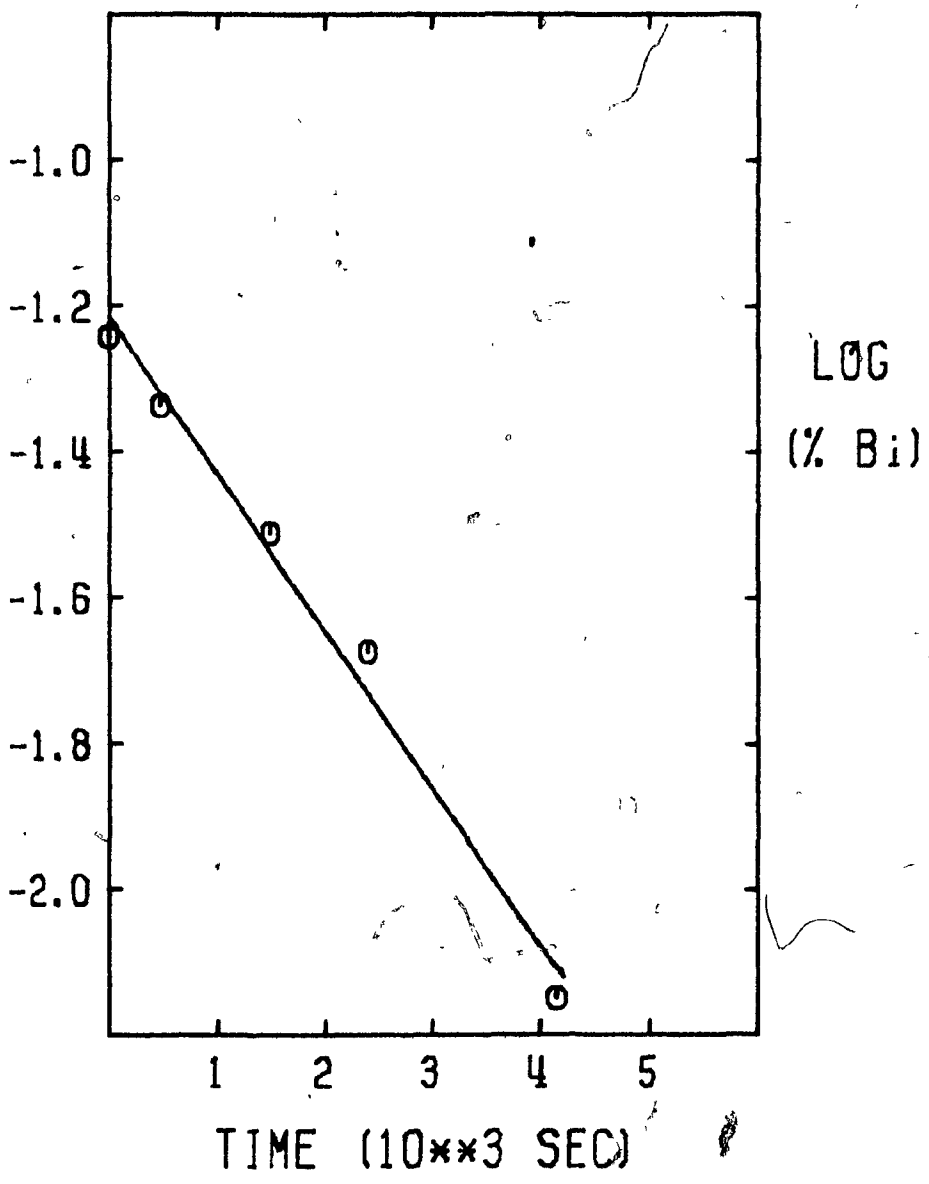

Figure 5.9a : Plot of Bismuth Removal in Test A-9

TEST NUMBER	:	A-10*
TYPE OF MELT	:	Doped Cathode Copper
MELT TEMPERATURE	:	1740 ± 5 K
CHAMBER PRESSURE	:	33.0 ± 1.0 Pa
AREA TO VOLUME	:	8.1 ± 0.4 m^{-1}
ELEMENTS TESTED	:	Bi Sb

TIME (SEC)	Wt.% Bi	Wt.% Sb**
0	0.003	0.050
1020	0.002	-
1980	0.001	-
2700	-	0.082

		Bi	Sb
K (10^{-5} m s^{-1})	:	5.0	-
% of initial content refined in 1 hour	:	77.3	-

* - About 1 % Fe is present in the melt for Test #'s A-10, A-11 & A-12; this resulted from a steel sample cup which fell into the melt and appears to have affected adversely the removal of Sb.

** - It is believed that the low value of Wt.% Sb for the initial sample was due to insufficient time between when the Sb was added and when the sample was taken

Figure 5.10 : Experimental Conditions and Results of Bismuth and Antimony Removal in Test A-10

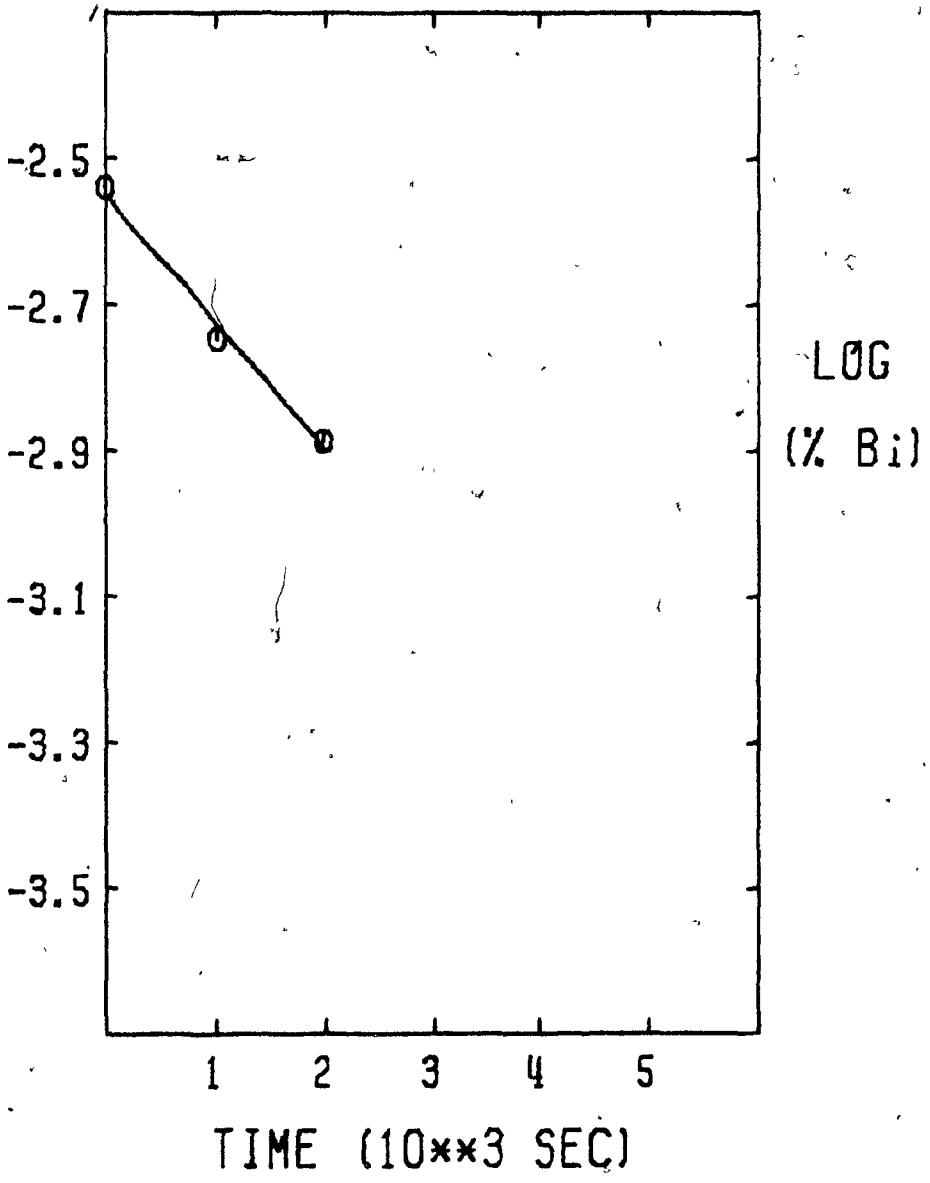

Figure 5.10a : Plot of Bismuth Removal in Test A-10

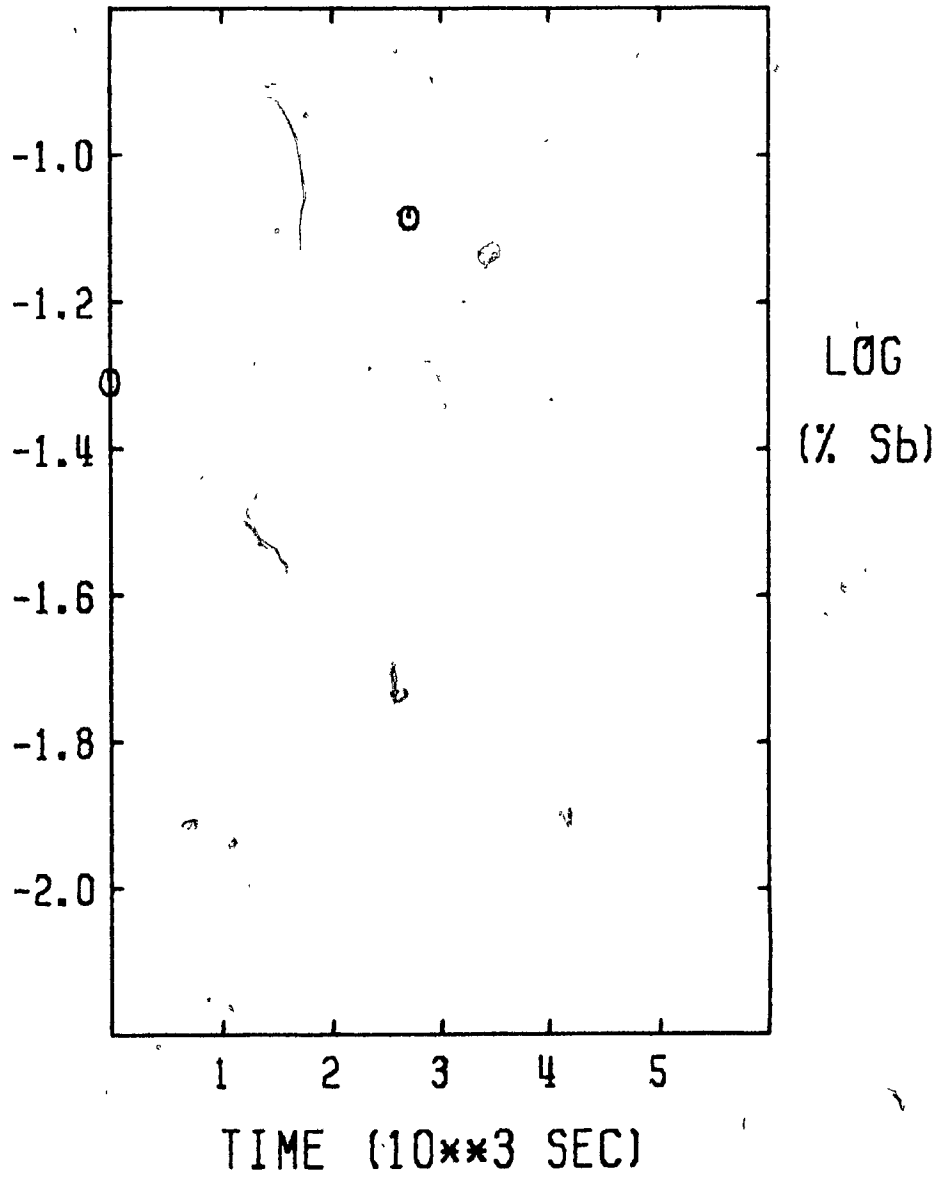

Figure 5.10b : Plot of Antimony Removal in Test A-10

TEST NUMBER	:	A-11*
TYPE OF MELT	:	Doped Cathode Copper
MELT TEMPERATURE	:	1743 ± 5 K
CHAMBER PRESSURE	:	28.5 ± 1.5 Pa
AREA TO VOLUME	:	9.0 ± 0.4 m^{-1}
ELEMENTS TESTED	:	Bi Sb As

TIME (SEC)	Wt.% Bi†	Wt.% Sb	Wt.% As
0	0.0023	0.078	0.089
660	0.0012	-	-
1680	0.0008	-	-
2640	0.0005	0.074	0.039

		Bi	Sb	As
K (10^{-5} m s^{-1})	:	6.1	0.2	3.5
% of initial content refined in 1 hour	:	87.7	6.9	67.5

* - melt contained about 1 % Fe (see Figure 5.10)

† - due to limits in analytical precision, the uncertainty of the fourth decimal place is large

Figure 5.11 : Experimental Conditions and Results of Bismuth, Antimony and Arsenic Removal in Test A-11

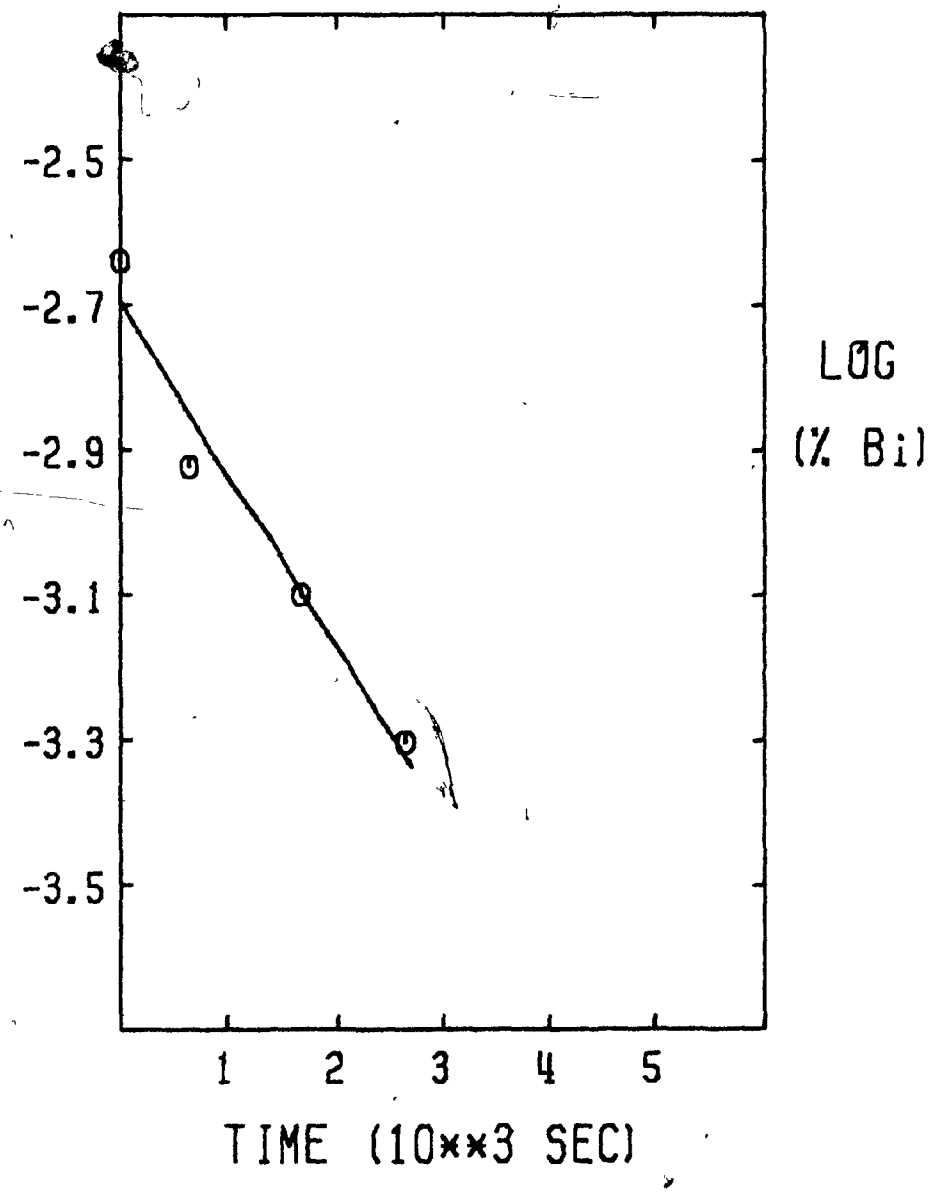

Figure 5.11a : Plot of Bismuth Removal in Test A-11

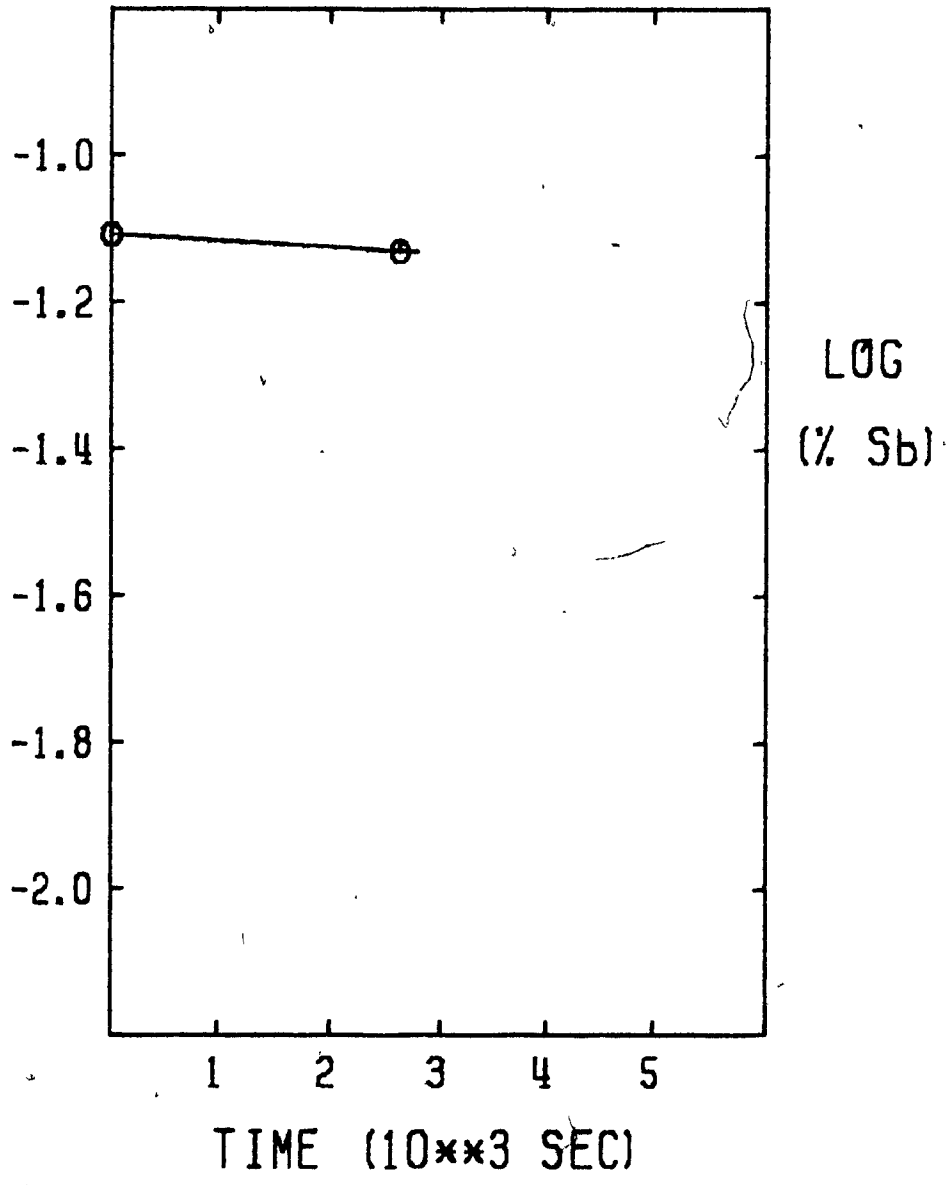

Figure 5.11b : Plot of Antimony Removal in Test A-11

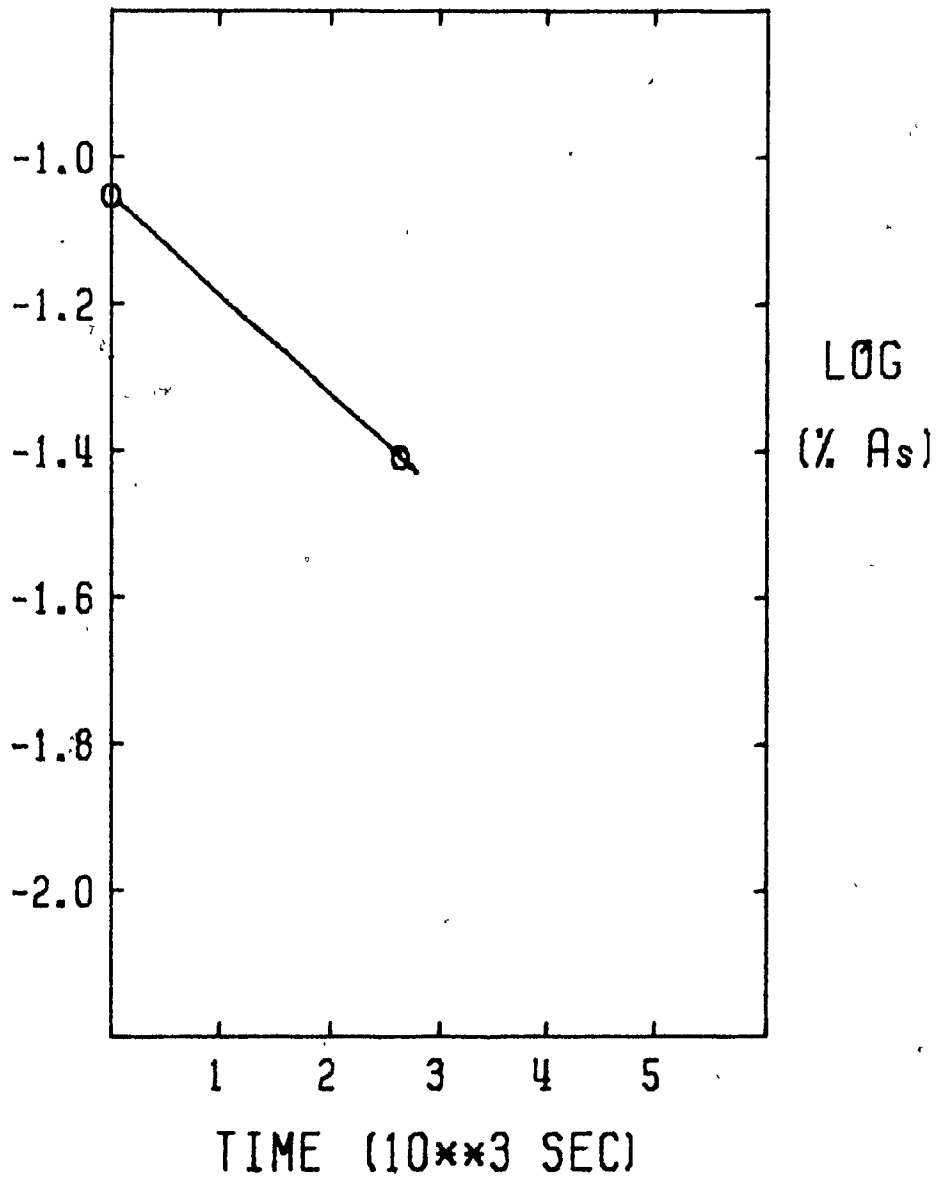

Figure 5.11c : Plot of Arsenic Removal in Test A-11

TEST NUMBER	:	A-12*
TYPE OF MELT	:	Doped Cathode Copper
MELT TEMPERATURE	:	1743 ± 5 K
CHAMBER PRESSURE	:	35.0 ± 4.0 Pa
AREA TO VOLUME	:	10.2 ± 0.4 m^{-1}
ELEMENTS TESTED	:	Bi Sb As

TIME (SEC)	Wt.% Bi	Wt.% Sb	Wt.% As
0	0.063	0.068	0.036
600	0.036	-	-
1800	0.019	0.069	0.025

		Bi	Sb	As
K (10^{-5} m s^{-1})	:	6.4	-	2.0
% of initial content refined in 1 hour	:	90.9	-	51.7

* - melt contained about 1 % Fe (see Figure 5.10)

Figure 5.12 : Experimental Conditions and Results of Bismuth, Antimony and Arsenic Removal in Test A-12

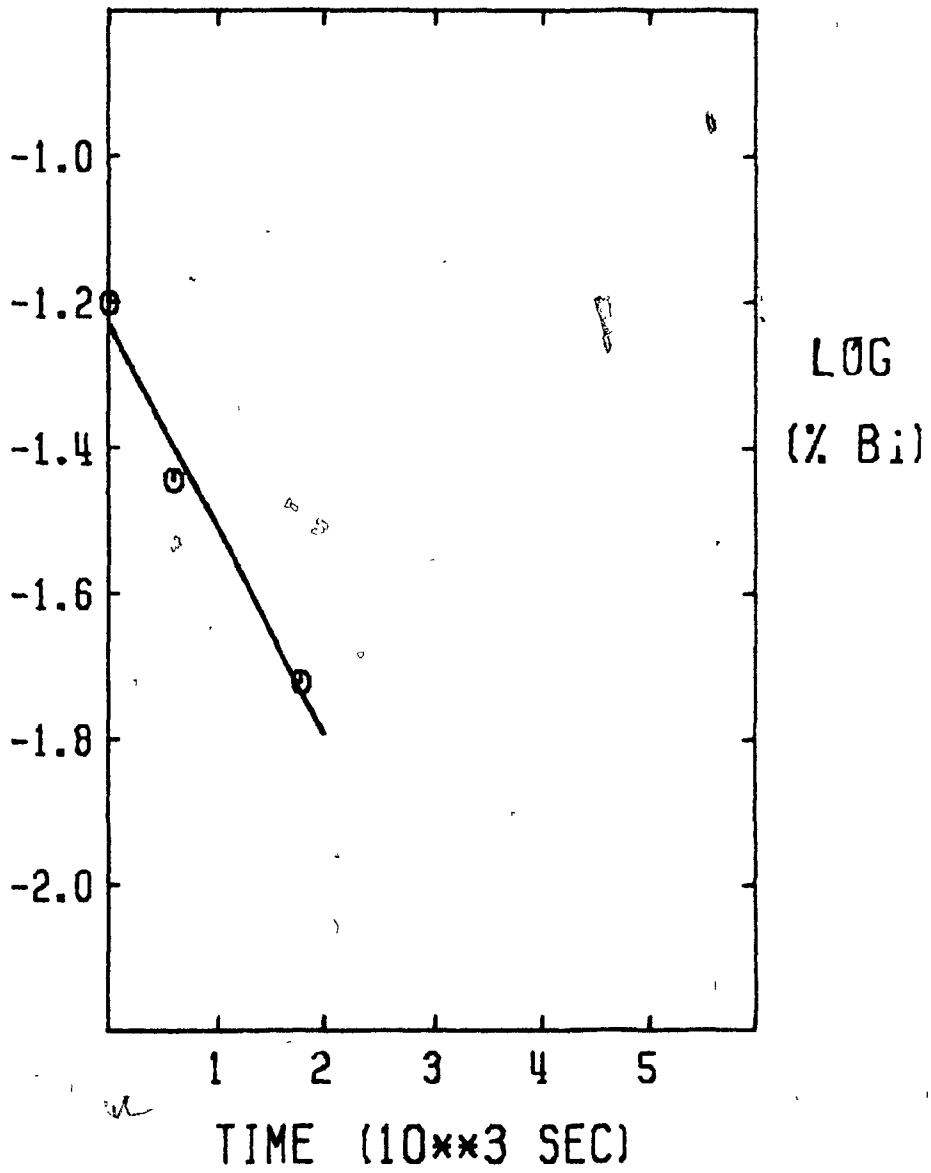

Figure 5.12a : Plot of Bismuth Removal in Test A-12

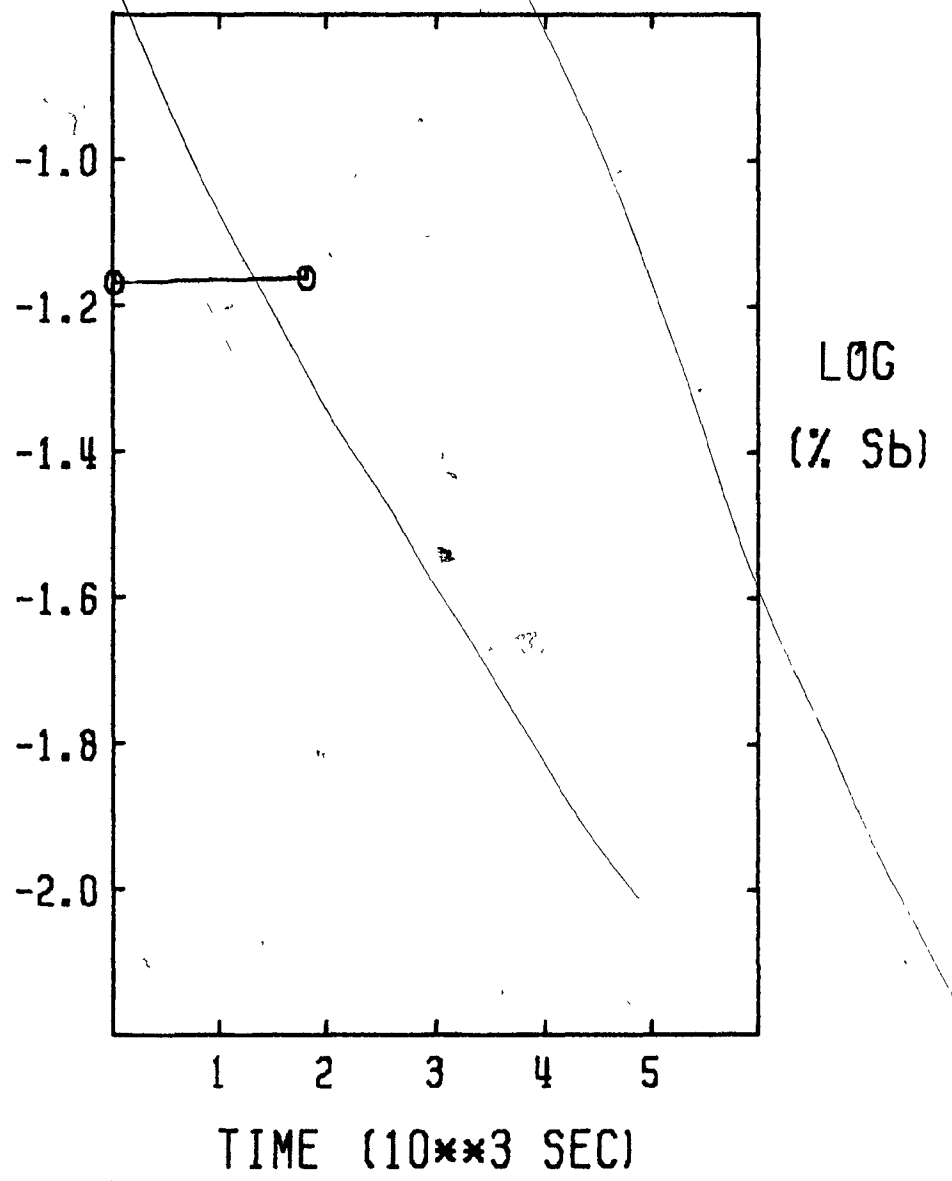

Figure 5.12b : Plot of Antimony Removal in Test A-12

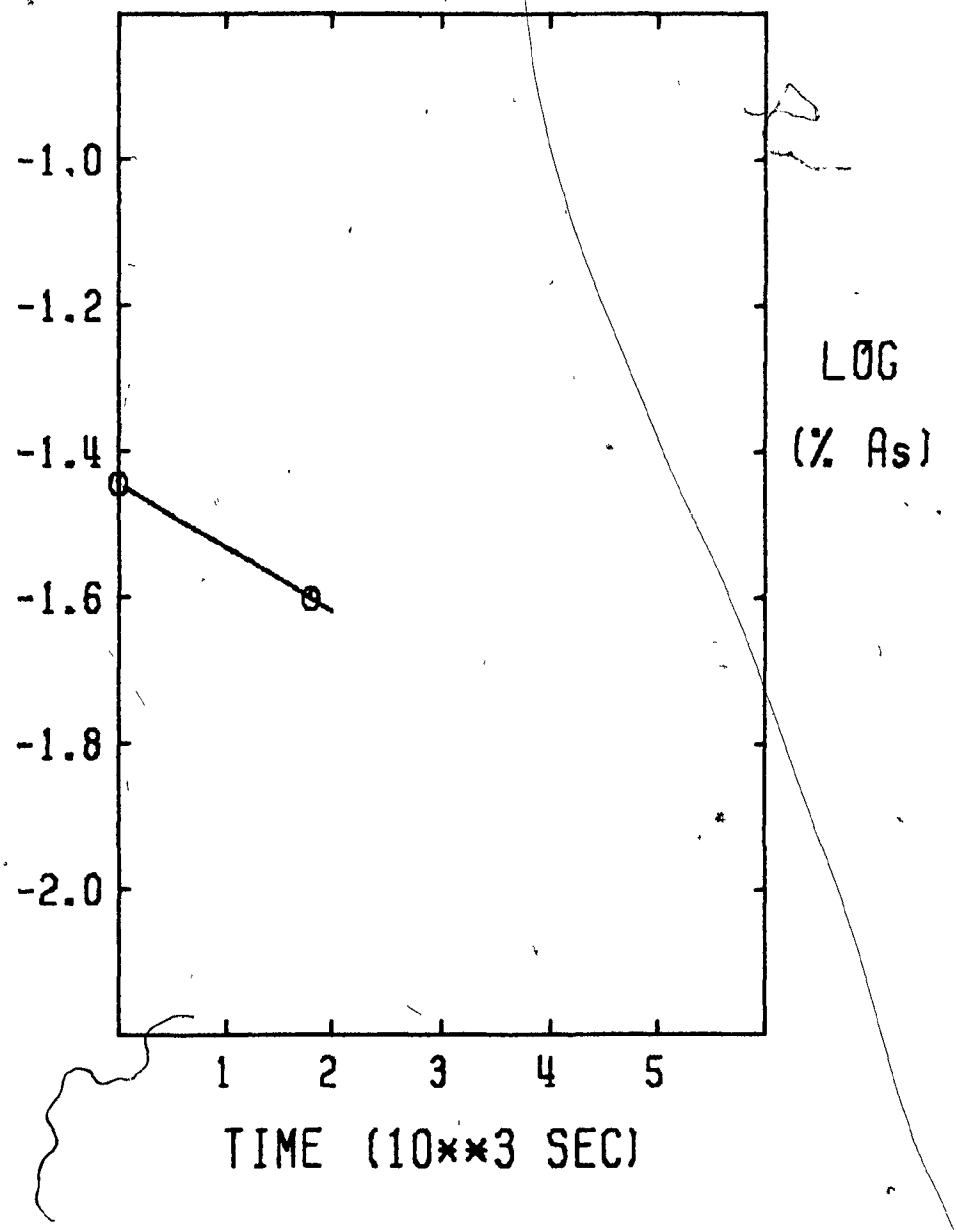

Figure 5.12c : Plot of Arsenic Removal in Test A-12

TEST NUMBER	:	A-13
TYPE OF MELT	:	Doped Cathode Copper
MELT TEMPERATURE	:	1645 ± 25 K
CHAMBER PRESSURE	:	126 ± 38 Pa
AREA TO VOLUME	:	6.9 ± 0.4 m^{-1}
ELEMENT TESTED	:	Bi

TIME (SEC)	Wt.% Bi
0	0.046
600	0.032
1500	0.032
2700	0.025
3900	0.024
5100	0.021

		Bi
K (10^{-5} m s^{-1})	:	1.9
% of initial content refined in 1 hour	:	46.6

Figure 5.13 : Experimental Conditions and Results of Bismuth Removal in Test A-13

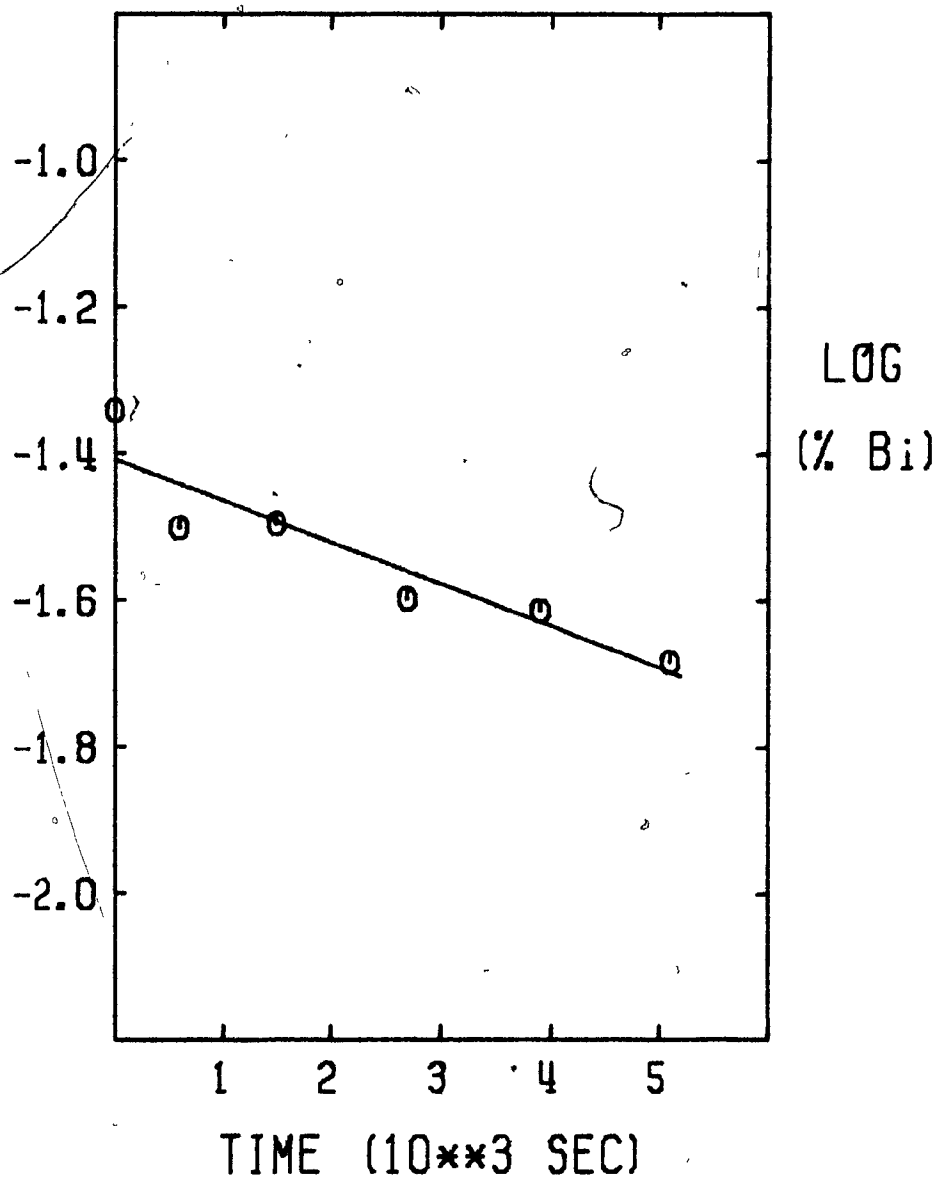

Figure 5.13a : Plot of Bismuth Removal in Test A-13

TEST NUMBER	:	A-14
TYPE OF MELT	:	Doped Cathode Copper
MELT TEMPERATURE	:	1608 ± 8 K
CHAMBER PRESSURE	:	96 ± 14 Pa
AREA TO VOLUME	:	8.0 ± 0.4 m^{-1}
ELEMENTS TESTED	:	Bi Sb

TIME (SEC)	Wt.% Bi	Wt.% Sb
0	0.012	0.058
900	0.011	-
2100	0.007	0.056
3300	0.006	0.054

		Bi	Sb
K (10^{-5} m s^{-1})	:	3.0	0.3
% of initial content refined in 1 hour	:	57.5	6.9

Figure 5.14: Experimental Conditions and Results of Bismuth and Antimony Removal in Test A-14

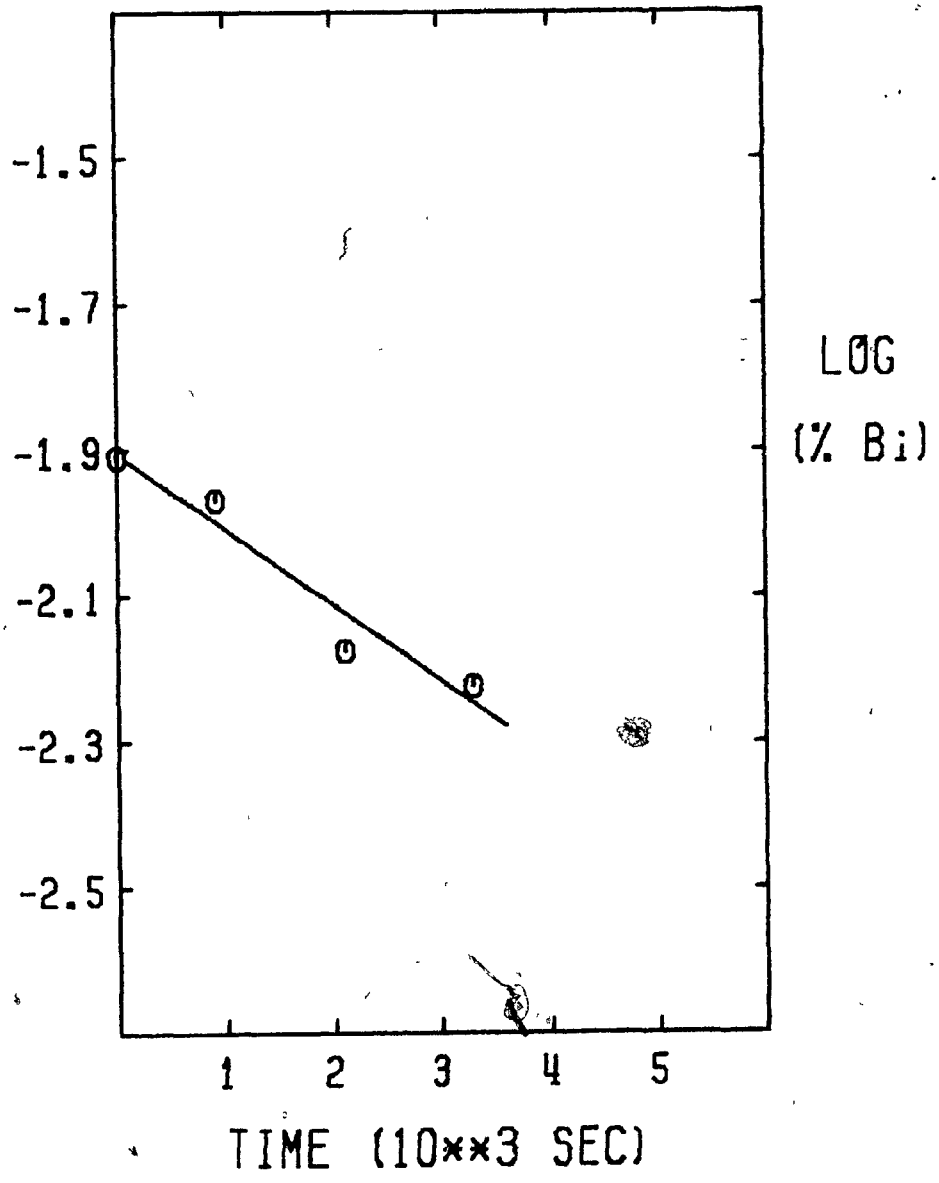

Figure 5.14a : Plot of Bismuth Removal in Test A-14

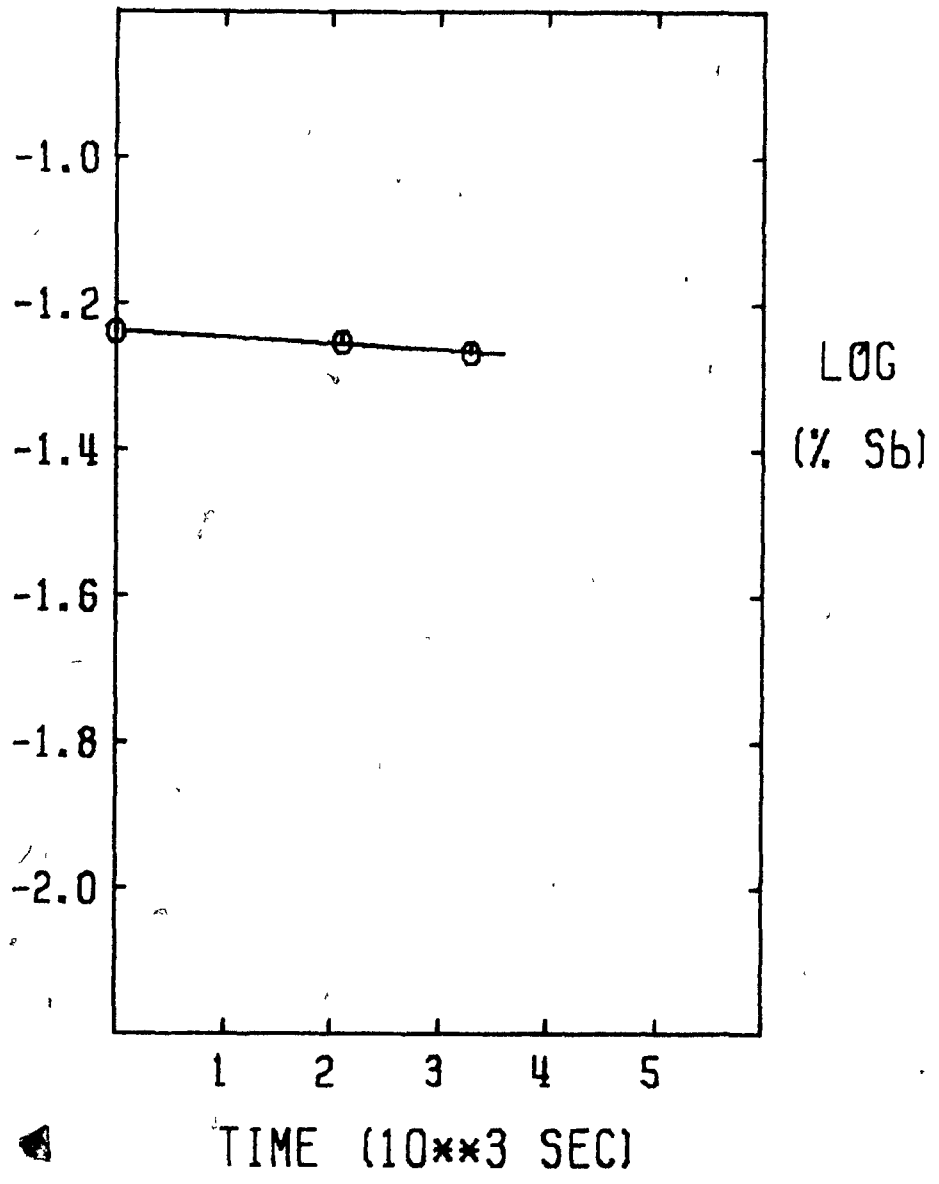

Figure 5.14b : Plot of Antimony Removal in Test A-14

TEST NUMBER	:	A-15
TYPE OF MELT	:	Doped Cathode Copper
MELT TEMPERATURE	:	1625 ± 10 K
CHAMBER PRESSURE	:	109 ± 14 Pa
AREA TO VOLUME	:	9.4 ± 0.4 m^{-1}
ELEMENTS TESTED	:	Bi Sb

TIME (SEC)	Wt.% Bi	Wt.% Sb
0	0.055	0.047
600	0.048	-
1500	0.031	-
3000	0.023	0.044

		Bi	Sb
K (10^{-5} m s^{-1})	:	3.2	0.2
% of initial content refined in 1 hour	:	66.5	7.8

Figure 5.15 : Experimental Conditions and Results of Bismuth and Antimony Removal in Test A-15

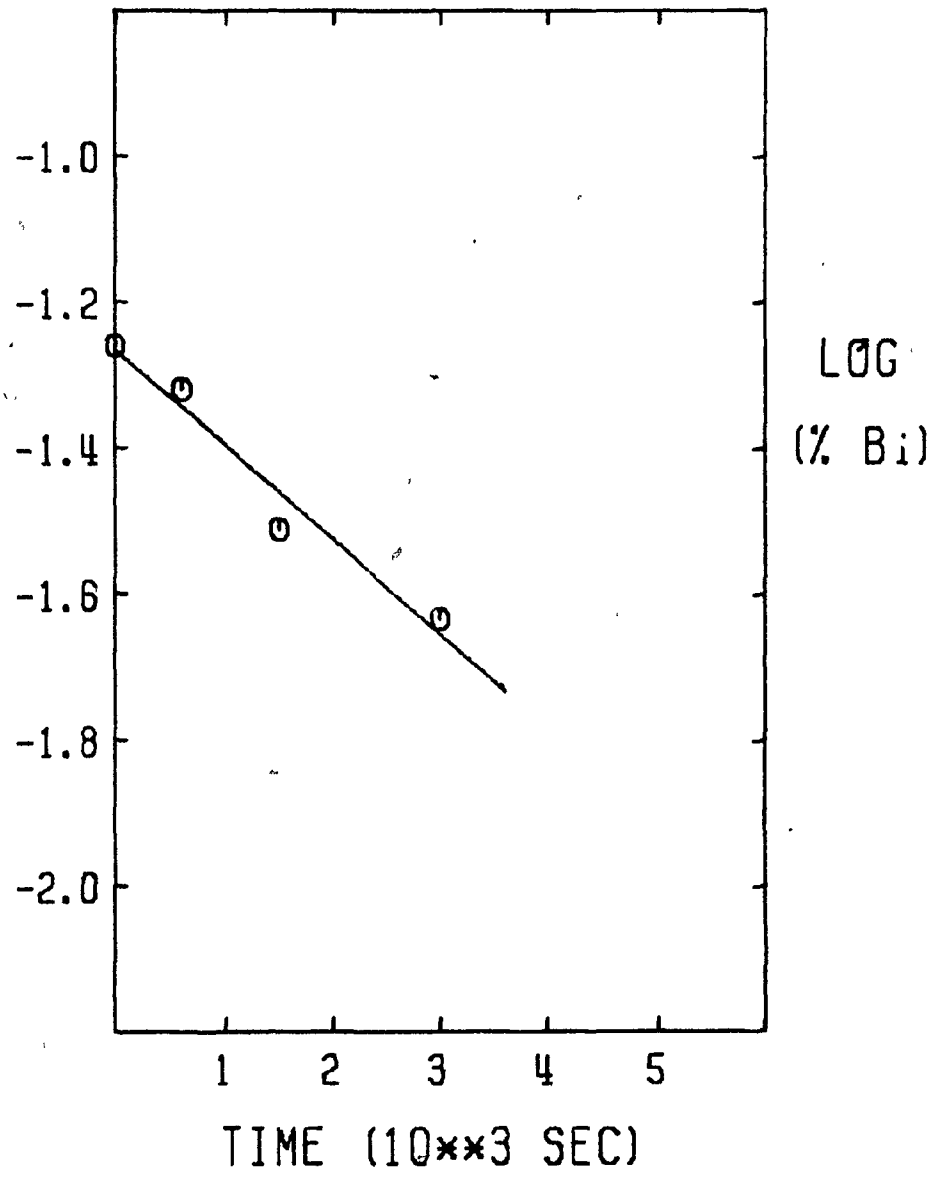

Figure 5.15a : Plot of Bismuth Removal in Test A-15

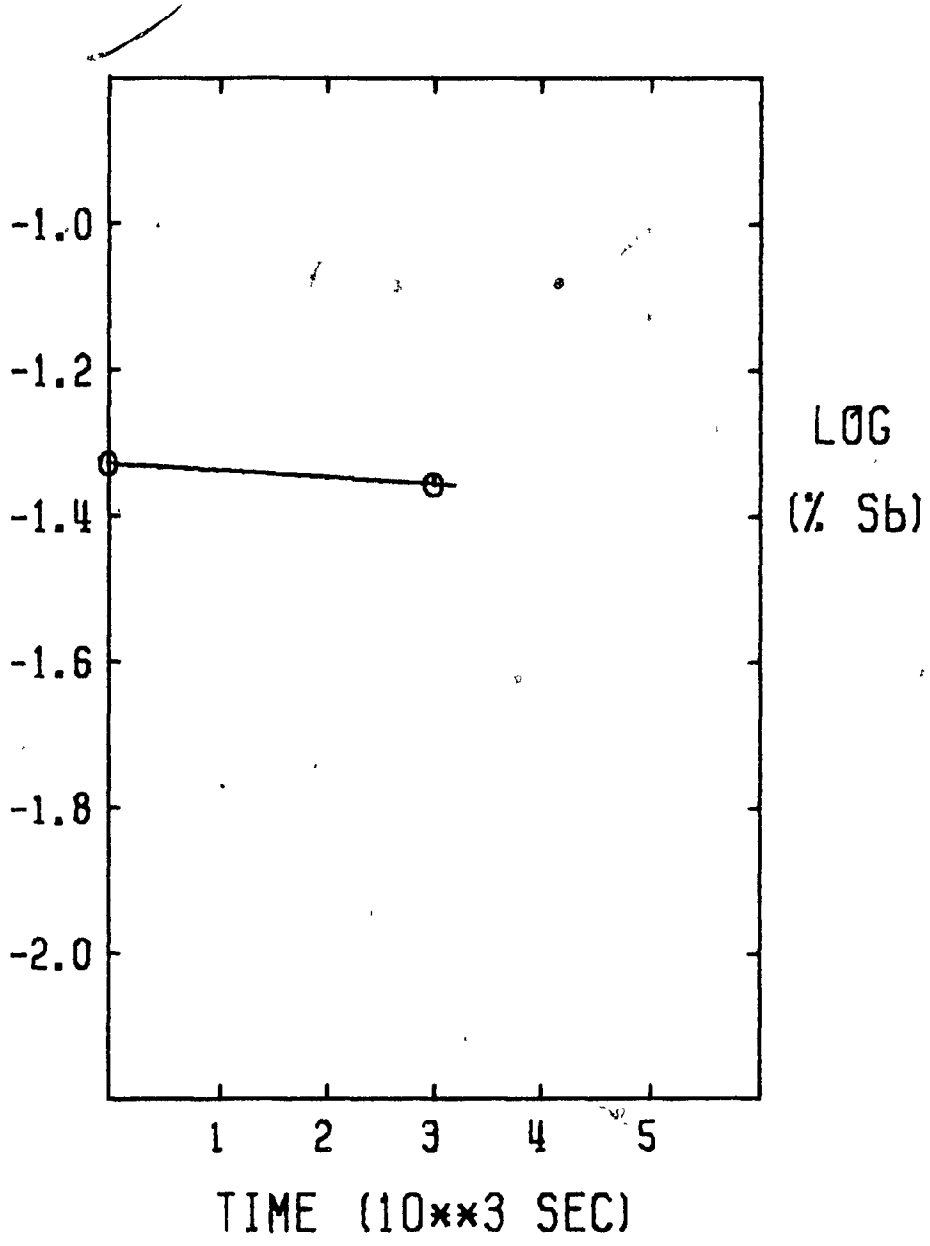

Figure 5.15b : Plot of Antimony Removal in Test A-15

TEST NUMBER	:	A-16*
TYPE OF MELT	:	Doped Blister Copper
MELT TEMPERATURE	:	1760 ± 30 K
CHAMBER PRESSURE	:	14.0 ± 1.0 Pa
AREA TO VOLUME	:	6.9 ± 0.4 m^{-1}
ELEMENT TESTED	:	Bi

TIME (SEC)	Wt.% Bi
0	0.124
540	0.060
1560	0.060
3060	0.055

		Bi
K (10^{-5} m s^{-1})**	:	0.6
% of initial content refined in 1 hour	:	13.0

* - a slag layer was maintained

** - K is calculated for last three points. It is thought that the discrepancy in the first point may be attributed to slow mixing of the bismuth in the melt due to the slag layer

Figure 5.16 : Experimental Conditions and Results of Bismuth in Test A-16

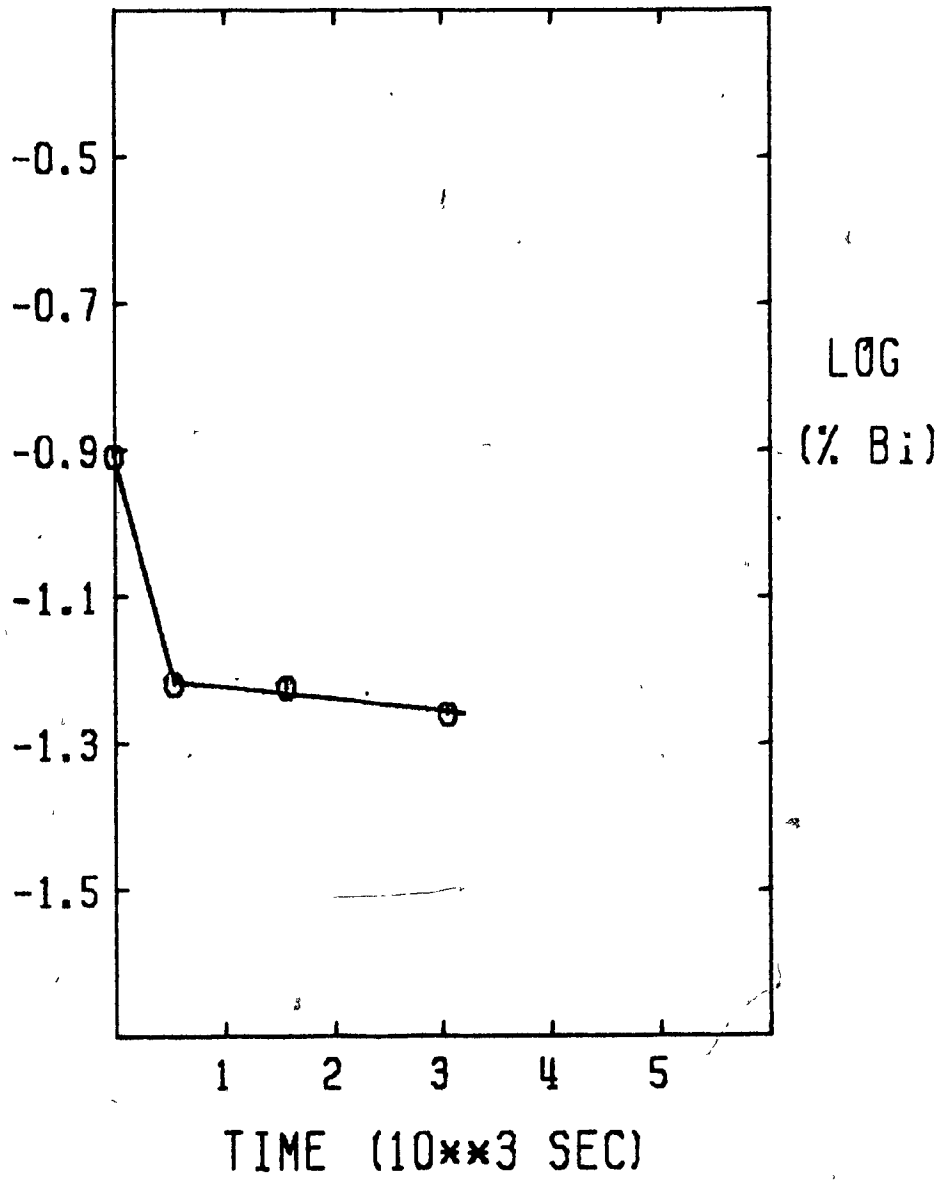

Figure 5.16a : Plot of Bismuth Removal in Test A-16

TEST NUMBER	:	A-17*
TYPE OF MELT	:	Doped Blister Copper
MELT TEMPERATURE	:	1740 ± 30 K
CHAMBER PRESSURE	:	18.0 ± 2.0 Pa
AREA TO VOLUME	:	7.5 ± 0.4 m^{-1}
ELEMENTS TESTED	:	Bi Sb

TIME (SEC)	Wt.% Bi	Wt.% Sb
0	0.052	0.089
2400	0.047	0.084

		Bi	Sb
K (10^{-5} m s^{-1})	:	0.6	0.3
% of initial content refined in 1 hour	:	14.1	8.5

* - a slag layer was maintained

Figure 5.17: Experimental Conditions and Results of Bismuth and Antimony Removal in Test A-17

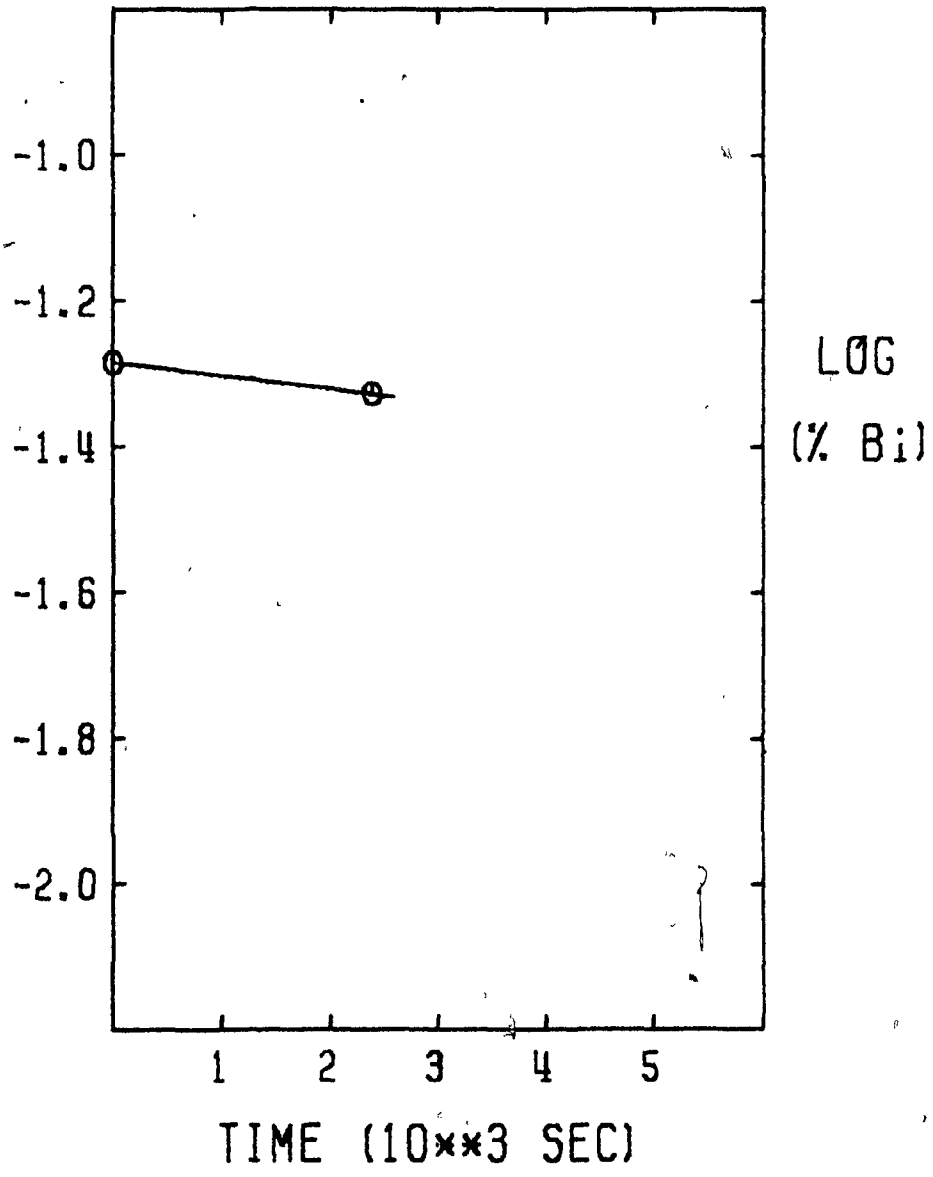

Figure 5.17a : Plot of Bismuth Removal in Test A-17

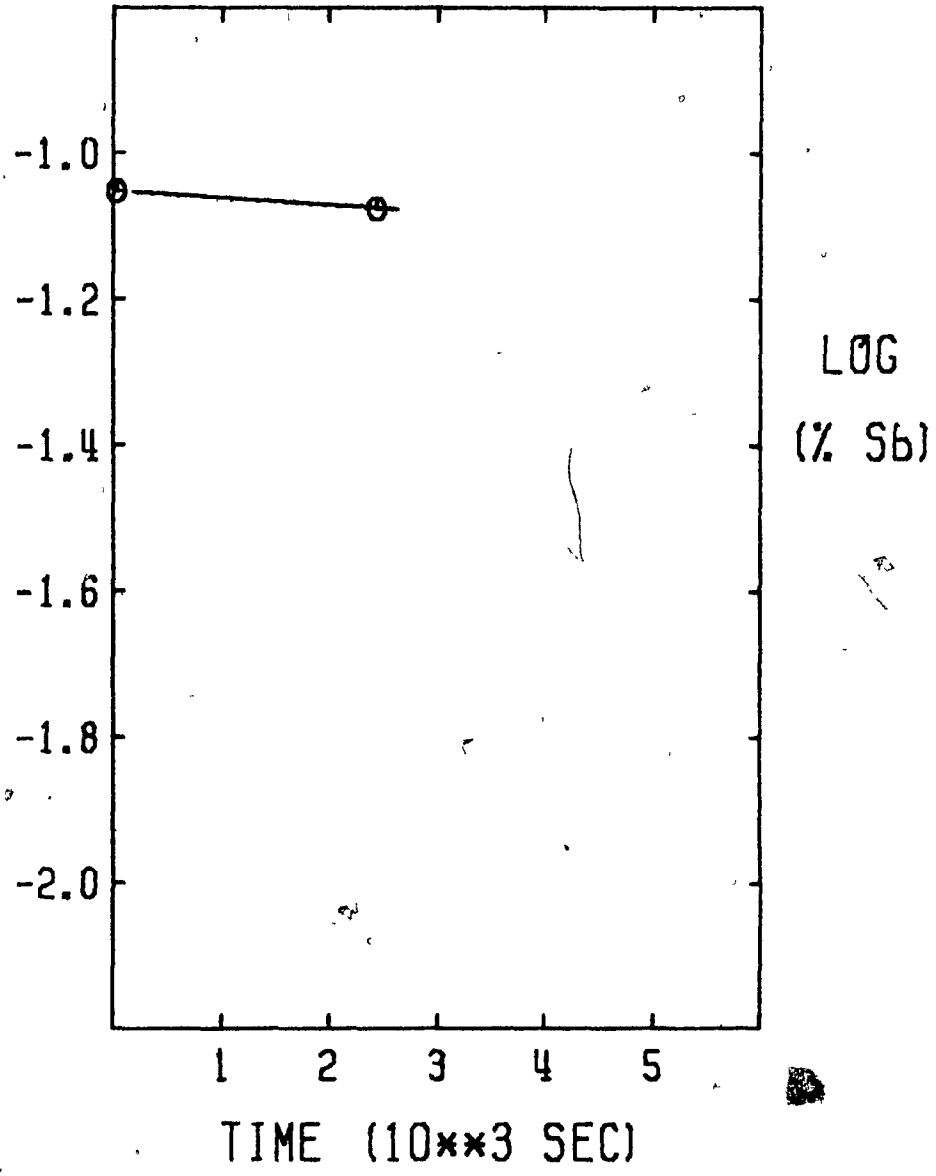

Figure 5.17b : Plot of Antimony Removal in Test A-17

TEST NUMBER	:	B-1
TYPE OF MELT	:	Blister Copper
MELT TEMPERATURE	:	1643 ± 28 K
CHAMBER PRESSURE	:	11.0 ± 2.0 Pa
AREA TO VOLUME	:	6.8 ± 0.4 m^{-1}
ELEMENT TESTED	:	Bi

TIME (SEC)	Wt.% Bi*
0	0.0026
720	0.0021
1440	0.0023
2100	0.0021
2820	0.0014
3720	0.0008
4620	0.0011

		Bi
K (10^{-5} m s^{-1})	:	3.5
% of initial content refined in 1 hour	:	54.4

* - due to limits in analytical precision, the uncertainty of the fourth decimal place is large

Figure 5.18 : Experimental Conditions and Results of Bismuth Removal in Test B-1

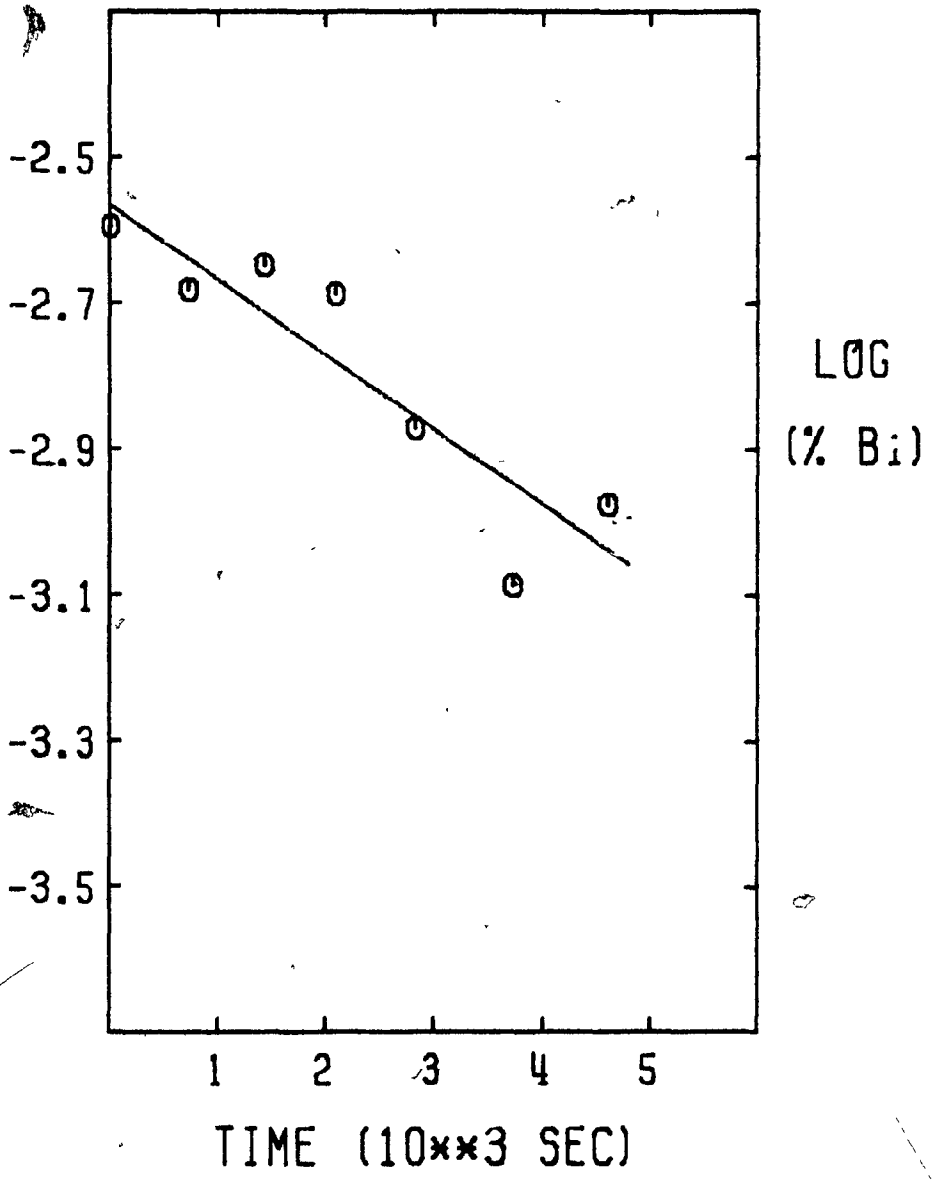

Figure 5.18a : Plot of Bismuth Removal in Test B-1

TEST NUMBER	:	B-2
TYPE OF MELT	:	Blister Copper
MELT TEMPERATURE	:	1730 ± 45 K
CHAMBER PRESSURE	:	24 ± 4 Pa
AREA TO VOLUME	:	6.7 ± 0.4 m^{-1}
ELEMENTS TESTED	:	Bi Sb As Se Te

TIME (SEC)	Wt.% Bi†	Wt.% Sb	Wt.% As
0	0.0028	<0.001	<0.002
3360	0.0017	<0.001	<0.002

TIME (SEC)	Wt.% Se	Wt.% Te†
0	0.035	0.0064
3360	0.035	0.0064

	Bi	Sb	As	Se	Te
K (10^{-5} m s^{-1}) :	2.2	-	-	0	0
% of initial content refined in 1 hour :	41.5	-	-	0	0

† - due to limits in analytical precision, the uncertainty of the fourth decimal place is large

Figure 5.19 : Experimental Conditions and Results of Bismuth, Antimony, Arsenic, Selenium and Tellerium Removal in Test B-2

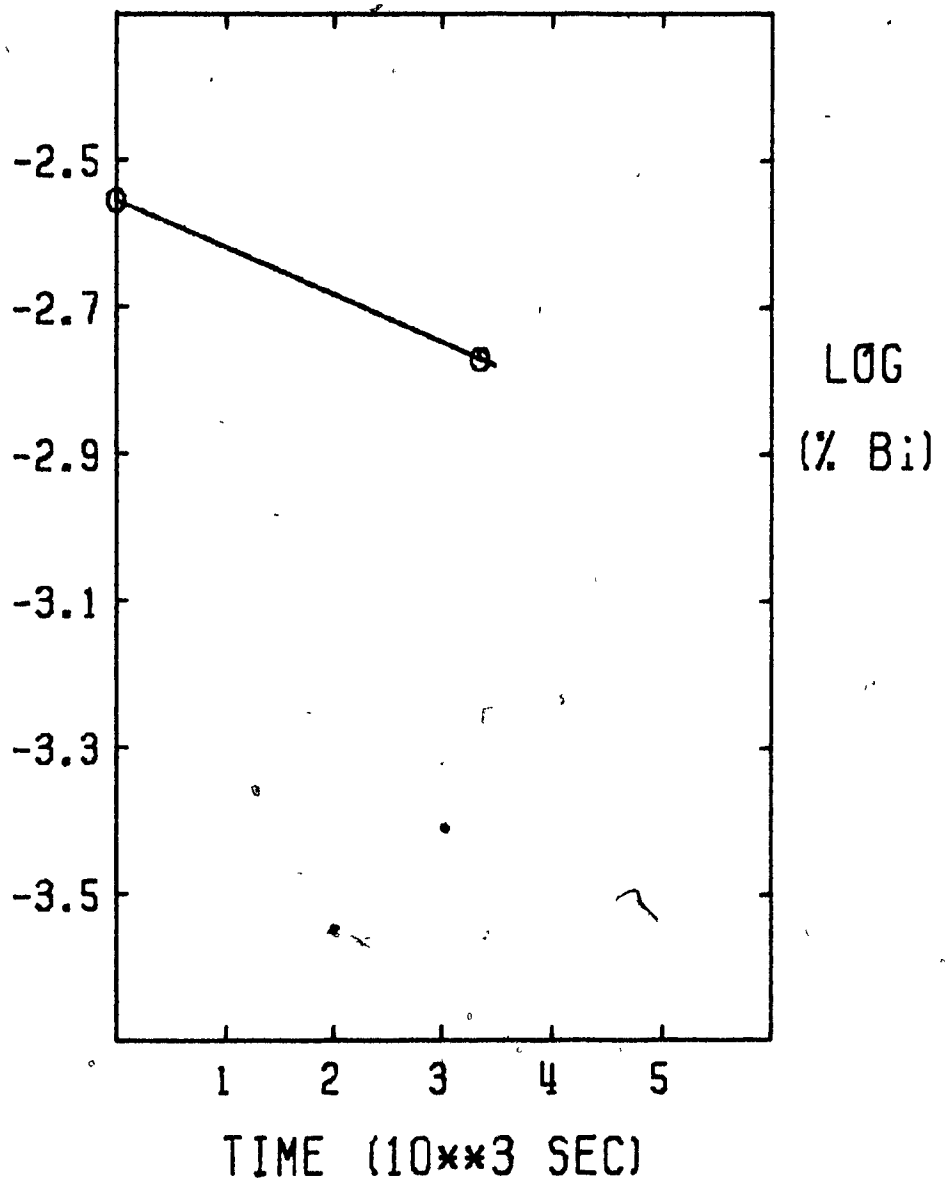

Figure 5.19a : Plot of Bismuth Removal in Test B-2

TEST NUMBER	:	C-1
TYPE OF MELT	:	White Metal (Cu_2S)
MELT TEMPERATURE	:	1528 ± 18 K
CHAMBER PRESSURE	:	187 ± 80 Pa
AREA TO VOLUME	:	6.4 ± 0.4 m^{-1}
ELEMENT TESTED	:	Bi

TIME (SEC)	Wt.% Bi
0	0.081
300	0.083
720	0.073
1440	0.059
2160	0.055
5400	0.034

		Bi
K (10^{-5} m s^{-1})	:	2.6
% of initial content refined in 1 hour	:	45.0

Figure 5.20 : Experimental Conditions and Results of Bismuth Removal in Test C-1

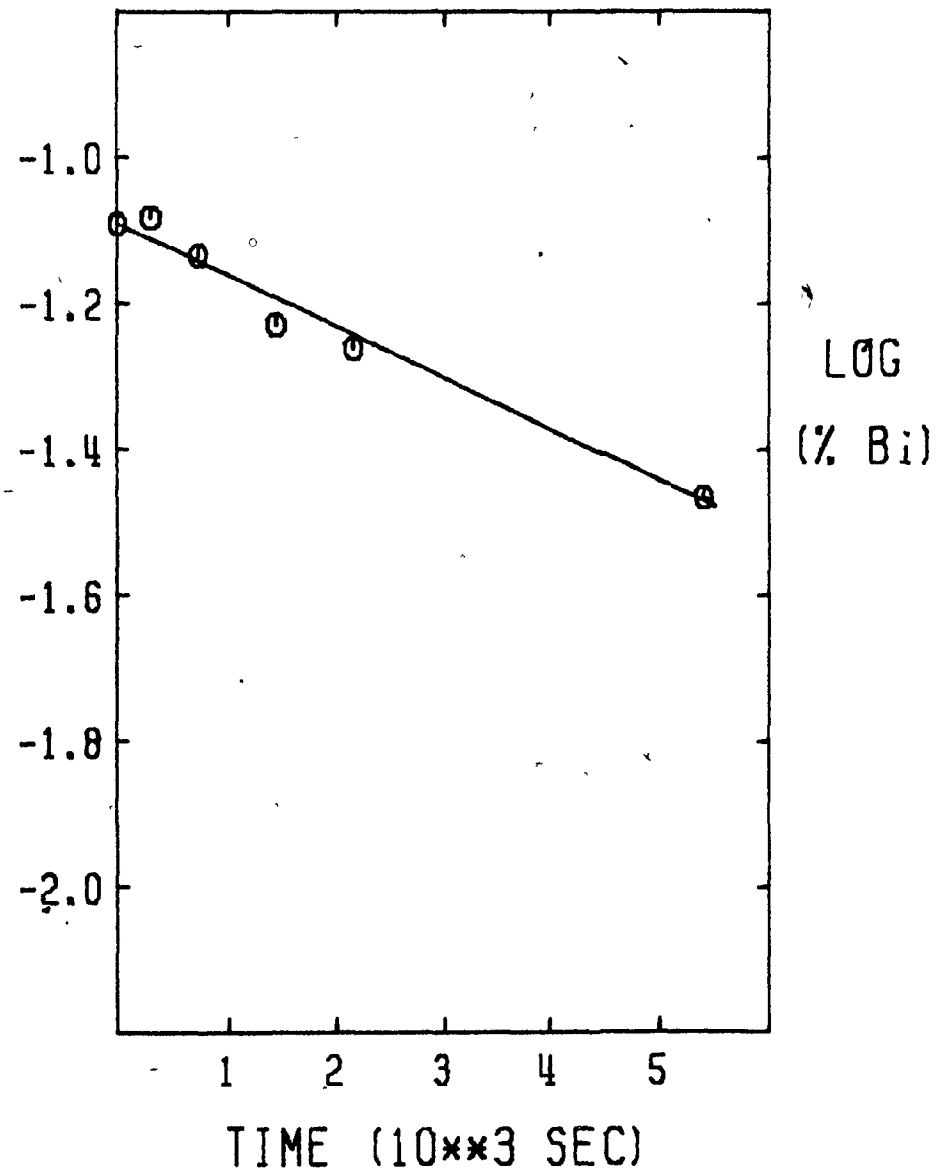

Figure 5.20a : Plot of Bismuth Removal in Test C-1

TEST NUMBER	:	C-2
TYPE OF MELT	:	White Metal (Cu_2S)
MELT TEMPERATURE	:	1545 ± 5 K
CHAMBER PRESSURE	:	120 ± 27 Pa
AREA TO VOLUME	:	6.7 ± 0.4 m^{-1}
ELEMENT TESTED	:	Bi

TIME (SEC)	Wt.% Bi
0	0.106
300	0.102
900	0.093
2100	0.075
3300	0.049
4200	0.056

		Bi
K (10^{-5} m s^{-1})	:	2.7
% of initial content refined in 1 hour	:	47.9

Figure 5.21 : Experimental Conditions and Results of Bismuth Removal in Test C-2

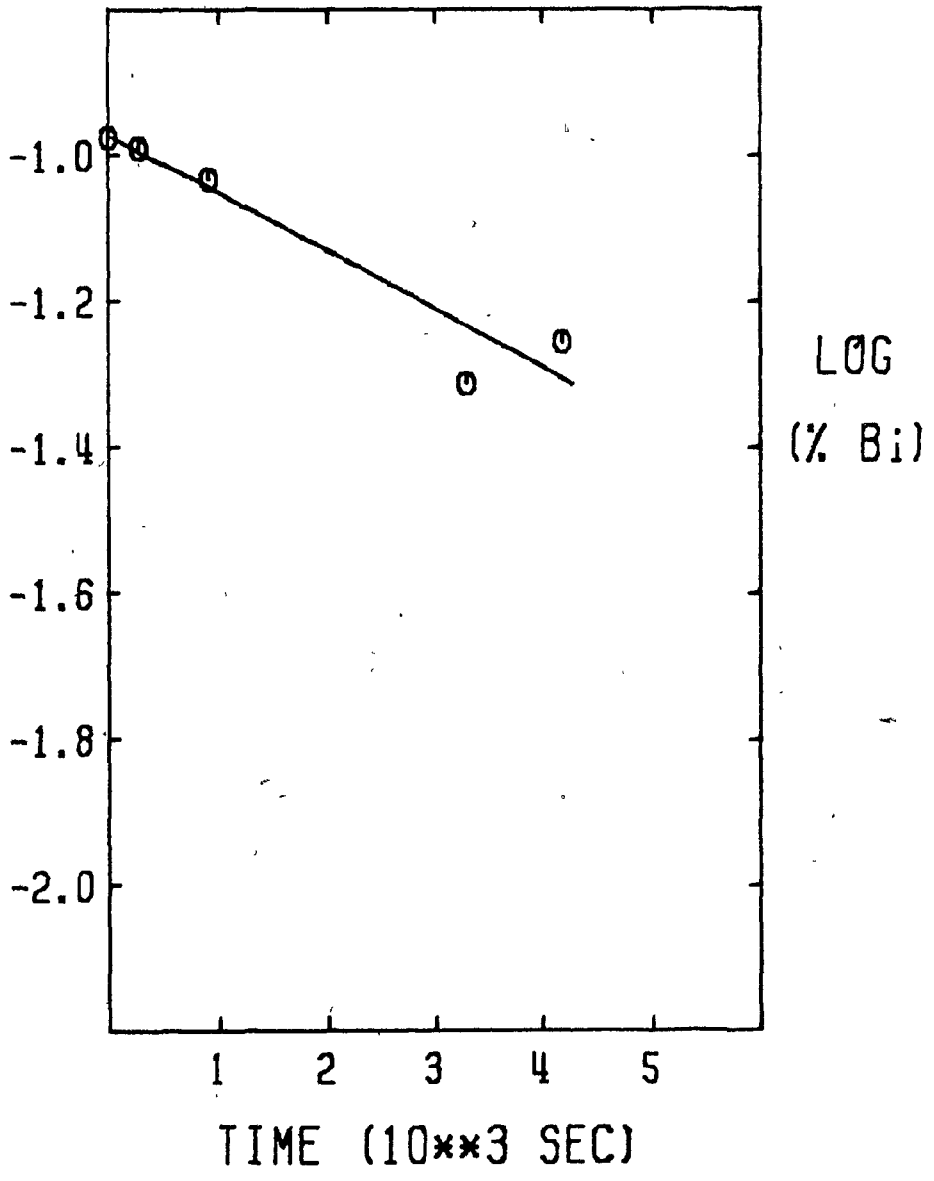

Figure 5.21a : Plot of Bismuth Removal in Test C-2

Day	Condensate Analysis			
	% Bi	% Sb	% As	% Cu
1	22.3	0.76	--	23.3
2	11.5	2.22	5.80	62.1
3	20.6	0.49	--	46.6

Table 5.9 : Condensate Analyses (by weight) for Three Different Days of Experimentation

CHAPTER SIX

DISCUSSION

SECTION 6.1 : INTRODUCTION

The objectives of this study were :

a) to determine rates of elimination of bismuth, antimony and arsenic from copper melts under vacuum and to examine the affects of the following parameters -

   i) melt temperature

   ii) chamber pressure

   iii) initial solute concentration

   iv) melt surface area to volume ratio

   v) presence of a slag layer

b) to develop a theoretical model which describes the elimination of bismuth, antimony and arsenic from copper melts under various conditions of vacuum distillation

and

c) to compare predictions of the theoretical model to experimental results.

The following discussion examines the experimental results of this study with the above objectives in mind.

SECTION 6.2 : VACUUM DISTILLATION OF DOPED COPPER MELTS

6.2.1 : GENERAL

It was found in the experiments that bismuth was readily removed from copper melts. Between 45 and 90 % of the initial content was eliminated in 1 hour (experiments with a slag layer being excepted). Removal of arsenic and antimony was more difficult, the elimination in 1 hour being 50 to 60 % of the initial arsenic content and nil to 60 % of the initial antimony content. In all experiments, melt temperature was in the range 1500-1790 K and chamber pressures were from 7 to 160 Pa. Melt surface area to volume ratio was 7-10 m^{-1} in all cases.

The very low antimony eliminations were thought to be due to the presence of iron in the copper. Experiments A-10, A-11 and A-12, which were a series of several high temperature experiments conducted on one melt, contained about 1 % iron due to a steel sample cup accidentally falling into that melt. No antimony was removed in two of the

experiments (A-10 & A-12). The third (A-11) showed only 7 % removed in 1 hour. Nothing unusual was noticed about bismuth and arsenic removal in any of these three experiments.

Two possible explanations for this phenomenom were :

a) the formation of iron and antimony compounds which have a lower vapour pressure above a copper melt than antimony alone

or

b) an interaction between dissolved iron and dissolved antimony in liquid copper which lowers the activity coefficient of antimony in the copper.

Although no data was found in the literature to support either consideration, the formation of FeSb and $FeSb_2$ is documented[29].

6.2.2 : EFFECT OF MELT TEMPERATURE

The effect of temperature on vacuum distillation is shown in Figure 6.1, where the overall refining rate coefficient is plotted against melt temperature. The results show that K_{Bi} increases from 2×10^{-5} to 7×10^{-5} m s^{-1}

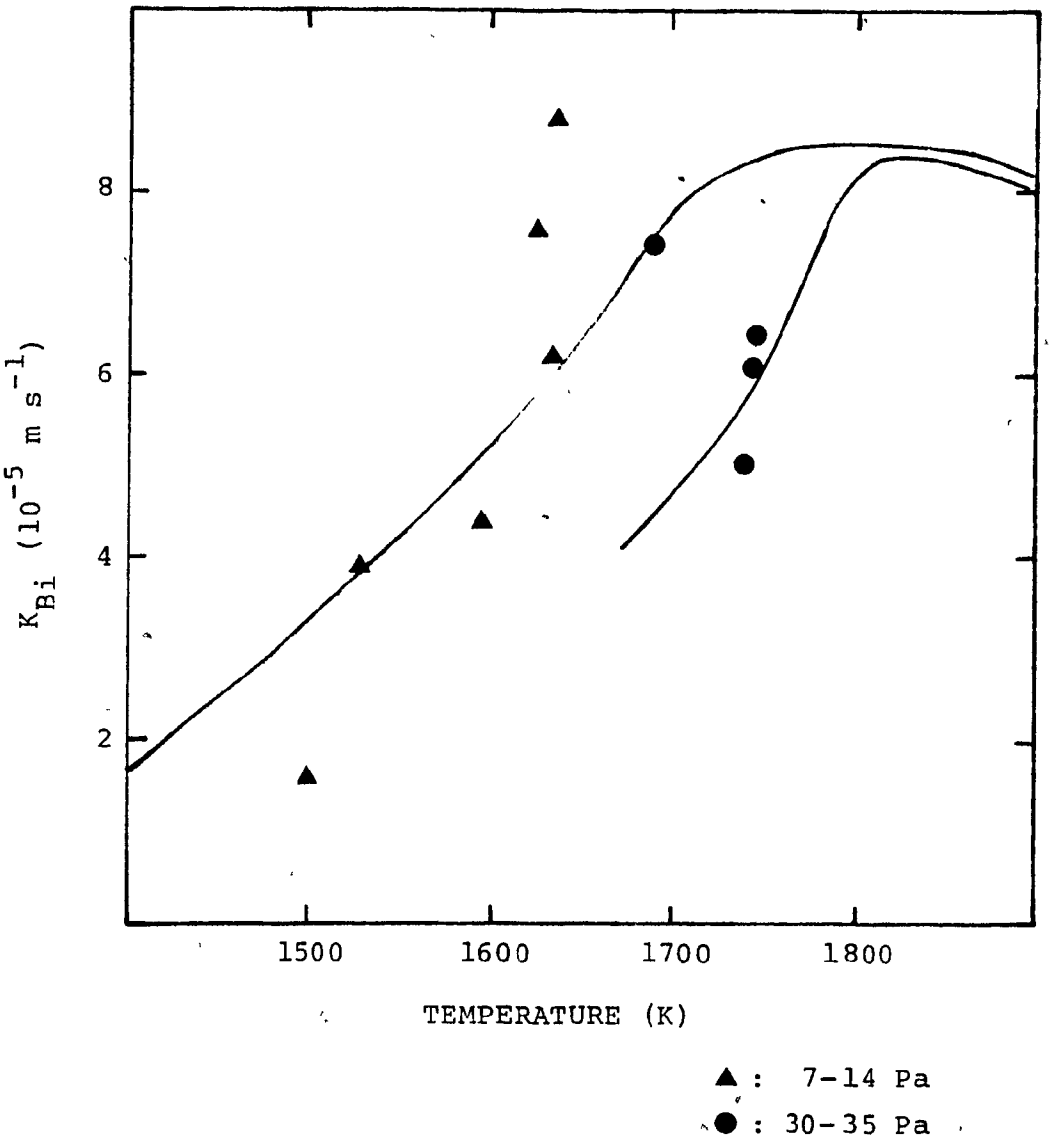

Figure 6.1a : Experimentally determined refining rate coefficients for bismuth plotted against melt temperature. Also shown are theoretically predicted rate coefficients for two sets of conditions - 11 Pa and 0.08 % Bi which were representative of most experiments with melt temperatures from 1500-1650 K; 32 Pa and 0.055 % Bi which was representative of most experiments with melt temperatures above 1650 K.

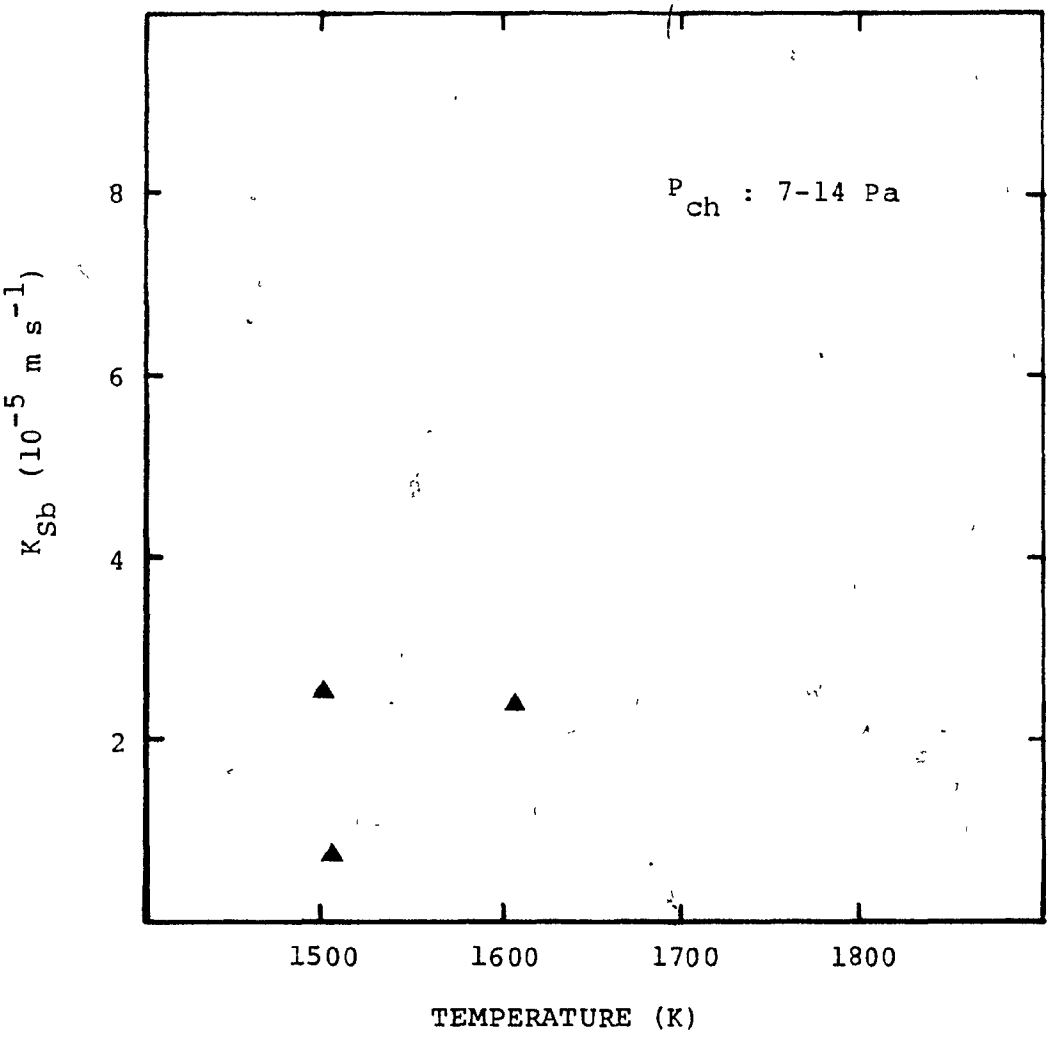

Figure 6.1b : Experimentally determined refining rate coefficients for antimony plotted against melt temperature.

when temperature is increased from 1500 to 1700 K.

The solid lines in Figure 6.1a which represent predictions of the theoretical model for bismuth elimination roughly agree with the experimental results. They also show that the refining rate drops off at higher temperatures. This is because the increase of vapour pressure above the melt with temperature is more rapid for copper than for bismuth (Figure 6.2). The same is true for the case of antimony but not for monatomic arsenic (see Section 3.10.1).

6.2.3 : EFFECT OF CHAMBER PRESSURE

Figures 6.3a and b plot refining rate coefficients against chamber pressure. The results show that K_{Bi} and K_{Sb} are significantly higher at pressures between 10 and 15 Pa than at pressures between 100 and 130 Pa. The model predictions for bismuth demonstrate the same effect. They also show that the greatest decrease occurs when the chamber pressure rises from 5 to 20 Pa. This can be explained by considering melt vapour pressure.

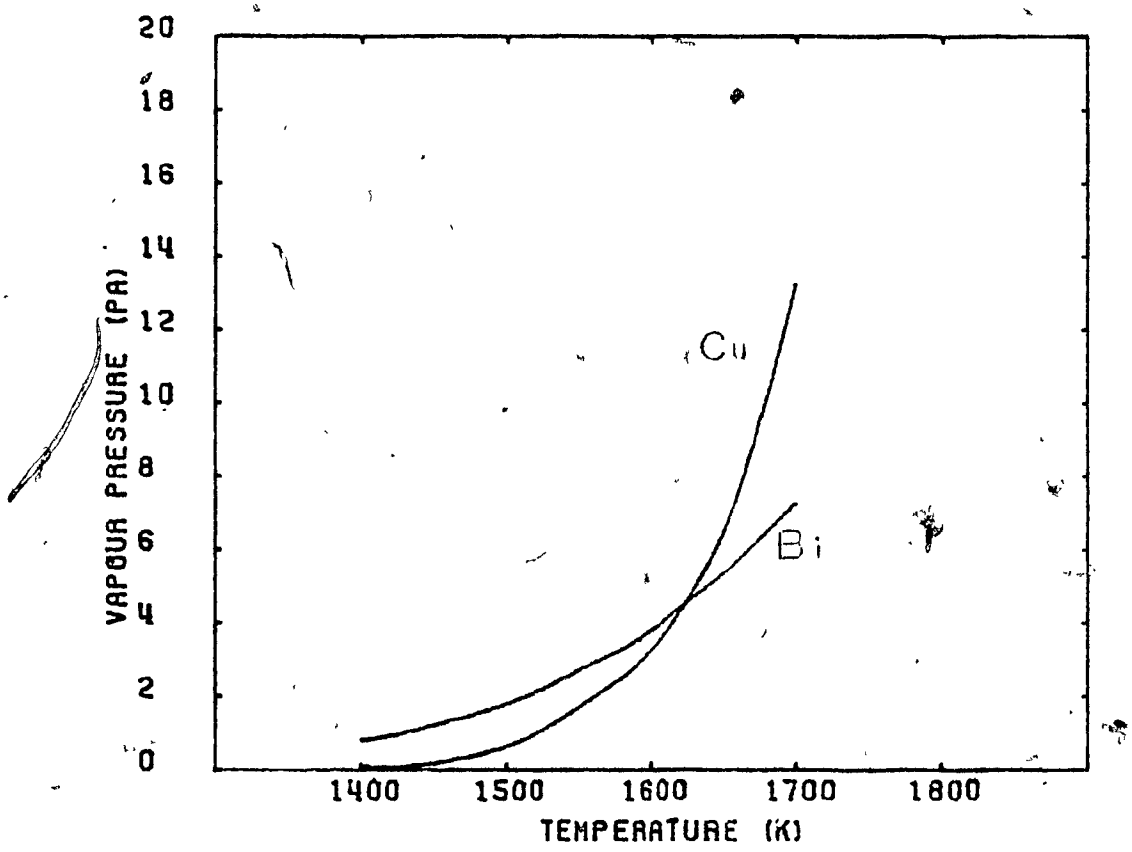

Figure 6.2 : Vapour Pressures of Copper and Bismuth above a Copper melt containing 0.08 % Bi plotted against Temperature

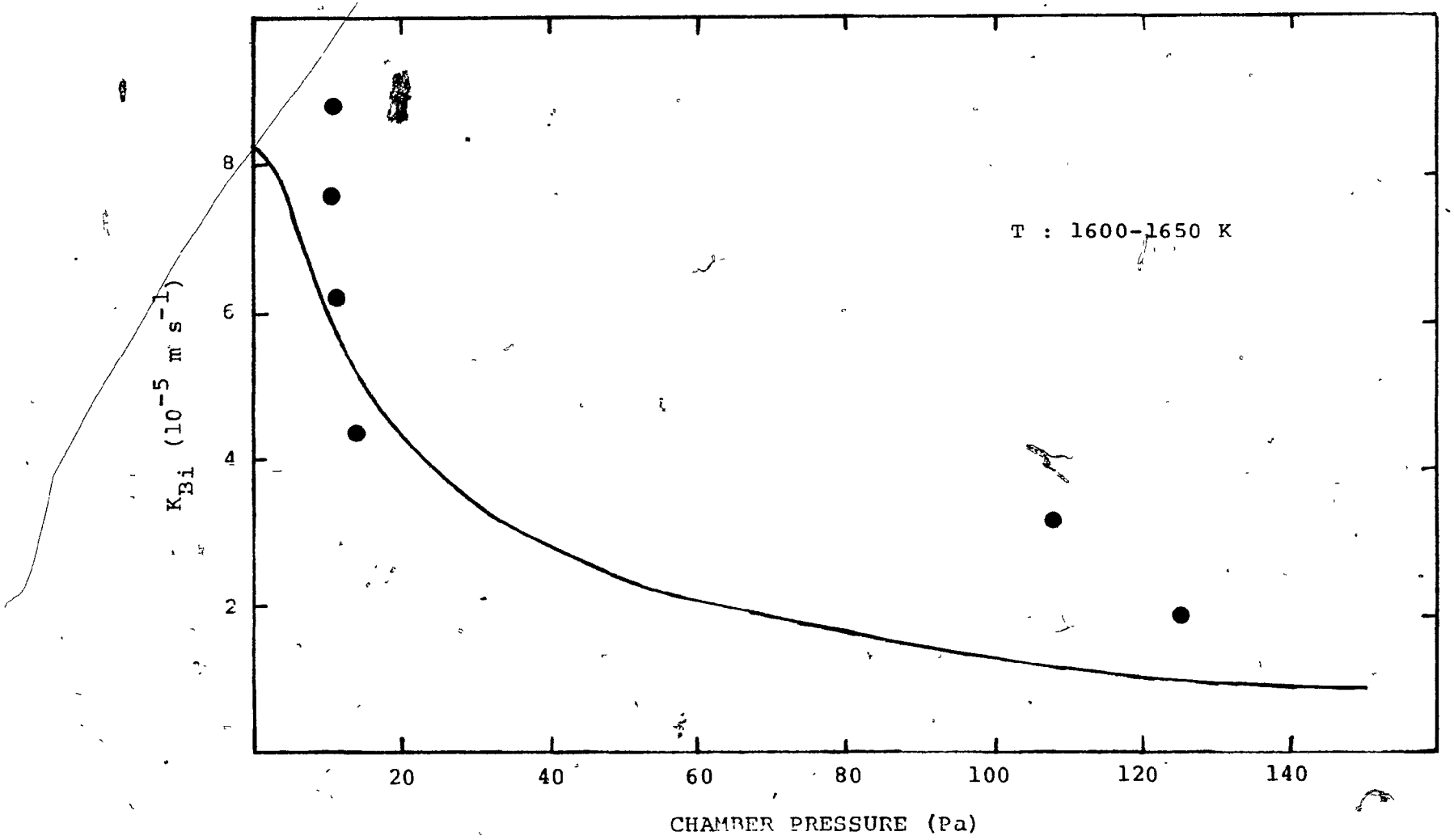

Figure 6.3a : Experimentally determined refining rate coefficients for bismuth plotted against chamber pressure. Also shown are theoretically predicted rate coefficients at 1630 K

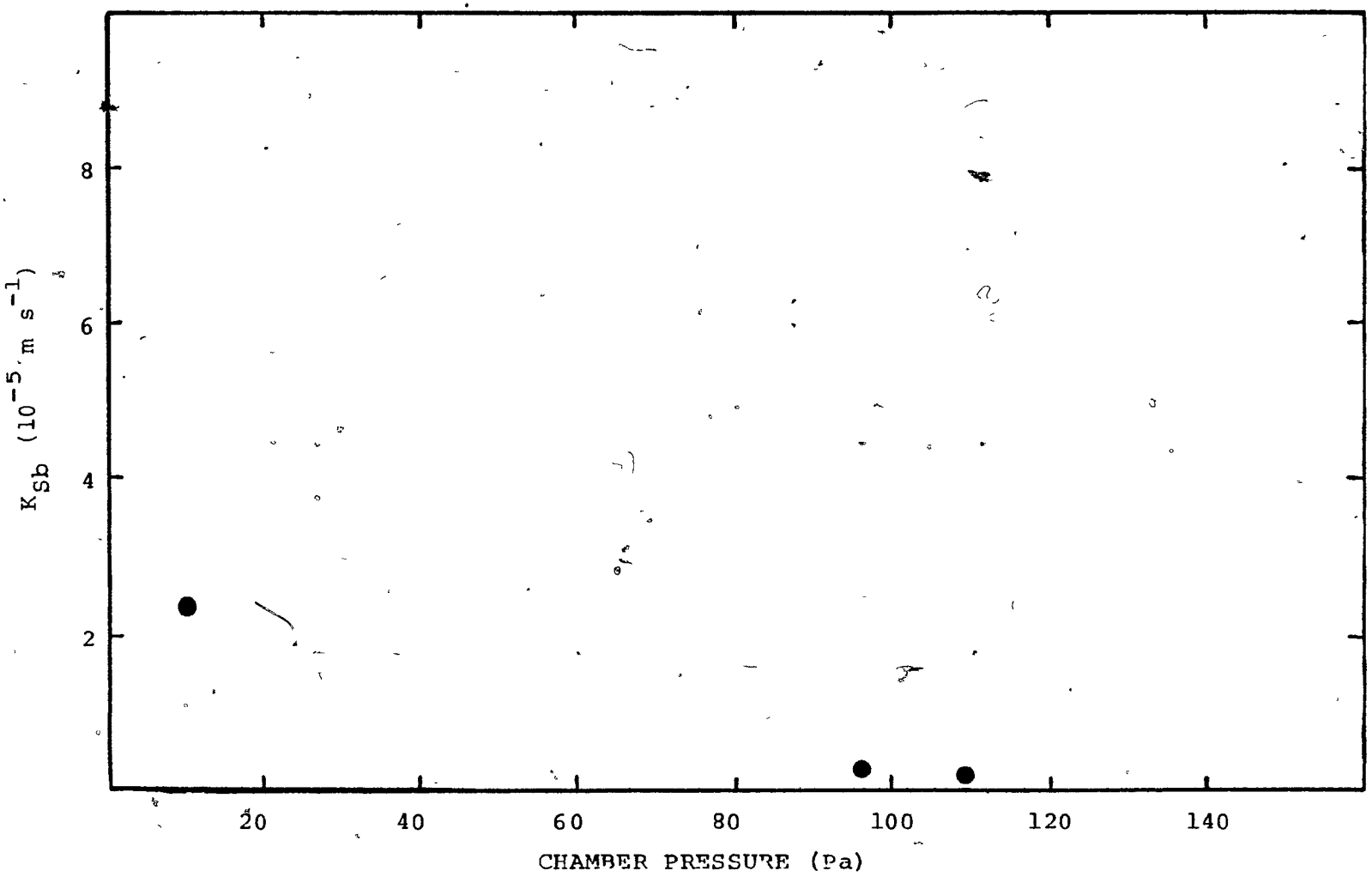

Figure 6.3b : Experimentally determined refining rate coefficient for antimony plotted against chamber pressure .

The total vapour pressure above a copper melt containing 0.08 % Bi by weight at 1630 K is 10.2 Pa. When the chamber pressure is much less than the total vapour pressure (i.e. chamber pressures less than 5 Pa in this case), the mass transfer rate is controlled by melt phase mass transfer and evaporation and will be independent of chamber pressure*. As the chamber pressure increases from 5 Pa, gas phase mass transfer resistance is no longer negligible and refining rate will decrease exponentially in accordance with the term $\Sigma N_i/P_{ch}$ in Equation 3.18. Numerically, the greatest effect of chamber pressure on refining rate will be seen at lower chamber pressures, that is between 5 and 20 Pa in this case.

6.2.4 : EFFECT OF INITIAL SOLUTE CONCENTRATION

Table 5.4 shows that, for experiments conducted at approximately the same temperature and pressure, the refining rate for bismuth tended to be lower at lower initial solute concentrations. This is similar to the effect of chamber pressure, that is, gas phase mass transport offers

---

* - Further evidence of this statement is seen in Figure 6.1a. At high melt temperatures, where the total vapour pressure above the melt is much higher than 32 Pa (≃ 60 Pa @ 1800 K, 0.08 % Bi), the refining rate at 11 Pa chamber pressure is equal to that at 32 Pa.

considerable resistance when melt vapour pressure is less than chamber pressure.

It is apparent from this section and the preceding one that the ratio of total vapour pressure to chamber pressure is an important parameter in terms of influencing the refining rate. Figure 6.4 plots K_{Bi} against the term '$\Sigma P_{vapour}/P_{ch}$' for the experiments in this study. The graph indicates that there is a fourfold increase in K_{Bi} when $\Sigma P_{vapour}/P_{ch}$ increases from 0.05 to 1.0. From consideration of the theoretical model, K_{Bi} is expected to reach a maximum for a value of $\Sigma P_{vapour}/P_{ch}$ equal to 2. At this point, K_{Bi} becomes independent of $\Sigma P_{vapour}/P_{ch}$ and will be affected only by the ratio P^{o}_{Bi}/P^{o}_{Cu}, which is a function of temperature. The inability of the apparatus to work at lower chamber pressures did not allow this to be investigated rigorously.

6.2.5 : EFFECT OF MELT AREA TO VOLUME RATIO

Figure 6.5 plots K_{Bi} against area to volume ratio for experiments with approximately the same temperature and pressure. The results are scattered and are deemed inconclusive for two reasons. The first is that the range of

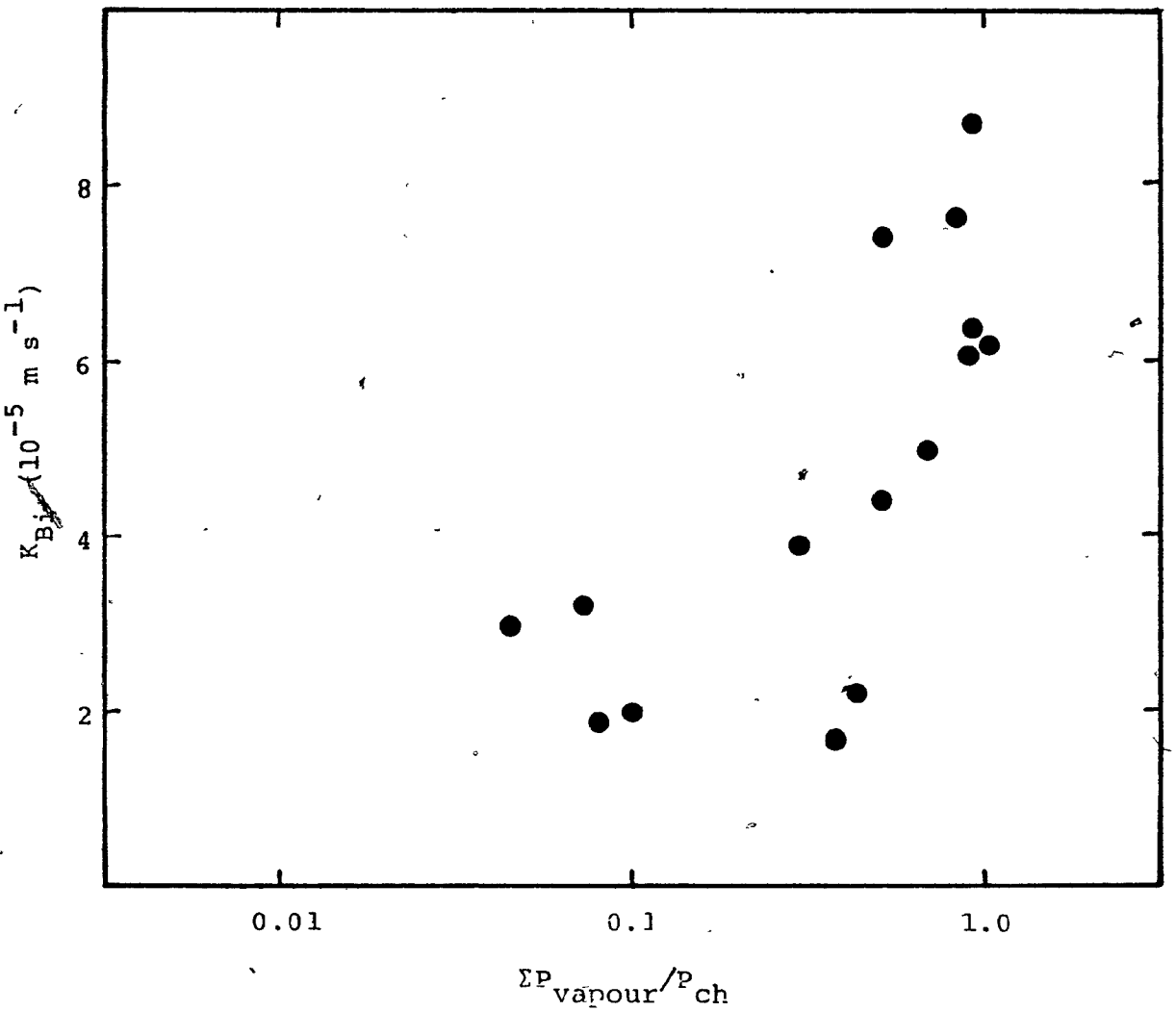

Figure 6.4 : Experimentally determined refining rate coefficients for bismuth plotted against the parameter $\Sigma P_{vapour}/P_{ch}$, where ΣP_{vapour} is the initial total vapour pressure.

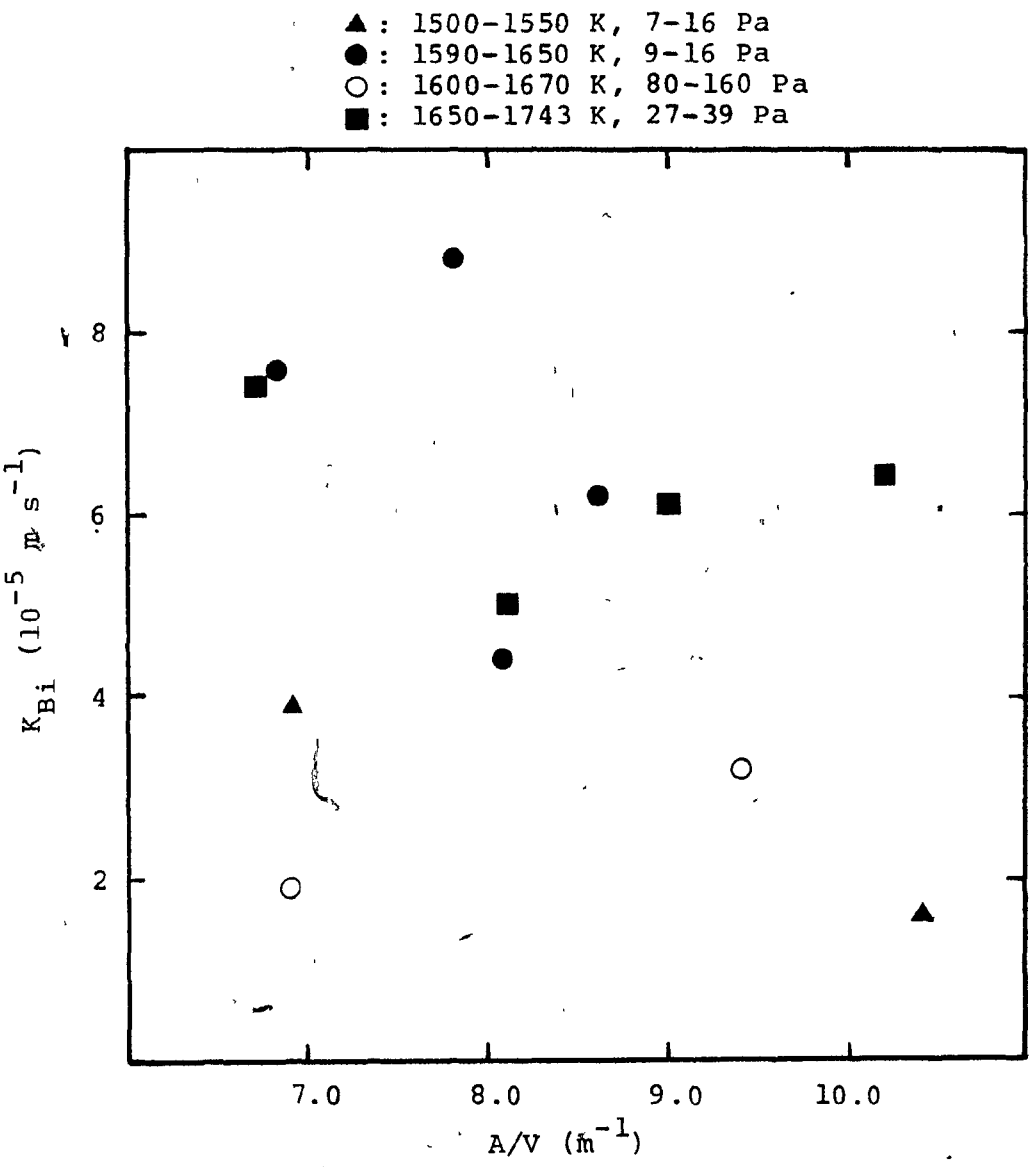

Figure 6.5 : Experimentally determined refining rate coefficients plotted against melt surface area to volume ratio

area to volume ratios examined was small, so that, considering experimental error, the difference between each value is insignificant. The second reason is that the other parameters were inconsistent within a set of A/V's and their effects are thought to outweigh the effect of a small change in A/V.

6.2.6 : EFFECT OF SLAG LAYER

The presence of a slag layer on the copper melt greatly reduced refining rates of all impurities tested. The refining rate coefficient of bismuth was 0.6×10^{-5} m s^{-1} in both experiments where a slag layer was maintained (A-16 & A-17). This was approximately an order of magnitude lower than that which was obtained in experiments where conditions were similar but no slag layer was present. The effect on antimony removal was the same, K_{Sb} being 0.3×10^{-5} m s^{-1} in Test A-17. These results suggest that mass transfer through the slag phase is rate controlling. Evidence that supports this hypothesis was given in a table of diffusion coefficients calculated by Szekely and Themelis[20]. The diffusion coefficients in molten slags were generally less than those in molten metals by one to two orders of magnitude.

SECTION 6.3 : VACUUM DISTILLATION OF BLISTER COPPER

Removal rates of bismuth in two experiments on blister copper (Tests B-1 & B-2) were in rough agreement with results obtained in doped copper experiments. Initial bismuth content of the blister copper was low (≃ 0.003 wt.%) in relation to most of the doped copper melts (0.01 to 0.09 wt.%). High melt temperatures (1640 & 1730°K) and low chamber pressures (11 & 24 Pa) were chosen in order to promote high rates of removal.

The removal rate of bismuth in Test B-1 was higher than that in Test A-5, for which experimental conditions were similar, the value of K_{Bi} being 3.5×10^{-5} m s^{-1} compared to 2.2×10^{-5} m s^{-1}. This is thought to be due to the higher melt temperature in Test B-1 (1643 K compared to 1608 K).

The refining rate in Test B-2 was lower than that in Tests A-10 and A-11 which had similar conditions. K_{Bi} was 2.2×10^{-5} m s^{-1} in Test B-2 compared to 5.0×10^{-5} and 6.1×10^{-5} m s^{-1} in Tests A-10 and A-11 respectively. It is believed that the low rate in Test B-2 was caused by the presence of some slag which covered about a third of the surface.

Removal of other elements from blister copper were examined in Test B-2. The initial contents of antimony and arsenic were below present detection limits and hence the rates of their removal are unknown. The contents of selenium and tellurium remained unchanged, indicating that no removal of these elements occurred. This behaviour is contrary to that expected from consideration of their volatility coefficients (Table 3.5a).

SECTION 6.4 : VACUUM DISTILLATION OF WHITE METAL

The removal of bismuth from white metal (Cu_2S) was examined in Tests C-1 and C-2. The melts were doped with bismuth so that the initial contents were close to those used in doped copper experiments. Melt temperature was kept low ($\simeq$ 1540 K) and chamber pressure high (100-250 Pa). Excessive splashing occurred when the temperature was increased or the pressure decreased.

Bismuth refining rate coefficients were 2.6×10^{-5} and 2.7×10^{-5} m s^{-1} for Tests C-1 and C-2 respectively. These rates were higher than those anticipated in view of rates measured on doped copper at low temperature or high pressure. The reason is that the activity coefficient of

bismuth is higher in white metal than in molten copper (6.1 compared to 2.3 at 1523 K)[30]. This reasoning is confirmed by the theoretical model. When γ^{o}_{Bi} is equal to 6.1, the model predicts values of K_{Bi} equal to 2.1×10^{-5} and 3.3×10^{-5} m s^{-1} for Tests C-1 and C-2 respectively. When γ^{o}_{Bi} is equal to 2.3, K_{Bi} becomes 1.0×10^{-5} and 1.7×10^{-5} m s^{-1}.

SECTION 6.5 : COPPER LOSSES

Condensate analyses for three different days of experiments were given in Table 5.9. Mass ratios of copper to bismuth evaporated may be derived from these results and used in conjunction with the results of bismuth elimination (Table 5.4) to calculate the amount of copper which was lost by evaporation during a day of experiments. Table 6.1 presents these values as percentages of the initial melt mass. Also listed for each day are :

a) the experimental tests conducted

b) the average melt temperature

c) the vacuum exposure time

and

d) theoretically predicted copper losses.

Day #	Experimental Tests Conducted	Average Melt Temperature (K)	Vacuum Exposure Time (hours)	Copper Losses (% of initial melt mass)	Predicted Copper Losses (% of initial melt mass)
1	A-6, A-7 A-8	1515	3.5	0.11	0.08
2	A-9, A-10 A-11, A-12	1725	4.0	0.45	0.55
3	A-13, A-14 A-15	1630	4.0	0.15	0.04

Table 6.1 : Copper Losses Recorded in a Day of Experimentation for Three Different Days

The table shows that experimental copper losses are between 0.1 and 0.5 % of the initial melt mass in about 4 hours. Losses increased with increasing temperature, as was predicted from consideration of volatility coefficients (Section 3.10.1).

The predicted copper losses are in close agreement with the experimentally determined losses in Days 1 and 2. Predicted losses in Day 3 are much lower than those obtained experimentally. This is consistent with all other results in high pressure experiments. Referring back to Figure 6.3a, the predicted evaporation rates of bismuth were considerably lower than those obtained experimentally.

SECTION 6.6 : DISCUSSION OF THEORETICAL MODEL

The theoretical model proposed in this study was incorporated into a computer program (Section 3.10.2) which calculated rates of refining of bismuth, antimony and arsenic from copper melts under vacuum and used these rates to predict changes in melt composition.

For each experiment of this study, the experimental parameters were input to the program and a simulation of

that experimental test was performed. The results of these simulations are compared to the actual experimental results in Figure 6.6, where measured final content is plotted against theoretically predicted final content for bismuth and arsenic.

The agreement was good for bismuth and arsenic, indicating that the model adequately describes vacuum distillation of these elements from copper. The model was less accurate at high chamber pressures, predicted refining rates being consistently lower than experimental refining rates.

There was no agreement for antimony, as the predicted values were always equal to the initial antimony content of the melt. This is thought to be due to an incorrect value for the activity coefficient of antimony in copper, the reason being as follows.

Azakami and Yazawa[31] plotted the activity coefficient in infinite dilution against the position of each element in the Periodic Table (Figure 6.7). The results show that the values for γ^{o}_{As} and γ^{o}_{Sb} represent discontinuities in their respective curves. The latest work by Lynch[19] calculated a higher value of γ^{o}_{As}. The new value, shown in

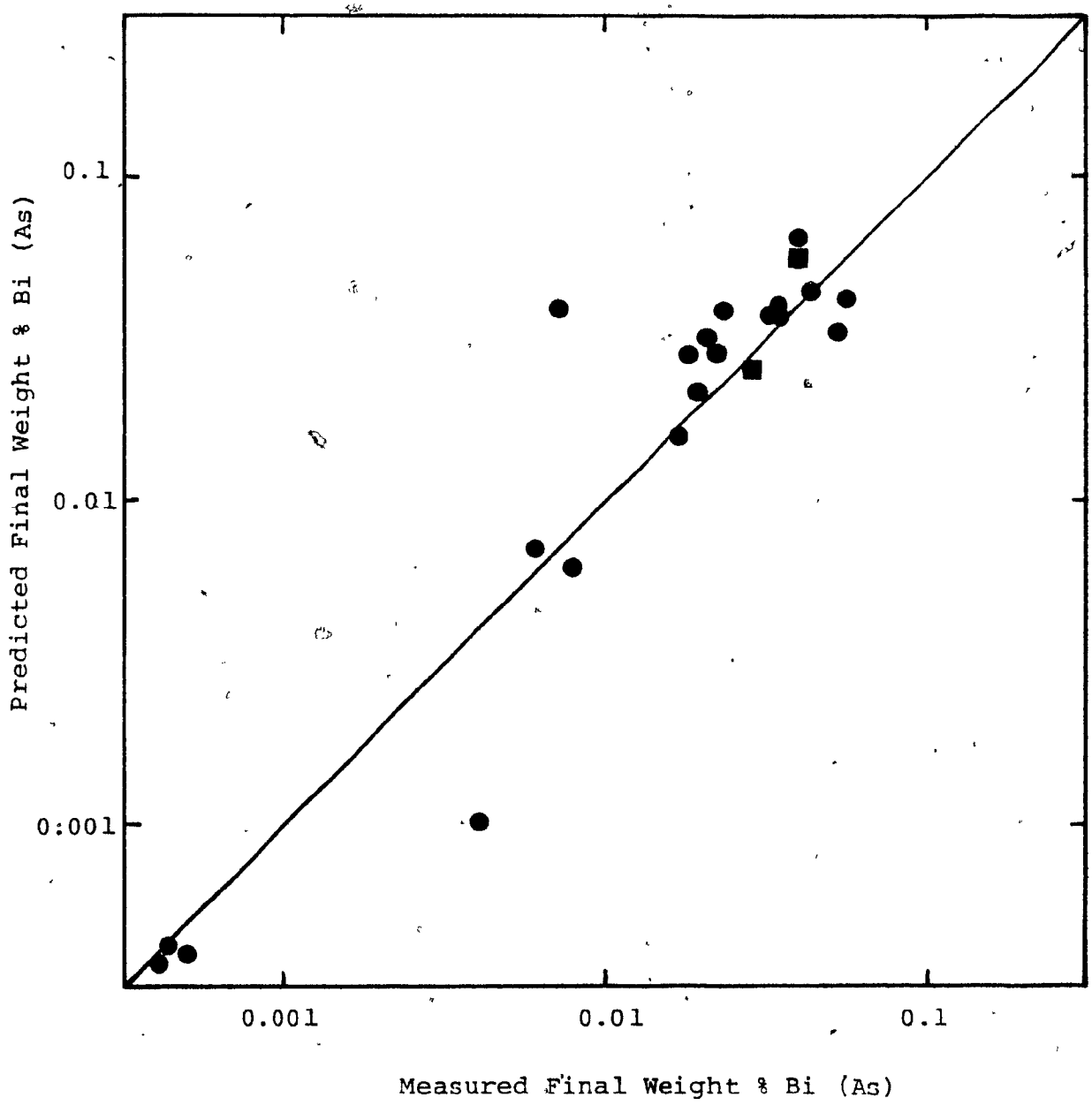

Figure 6.6 : Comparison Between Theoretically Predicted and Experimentally Measured Final Bismuth(●) and Arsenic(■) Content

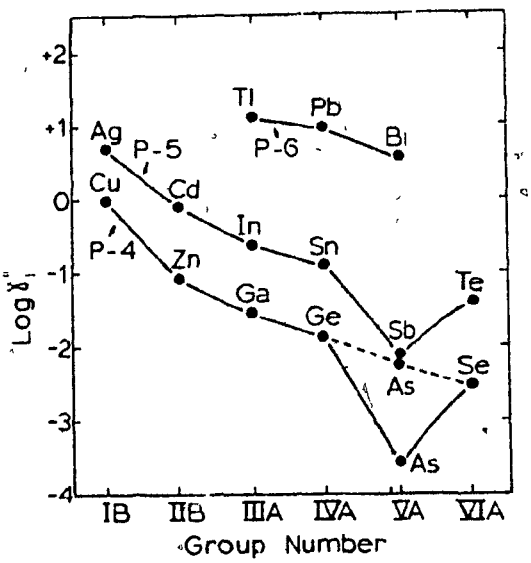

Figure 6.7 : Activity Coefficients of elements in infinite dilution plotted against their position in the Periodic Table (Azakami and Yazawa[31])

Figure 6.7 by the hatched line, is in better agreement with the curve. When used in the present study this value yielded theoretical predictions which were in closer agreement with the results than were seen with previous values of γ^{o}_{As}. Lynch suggested, in light of his findings, that further analysis of the activity of antimony in dilute solution in liquid copper may result in larger values of γ^{o}_{Sb} than previously reported. A value of 1.0×10^{-1}, which was taken from the curve in Figure 6.7, was incorporated into the computer program. The new predictions were slightly closer to but still much lower than experimentally measured values.

SECTION 6.7 : COMPARISON WITH PREVIOUS WORK

A summary of previous work (Tables 3.1, 3.2 & 3.3) is combined with the results of this study and shown in Tables 6.2, 6.3 and 6.4. Melt surface area to volume ratio was not given nor able to be calculated for most of the studies, so that a comparison of refining rates using overall rate coefficients was not possible.

The percentage eliminations of bismuth, antimony and arsenic in this study were lower than those in most of the

Source	Melt Mass (kg)	Melt Temperature (K)	Chamber Pressure (Pa)	Area Volume (m^{-1})	Initial Wt.% Bi	Processing Time (min)	% Elimination	K_{Bi} (10^{-5} m s^{-1})
Kameda[4]	0.03	1373	13	-	-	60	50-80	(20-45)/(A/V)
Kameda[4]	0.03	1473	13	-	-	60	+90	64/(A/V)
Ohno[5]	0.15	1473-1573	0.1-1	50-60	0.5	5-15	+95	8-27
Bryan[6]	0.02	1443	10	-	0.126	60	+99	128/(A/V)
Bryan[6]	4	1473-1573	1-150	15-20	0.02-0.3	50-60	80-95	1-8
Bryan[6]*	0.02	1443	10	-	0.32	60	80	50/(A/V)
Strel'tsov[7]	0.04	1473	0.01	55	0.9	25	90	2.8
Komorova[8]	0.03	1473	1	-	-	120	50-80	(10-22)/(A/V)
Golovko[9]	-	1473	13-67	-	-	5-15	93	443/(A/V)
Kametami[10]	0.6-6.0	1473	130-270	Vacuum Lift Refining	-	15-90	10	(2-12)/(A/V)
Taubenblat[11]	25	1423-1573	0.01	-	-	30	50	39/(A/V)
Ozberk[12]	34	1423-1623	8-40	6.7-10.2	0.02-0.04	120	40-80	1-3
Present	35	1500-1790	7-160	6.8-10.2	0.003-0.1	30-90	45-90	2-8
Present*	20	1540	120-200	6.4-6.7	0.08-0.1	70-90	45	2.7

* - the melt was Cu_2S

Table 6.2 : Summary of Results from Previous and Present Vacuum Refining Studies Showing Bismuth Elimination from Molten Copper

Source	Melt Mass (kg)	Melt Temperature (K)	Chamber Pressure (Pa)	Area Volume (m^{-1})	Initial Wt.% Sb	Processing Time (min)	% Elimination	K_{Sb} (10^{-5} m s^{-1})
Kameda[4]	0.03	1373	13	-	-	60	50-55	20/(A/V)
Kameda[4]	0.03	1473	13	-	-	60	30-40	10/(A/V)
Komorova[8]	0.03	1473	1	-	-	120	50-75	(10-20)/(A/V)
Golovko[9]	-	1473	13-67	-	-	5-15	20	40/(A/V)
Kim[13]	-	-	-	-	-	-	40	-
Kametami[10]	0.6-6.0	1473	130-270	Vacuum Lift Refining	-	15-90	20	(4-25)/(A/V)
Ozberk[12]	34	1523	13	7.1	0.15-0.25	120	0	0
Present	35	1500-1790	7-160	8.0-10.2	0.05-0.1	30-80	0-60	0-3

Table 6.3 : Summary of Results from Previous and Present Vacuum Refining Studies showing Antimony Elimination from Molten Copper

Source	Melt Mass (kg)	Melt Temperature (K)	Chamber Pressure (Pa)	Area / Volume (m^{-1})	Initial Wt.% As	Processing Time (min)	% Elimination	K_{As} (10^{-5} m s^{-1})
Kameda[4]	0.03	1373	13	-	-	60	10-30	(3-10)/(A/V)
Kameda[4]	0.03	1473	13	-	-	60	40-70	(15-30)/(A/V)
Komorova[8]	0.03	1473	1	-	-	120	50-80	(10-25)/(A/V)
Golovko[9]	-	1473	13-67	-	-	5-15	20	40/(A/V)
Kim[13]	-	-	-	-	-	-	30-50	-
Kametami[10]	0.6-6.0	1473	130-270	Vacuum Lift Refining	-	15-90	10-20	(2-25)/(A/V)
Ozberk[12]	34	1523	13	7.1	0.3-0.4	120	0	0
Present	35	1743	30	9.0-10.2	0.04-0.09	30-45	50-60	2-3.5

Table 6.4 : Summary of Results from Previous and Present Vacuum Refining Studies Showing Arsenic Elimination from Molten Copper

laboratory scale experiments. This may be attributed to the generally lower chamber pressures (Ohno[14], Streltsov[7], Komorova[8]), higher initial solute contents (Ohno, Streltsov, Bryan[6]) and higher melt surface area to volume ratios (Ohno, Streltsov) which were used in the laboratory scale experiments. The chamber pressures in the works of Kameda[4] and Golovko[9] were similar to those used in the present work and hence this does not explain why higher elimination rates were obtained. It is speculated that melt area to volume ratios were higher than those used in this study (7-10 m^{-1}).

Pilot plant scale studies by Bryan[6] and Taubenblat[11] showed rates for bismuth removal which were close to those in this work. Taubenblat's results, however, were obtained under chamber pressures of about 0.1 Pa whereas the present low pressure experiments used values of about 10 Pa. Many of Bryan's experiments were also at lower pressures (1-7 Pa) than the present work. The conditions in one of Bryan's experiments (1513 K and 7 Pa) closely ressembled the conditions in the low temperature experiments of this study, except that the area to volume ratio was higher in the case of Bryan by a factor of two. Bryan's overall rate coefficient was 3.76×10^{-5} m s^{-1} compared to 3.9×10^{-5}, 2.0×10^{-5} and 1.6×10^{-5} m s^{-1} obtained in Tests A-6, A-7 and A-8 respectively.

The most significant comparison may be made between the present work and that of Ozberk[12]. The experiments in these two studies were carried out in the same vacuum induction furnace under similar conditions of melt mass, melt temperature, chamber pressure and melt surface area to volume ratio.

The overall refining rate coefficients for bismuth in Ozberk's study were generally lower than those of the present study by a factor of two. Ozberk also obtained no removal of antimony or arsenic in the two experiments where these elements were considered, which was contrary to the findings of the present work. Two possible explanations for this discrepancy are considered below.

Firstly, initial impurity contents in Ozberk's study were different from those in the present study in that, in the former case, bismuth contents were lower and lead was present. Differences in initial impurity content affect refining rate by changing the total vapour pressure above the melt (Section 6.2). Hence, total vapour pressures above a number of different melts, covering the range of initial contents studied by Ozberk, are given in Table 6.5. The same data is presented in Table 6.6 for the present work. It can be seen that, for experiments

Initial Content		Temperature	ΣP_{vapour}	K_{Bi}
Wt.% Bi	Wt.% Pb	(K)	(Pa)	
0.020	0.028	1523	2.89	1.86
0.038	0.059	1523	4.89	2.76
0.039	0.125	1523	8.03	1.34
0.030	0.059	1623	11.66	3.15

Table 6.5 : Total Vapour Pressures above Selected Melts in the work of Ozberk[12]

Initial Content		Temperature	ΣP_{vapour}	K_{Bi}
Wt.% Bi	Wt.% Sb	(K)	(Pa)	
0.014	0.093	1505	1.09	2.0
0.098	-	1530	4.20	3.9
0.072	-	1625	9.17	7.6
0.072	-	1633	9.98	8.8
0.088	-	1635	11.26	6.2

Table 6.6 : Total Vapour Pressures above Selected Melts in the Present Study

with the same total vapour pressure, K_{Bi} is higher in the present work than in Ozberk's work. This indicates that differences in initial impurity content do not explain why lower refining rates were obtained in Ozberk's study.

Secondly, all crucibles used in Ozberk's work were placed in the furnace without being shortened and are schematically shown in Figure 6.8a containing the copper melt (34 kg). It is clear that a portion of the evaporated species could condense on the crucible walls and wash back into the melt by melt splashing. This phenomenom has been observed by Harris[15] during vacuum refining steel. Figure 6.8b shows the present experimental configuration and indicates that refluxing from the crucible wall was not possible.

SECTION 6.8 : INDUSTRIAL APPLICABILITY

Table 6.7 lists levels of bismuth, antimony and arsenic in typical blister copper[1,2,25,32] and Noranda Reactor copper[32]. Also given are maximum permissible impurity levels for vacuum refined copper[32]. These figures indicate that a vacuum refining process must remove about 60 % of each of the impurity elements from blister copper.

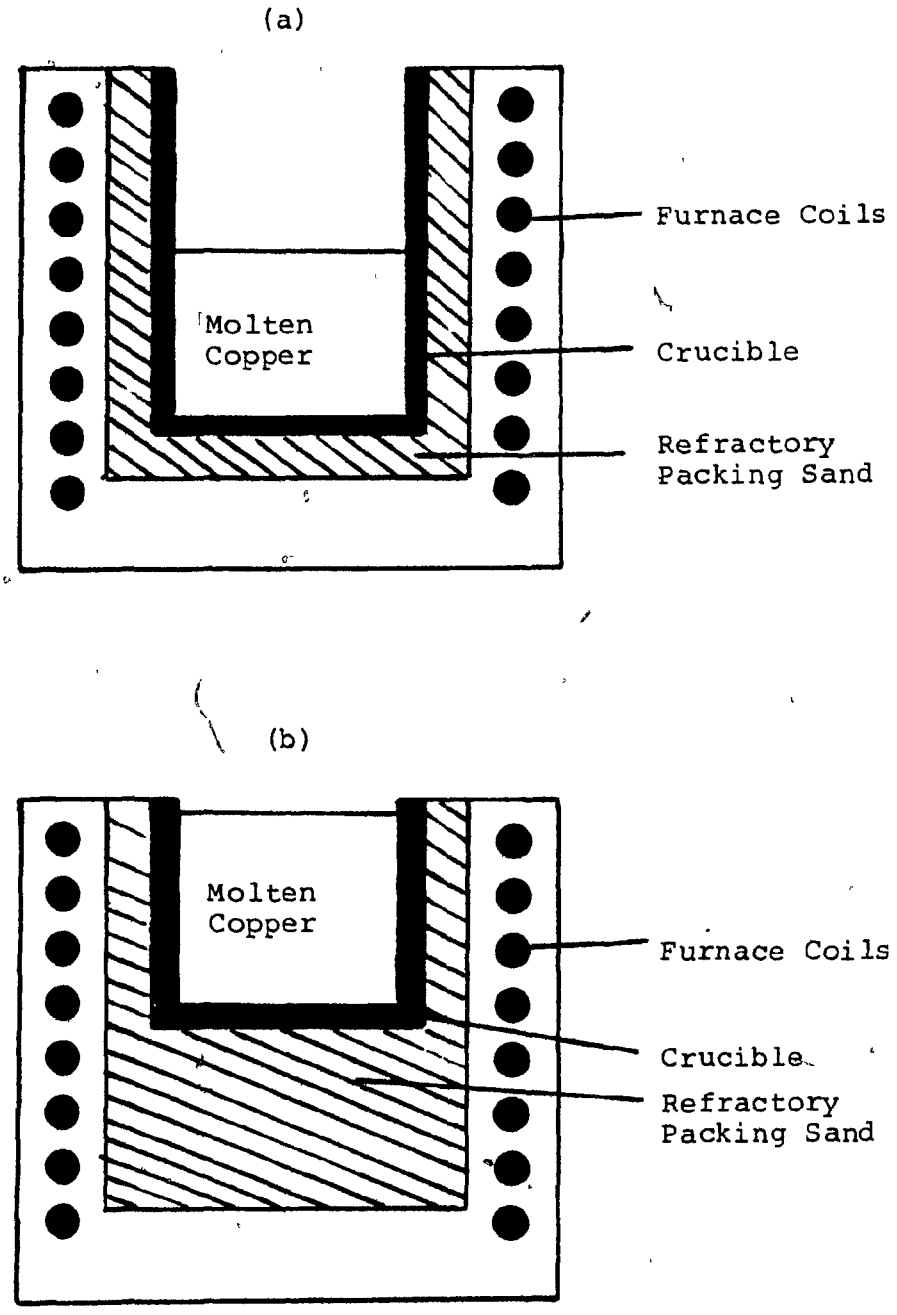

Figure 6.8 : Placement of 34 kg of Molten Copper in Crucibles for Experiments in (a) Ozberk's work and (b) the present study

	Bi	Sb	As
Typical Impurity Levels in Blister Copper :	0.02	0.02	0.1
Impurity Levels in Noranda Reactor Copper :	0.028	0.119	0.296
Vacuum Refined Copper (Maximum Impurity Levels) :	0.008	0.012	0.044

Table 6.7 : Levels of Bismuth, Antimony and Arsenic in Typical Blister Copper, Noranda Reactor Copper and Vacuum Refined Copper

In the case of Reactor copper, 70 % of the bismuth, 90 % of the antimony and 85 % of the arsenic must be eliminated.

This study has shown that 60-70 % of the initial bismuth may be removed from a 35 kg copper melt in about 60 minutes at 1500 K and 10-15 Pa and in about 35 minutes at 1600-1750 K and 10-35 Pa.

Experiments A-11 and A-12 (Figures 5.11 and 5.12) showed that 60 % of the arsenic could be removed in about 1 hour at 1750 K and 30 Pa. Extrapolation indicates that removal of 85 % of the arsenic would require about 2 hours.

The removal of antimony in this study was erratic. Consequently, it is not possible to obtain a definite value for the time required to remove a certain amount of antimony. Tests A-5 and A-8 showed the highest rates of antimony removal, ≈ 60 % in 1 hour at 1500-1600 K and 7-10 Pa.

Refining rate coefficients during vacuum refining blister copper on an industrial scale are expected to be similar to the present results as long as the chamber pressure is close to, or if possible, lower than the total vapour pressure of the melt. Using the initial impurity levels in Table 6.7 and not including other

impurities, the vapour pressures above a typical blister copper melt are calculated to be 1.2 Pa at 1500 K, 4.6 Pa at 1600 K and 17 Pa at 1700 K. The inclusion of other impurities such as lead and zinc in the calculations is expected to increase these values by at least a factor of 2. Therefore, the vacuum levels required in industry are expected to be approximately 10 Pa.

Impurity removal from Noranda Reactor copper is expected to be more rapid than from blister copper since the impurity contents and hence the melt vapour pressures are higher. The impurity levels listed in Table 6.7 were used to determine the vapour pressures above Reactor melts. The values were calculated to be 1.5, 5.6 and 21 Pa at 1500, 1600 and 1700 K respectively. Taking into consideration other impurities, the required vacuum levels are expected to about 20 Pa.

An important consideration in vacuum refining copper on an industrial scale is the melt surface area to volume ratio. Industrial values for this parameter are between 0.5 and 1 m^{-1}, and not between 7 and 10 m^{-1} as was used in this study. These low values must somehow be compensated for if vacuum refining copper is to be used in industry. It is thought that technology which already exists

in the steel industry, that is spray degassing or D.H. and R.H. type units[33], can be adopted for use in the copper industry.

SECTION 6.9 : FUTURE WORK

Future theoretical investigations on vacuum refining copper should aim at developing a mass transfer model which will describe vacuum distillation of antimony from copper. Vacuum refining processes should also be studied from an economics point of view by examining costs and benefits of the process.

Future pilot plant scale experiments should concentrate on :

a) developing a metal spraying or metal transfer technique to compensate for low melt surface area to volume ratios presently encountered in industry.

b) investigating more thoroughly the effect of various parameters on arsenic and antimony elimination.

c) purging oxygen or chlorine through the melt to increase melt turbulence and form volatile oxides

and chlorides with antimony and arsenic. The latter effect would not only enhance the vacuum distillation of antimony and arsenic but would also benefit the vacuum refining process by increasing the total vapour pressure above the melt.

d) vacuum refining industrial copper melts of high impurity content such as those produced from low grade ores or by continuous copper making processes.

CHAPTER SEVEN

CONCLUSIONS

1. Experiments have shown that 45 to 90 % of the initial bismuth, 50 to 60 % of the initial arsenic and nil to 60 % of the initial antimony were removed from molten copper in 1 hour by vacuum refining 35 kg melts at 1500-1790 K under 7-160 Pa. About 40 % of the initial bismuth was removed in 1 hour from molten white metal (Cu_2S) by vacuum purifying 20 kg melts at 1500-1550 K under 100-250 Pa.

2. The effects of melt temperature and chamber pressure on bismuth refining rate were found to be significant in the ranges examined in this study. An increase in melt temperature from 1500 K to 1700 K increases the refining rate coefficient of bismuth from 2×10^{-5} to 7×10^{-5} m s^{-1}. A decrease in chamber pressure from 150 Pa to 10 Pa increases the rate coefficient from 3×10^{-5} to 7×10^{-5} m s^{-1}.

3. Experimental results have shown that refining rate increases with an increase in the value of $\Sigma P_{vapour}/P_{ch}$.

which is in turn increased by increasing melt temperature, decreasing chamber pressure or increasing the concentration of solute elements more volatile than copper.

4. Theoretical calculations agreed with this finding and showed that, for values of $\Sigma P_{vapour}/P_{ch}$ greater than approximately 2, refining rate will become independent of this ratio and depend solely upon the ratio P_i^o/P_{Cu}^o. The latter ratio varies only with melt temperature.

5. The presence of a slag layer on the copper melt decreases refining rate by a factor of approximately ten due to the relatively slow rate of mass transfer through the slag phase.

6. The presence of iron in molten copper is thought to inhibit the removal of antimony by vacuum distillation due to atom-atom interaction between iron and antimony.

7. It was discovered that the elements which can exist as polyatomic gaseous species evaporate predominantly in the monatomic form, that is, volatility coefficients for As_2 and Bi_2 were approximately 1/500 and 1/3000 of that for As and Bi respectively.

8. A theoretical model was developed to describe the vacuum distillation process using kinetic theory of melt phase mass transfer, evaporation and gas phase mass transfer.

9. The model adequately predicts removal of bismuth and arsenic from molten copper and bismuth from molten white metal. The model consistently predicted values of antimony removal rates which were lower than those observed. The use of a higher value of γ^{o}_{Sb} as suggested by Lynch only partially compensates for the inaccuracy.

10. Experimental results and theoretical calculations indicate that removal of bismuth from copper melts by vacuum distillation can become a viable industrial process. Efficient removal of antimony and arsenic on an industrial level may require a process which combines vacuum distillation with oxidation and chlorination.

BIBLIOGRAPHY

1. Biswas, A.K. and Davenport, W.G., Extractive Metallurgy of Copper, Pergammon, Oxford, 1976, a. typ. 2, b. pp 178-296

2. Yazawa, A., 'Thermodynamic Considerations in the Removal of Impurities in Copper Smelting', Bulletin of the Research Institute of Mineral Dressing and Metallurgy, Tohoku University, Vol. 23, No. 1, June 1967, pp. 67-75.

3. Yazawa, A., Yutaka, K. and Ujiie, H., 'Refining of Crude Copper by Addition of Chlorides', Bulletin of the Research Institute of Mineral Dressing and Metallurgy, Tohoku University, Vol. 27 No. 1,2, Oct. 1971, pp. 209-216.

4. Kameda, M. and Yazawa, A., 'Refining of Crude Copper by Vacuum Melting', Tohoku Diagaku Senko Seiren Kenkgusho Iho, 19 (1), 1963, pp. 57-68, Cited by E. Ozberk[12].

5. Ohno, R., 'Rates of Evaporation of Silver, Lead and Bismuth from Copper Alloys in VAcuum Induction Melting', Met. Trans. B, Vol. 7B, Dec. 1976, pp. 647-653.

6. Bryan, R., Pollard, D.M. and Willis, G.M., 'Removal of Bismuth from Copper by Vacuum Refining', Australia Japan Extractive Metallurgy Symposium, 1980.

7. Strel'tsov, F.N., Trankovskii, E.G. and Moldavskii, O.D., 'Refining Copper During Melting in Vacuum Furnaces', Tsventnye Metally/Non Ferrous Metals, pp. 45-47.

8. Komorova, L., 'Vacuum Refining Technique for Removal of Impurities from Copper', Hutnicke Listy, (Czech), 8, 1973, pp. 577-582, Translation BISI 12425, The Metals Society, London, Cited by E. Ozberk[12].

9. Golovko, V.V. and Isakova, R.A., 'Removal of Impurities from Binary Alloys and Crude Copper by a Vacuum Method', Trans. Inst. Met. i Obegashch, Akad. Naik Kaz. SSR, 13, 1965, pp. 32-37, Cited by E. Ozberk[12].

10. Kametami, H. and Yamauchi, C., 'Vacuum Lift Refining in Copper Smelting', Trans. Nat. Res. Met., Vol. 20, No. 1, 1978, pp. 22-59.

11. Taubenblat, P.W., Brockup, F.H. Oswald, R.S. and Ohring, M., 'Vacuum Melting and Casting Copper', Vacuum Metallurgy, Edited by R.C. Krutenat, Proceedings of 1977 Vacuum Met. Conf., Pittsburgh, Penn. June 1977, pp. 543-568

12. Ozberk, E., 'Vacuum Refining of Copper', M. Eng Thesis, McGill University, 1980.

13. Kim, G.V., Kuyatkovskii, A.N. et al., 'Vacuum Processing of Crude Copper', Trans. Altaisk Gorno-Met., Nauchn.-Issled. Inst., Cited by E. Ozberk[12].

14. Ohno, R., Liquid Metals, Chemistry and Physics, S.Z. Beer, editor, Marcel Dekker Inc. N.Y., 1972, pp. 37-80.

15. Harris, R., 'Vacuum Refining Molten Steel', PhD Thesis, McGill University, 1980.

16. Machlin, E.S., 'Kinetics of Vacuum Induction Refining - Theory', Trans. Met. Soc. of AIME, Vol. 218, April 1960, pp. 314-326.

17. Persson, H.A., 'Vacuum Removal of Sulphur and Tin from Liquid Steel', M. Eng. Thesis, McGill University, 1981.

18. Winkler, O., 'Thermodynamics and Kinetics in Vacuum Metallurgy', Vacuum Metallurgy, O. Winkler and R. Bakish Editors, Elservier Publishing, Ch.I, 1971.

19. Lynch, D.C., 'Activity of Arsenic in Copper', Met. Trans. Soc. of AIME, Vol. 11B Dec. 1980 pp. 623-629.

20. Szekely, J. and Themelis, N.J., Rate Phenomena in Process Metallurgy, Wiley-Interscience, NewYork, 1971, PP. 361-454.

21. Richardson, F.D., Physical Chemistry of Melts in Metallurgy, Vol. 2, Academic Press, 1974, pp. 483-493.

22. Irons, G.A., Chang, C.W., Guthrie, R.I.L. and Szekely, J., 'The Measurement and Prediction of the Vaporization of Magnesium from an Inductively Stirred Melt', Met. Trans., 9B, March 1978, pp. 151-154.

23. Szekely, J. and Chang, C.W., 'Melt Velocities, Temperature Profiles, Tracer Dispersion Rates and Scrap Melt Kinetics in Vacuum Induction Melting', Vacuum Metallurgy, R.C. Krutenat Editor, Proceeding of 1977 Vac. Met. Conf., Pittsburgh, Penn., June 1977, pp. 15-48.

24. Nagamori, M., Mackey, P.J. and Tarasoff, P., 'Copper Solubility in $FeO-Fe_2O_3-SiO_2-Al_2O_3$ Slag and Distribution Equilibria of Pb, Bi, Sb and As between Slag and Metallic Copper', Met. Trans. 6B, June 1975, pp. 295-301.

25. Yazawa, A., 'Thermodynamic Considerations of Copper Smelting', Can. Met. Quart., Vol. 13, No. 3, 1974, pp. 443-453.

26. Hultgren, R. et al., Selected Values of the Thermodynamic Properties of the Elements, ASM, 1973.

27. Bird, R.B., Stewart, W.E. and Lightfoot, E.W., Transport Phenomena, John Wiley & Sons, 1960, pp. 495-518.

28. Olette, M., 'Vacuum Distillation of Minor Elements from Liquid Ferrous Alloys', Physical Chemistry of Process Metallurgy, Part 2, Interscience, NewYork, 1961, pp. 1065-1087.

29. Hultgren, R. et al., Selected Values of the Thermodynamic Properties of Binary Alloys, ASM, 1973.

30. Arac, S. and Geiger, G.H., 'Thermodynamic Behavior of Bismuth in Copper Pyrometallurgy : Molten Matte, White Metal and Blister Copper Phases', Met. Trans. 12B, Sept. 1981, pp. 569-578.

31. Azakami, T. and Yazawa, A., 'Activity Measurements of Liquid Copper Binary Alloys', Can. Met. Quart., Vol 15, No. 2, 1976, pp. 111-121.

32. Poggi, D., 'Typical Lead Bullion and Blister Copper Compositions for Vacuum Refining', Noranda Research Center, Montreal, May 26, 1981.

33. Rüttiger, K.,'Vacuum Degassing in the Liquid State', Vacuum Metallurgy, O. Winkler and R. Bakish Editors, Elsevier Publishing, Ch. IV, Section 1, 1971.

34. Krüger, J., 'Use of Vacuum Techniques in Extractive Metallurgy and Refining of Metals', Vacuum Metallurgy, O. Winkler and R. Bakish Editors, Elservier Publishing, Ch. III, 1971.

35. Reichel, W. and Bleakly, B.G., 'Concentration and Determination of Trace Impurities in Copper by Atomic Absorption Spectrophotometry', Analytical Chemistry, Vol. 46, No. 1, Jan. 1974, pp. 59-61.

36. Gomez, M. et al., 'Densities of Molten Copper and Molten Bismuth-Copper Alloys', Z. Metallkde, 1976, pp. 131-134.

37. Kubaschewski, O. and Alcock, C.B., Metallurgical Thermochemistry, 5'th Edition, Pergamon, Oxford, 1979,pp.358-377.

APPENDIX 1

THERMODYNAMIC DATA

1-1 Density of Copper :

$$\rho_{Cu} = (7.936 - 7.862 \times 10^{-4} (T - 1356)) \times 1000, \text{ kg m}^{-3}$$ [36]

1-2 Raoultian Activity Coefficients in Infinite Dilution In Molten Copper Melts

$$\log \gamma^{o}_{Bi} = 1900\ T^{-1} - 0.885$$ [24]

$$\gamma^{o}_{Sb} = 2.2 \times 10^{-2} \text{ at } 1573 \text{ K}$$ [24]

$$\gamma^{o}_{As} = 5 \times 10^{-3} \text{ at } 1373 \text{ K}$$ [19]

1-3 Vapour Pressures of Species in their Pure States

$$\log P^{o}_{Cu} = -17520\ T^{-1} - 1.21 \log T + 13.21, \text{ mm Hg}$$ [37]

$$\log P^{o}_{Bi} = -10400\ T^{-1} - 1.26 \log T + 12.35, \text{ mm Hg}$$ [37]

$$\log P^{o}_{Bi_2} = -10730\ T^{-1} - 3.02 \log T + 18.10, \text{ mm Hg}$$ [37]

$$\ln P^{o}_{Sb} = -2.80 \times 10^{4}\ T^{-1} + 11.95, \text{ atm.}^{*}$$

$$\ln P^{o}_{Sb_2} = -1.94 \times 10^{4}\ T^{-1} + 10.27, \text{ atm.}^{*}$$

$$\ln P^{o}_{As_4} = -1.59 \times 10^{4}\ T^{-1} + 18.22, \text{ atm.}^{*}$$

$$\ln P^{o}_{As_2} = -3.14 \times 10^{4}\ T^{-1} + 25.88, \text{ atm.}^{**}$$

$$\ln P^{o}_{As} = -4.73 \times 10^{4}\ T^{-1} + 29.17, \text{ atm.}^{**}$$

---

* - These equations were obtained by taking data given by Hultgren et al.[26] and performing a linear regression on ln P versus 1/T. The correlation coefficients were always better than -0.9999.

** - see Appendix 2

APPENDIX 2

CALCULATION OF $P^{o}_{As_2}$ AND P^{o}_{As}

a) Lynch[19] derived the following equilibrium constant equations from the data of Hultgren et al.[26] :

1. $As_4(g, 1 \text{ atm.}) = 2\ As_2(g, 1 \text{ atm.})$

$$\ln K_1 = -33960\ T^{-1} + 17.3 \quad (900\text{-}1200 \text{ K})$$

2. $As_2(g, 1 \text{ atm.}) = 2\ As(g, 1 \text{ atm.})$

$$\ln K_2 = -46500\ T^{-1} + 13.7 \quad (400\text{-}1200 \text{ K})$$

Combining 1 and 2 :

3. $As_4(g, 1 \text{ atm.}) = 4\ As(g, 1 \text{ atm.})$

$$\ln K_3 = \ln K_1 + 2 \ln K_2$$
$$= -126960\ T^{-1} + 44.7 \quad (900\text{-}1200 \text{ K})$$

b) K_1 was evaluated at several high temperatures. Here, $K_1 = (P_{As_2})^2/P_{As_4}$, where P_{As_2} and P_{As_4} are the partial pressures of As_2 and As_4 respectively when the total pressure, P_T, is 1 atm. Because $P_{As_4} = P_T - P_{As_2}$ when only As_2 and As_4 are present, then :

$$K_1 = \frac{(P_{As_2})^2}{1 - P_{As_2}}$$

This solves by the quadratic rule to :

$$P_{As_2} \ (@\ P_T = 1 \text{ atm.}) = \frac{-K_1 + (K_1^2 + 4K_1)^{\frac{1}{2}}}{2}$$

This is the partial pressure of P_{As_2} when the total pressure is equal to 1 atm. If it is assumed that the ratio of P_{As_2} to P_T is the same for any value of P_T, then P_{As_2} at a value of P_T other than 1 atm. is given by :

$$P_{As_2} \text{ (@ } P_T) = P_{As_2} \text{ (@ 1 atm.) x } P_T$$

$$\simeq P_{As_2} \text{ (@ 1 atm.) x } P_{As_4} \text{ (@ } P_T)$$

Solving for P_{As_2} at several temperatures yields :

$$\ln P_{As_2} = -3.14 \times 10^4 \, T^{-1} + 25.88$$

c) K_3 was evaluated at several high temperatures. Here, $K_3 = (P_{As})^4 / P_{As_4}$ and, since $P_T = P_{As_4} + P_{As} = 1$ atm., then $P_{As_4} = 1 - P_{As}$ and :

$$K_3 = \frac{(P_{As})^4}{1 - P_{As}}$$

Because K_3 is always very small (10^{-18} at 1500 K to 10^{-14} at 1700 K), the term P_{As} in the denominator may be neglected, and P_{As} solves to :

$$P_{As} \text{ (@ } P_T = 1 \text{ atm.)} = (K_3)^{0.25}$$

This value of P_{As} is for a total pressure of 1 atm. The value of P_{As} at a total pressure other than 1 atm. is approximately given by :

$$P_{As} \text{ (@ } P_T) = P_{As} \text{ (@ 1 atm.) x } P_{As_4} \text{ (@ } P_T)$$

solving for P_{As} at several temperatures yields :

$$\ln P_{As} = -4.73 \times 10^4 \, T^{-1} + 29.17$$

APPENDIX 3

CALCULATION OF GAS PHASE BOUNDARY LAYER THICKNESS, ℓ, IN BRYAN'S WORK

Given :

$$\text{Overall } K_{Bi} = 1.24 \times 10^{-5} \text{ m s}^{-1}$$

$$K^{m}_{Bi} = 1.80 \times 10^{-4} \text{ m s}^{-1}$$

$$K^{e}_{Bi} \cdot \phi_{Bi} = 2.57 \times 10^{-4} \text{ m s}^{-1}$$

$$\text{Melt T} = 1513 \text{ K}$$

$$P_{ch} = 26.7 \text{ Pa}$$

$$\text{Initial \% Bi} = 0.02$$

By Equation 3.21d : $\phi_{Bi} = 3931\ (2.55)\ (0.0081) = 81.45$

By Equation 3.22 :

$$1.24 \times 10^{-5} = \left(\frac{1}{1.8 \times 10^{-4}} + \frac{1}{2.37 \times 10^{-4}} + \frac{1}{K^{g}_{Bi}\ (81.45)}\right)^{-1}$$

$$\therefore K^{g}_{Bi} = 1.724 \times 10^{-7}$$

By Equation 3.21 : $\Sigma N_i \simeq \Sigma N_{Bi} = 1.24 \times 10^{-5}\ (0.025)$

$$= 3.04 \times 10^{-7}$$

By Equation 3.21c :

$$1.724 \times 10^{-7} = \frac{3.04 \times 10^{-7}}{26.7}\left(1 - \exp\left(\frac{3.04 \times 10^{-7}\ (8314)(1513)\,\ell}{0.385(26.7)}\right)^{-1}\right)$$

$$\therefore \underline{\ell = 0.19 \text{ m}}$$

APPENDIX 4

COMPUTER SIMULATION OF VACUUM REFINING COPPER

```
/LOAD WATFIV
      REAL MASS,MCU,MBI,MAS,MSB,NCU,NBI,NAS,NSB,
     #KM,KE,KECU,KEBI,KEAS,KESB,KG,L,KEBI2,KESB2,KEAS2
      DOUBLE PRECISION ABI2,BBI2,CBI2,ASB2,BSB2,CSB2,AAS2,BAS2,CAS2,
     #NBI2,NSB2,NAS2
      WRITE(6,101)
101   FORMAT(///'ENTER THE FOLLOWING MELT PROPERTIES'///
     #10X,'1.  MELT DIAMETER  (M)'/
     #10X,'2.  MELT MASS  (KG)'/10X,'3.  MELT',
     #' TEMPERATURE  (K)'///)
      READ(9,*)DIA,MASS,T
      WRITE(6,102)
102   FORMAT(//'ENTER THE CHAMBER PRESSURE (PA)'//)
      READ(9,*)PCH
      WRITE(6,103)
103   FORMAT(//'ENTER THE WEIGHT PERCENTS OF BI,AS,SB & CU'//)
      READ(9,*)PERBI,PERAS,PERSB,PERCU
      WRITE(6,105)
105   FORMAT(//'ENTER DURATION OF EXPERIMENT  (SEC)'//)
      READ(9,*)TEXP
      DM=3E-9
      VEL=.1
      PI=3.14159265
      MCU=63.54
      MBI=208.98
      MAS=74.92
      MSB=121.75
      DEN=1000.*(7.936-7.862E-4*(T-1356.))
      CCU=PERCU*DEN/MCU/100.
      CBI=PERBI*DEN/MBI/100.
      CAS=PERAS*DEN/MAS/100.
      CSB=PERSB*DEN/MSB/100.
      DELT=10.0
      TIME=DELT
      A=PI*DIA**2./4.
      V=MASS/DEN
      R=8.314E3
      KM=SQRT(8.*DM*VEL/PI/DIA*2.)
      KE=SQRT(0.5/PI/R/T)
      KECU=KE/SQRT(MCU)
      KEBI=KE/SQRT(MBI)
      KEBI2=KE/SQRT(2*MBI)
      KEAS=KE/SQRT(MAS)
      KEAS2=KE/SQRT(2*MAS)
      KESB=KE/SQRT(MSB)
      KESB2=KE/SQRT(2*MSB)
```

```
      GAMCU=1.0
      GAMBI=EXP((1900/T-0.885)*2.303)
      GAMSB=2.0E-1
      GAMAS=5.0E-3
      POCU=10**(-17520/T-1.21*ALOG10(T)+13.21)*133.322
      POBI=10**(-10400/T-1.26*ALOG10(T)+12.35)*133.322
      POBI2=10**(-10730/T-3.02*ALOG10(T)+18.1)*133.322
      POSB=EXP(-2.8E4/T+11.95)*101325
      POSB2=EXP(-1.94E4/T+10.27)*101325
      POAS=EXP(-4.73E4/T+29.17)*101325
      POAS2=EXP(-3.14E4/T+25.88)*101325
      PHICU=GAMCU*POCU*MCU/DEN
      PHIBI=GAMBI*POBI*MCU/DEN
      PHIBI2=POBI2*(GAMBI*MCU/DEN)**2
      PHISB2=POSB2*(GAMSB*MCU/DEN)**2
      PHIAS=POAS*GAMAS*MCU/DEN
      PHIAS2=POAS2*(GAMAS*MCU/DEN)**2
      PHISB=GAMSB*POSB*MCU/DEN
      NCU=CCU*KECU*PHICU
      NBI=CBI/(1/KM+1/KEBI/PHIBI)
      NSB=CSB/(1/KM+1/KESB/PHISB)
      SUMNI=NCU+NBI+NSB
      DG=1.8194E-4*T**1.5/PCH
      L=0.1
      KG=SUMNI/PCH/(1.-EXP(-SUMNI*R*T*L/DG/PCH))
      ICSTOP=TEXP/100.
      WRITE(6,450) PERCU,PERBI,PERAS,PERSB
450   FORMAT(//'TIME',3X,'% CU',4X,'% BI',3X,'% AS',
     #3X,'% SB',6X,'NBI',6X,'NBI2',6X,'NSB',6X,'NSB2'/
     #'    0 ',4F7.3)
      DO 600 I=1,ICSTOP
      DO 500 J=1,10
      NCU=CCU/(1/KECU/PHICU+1/KG/PHICU)
      NBI=CBI/(1/KM+1/KEBI/PHIBI+1/KG/PHIBI)
      NAS=CAS/(1/KM+1/KEAS/PHIAS+1/KG/PHIAS)
      NSB=CSB/(1/KM+1/KESB/PHISB+1/KG/PHISB)
      ABI2=2/KM**2
      ASB2=2/KM**2
      AAS2=2/KM**2
      BBI2=4*CBI/KM+1/KEBI2/PHIBI2+1/KG/PHIBI2
      BSB2=4*CSB/KM+1/KESB2/PHISB2+1/KG/PHISB2
      BAS2=4*CAS/KM+1/KEAS2/PHIAS2+1/KG/PHIAS2
      CBI2=2*CBI**2
      CSB2=2*CSB**2
      CAS2=2*CAS**2
      NBI2=(BBI2-DSQRT(BBI2**2-4*ABI2*CBI2))/2/ABI2
      NSB2=(BSB2-DSQRT(BSB2**2-4*ASB2*CSB2))/2/ASB2
      NAS2=(BAS2-DSQRT(BAS2**2-4*AAS2*CAS2))/2/AAS2
      SUMNI=NCU+NBI+NBI2+NSB+NSB2+NAS+NAS2
      SUMV=(NCU*MCU+NBI*MBI+NBI2*2*MBI+NSB*MSB+NSB2*2*MSB
     #+NAS*MAS+NAS2*2*MAS)*A*DELT/DEN
      CCU=(CCU*V-NCU*A*DELT)/(V-SUMV)
      CBI=(CBI*V-(NBI+2*NBI2)*A*DELT)/(V-SUMV)
      CSB=(CSB*V-(NSB+2*NSB2)*A*DELT)/(V-SUMV)
      CAS=(CAS*V-(NAS+2*NAS2)*A*DELT)/(V-SUMV)
      V=V-SUMV
      KG=SUMNI/PCH/(1.-EXP(-SUMNI*R*T*L/DG/PCH))
      PERCU=CCU*MCU*100/DEN
```

```
      PERBI=CBI*MBI*100/DEN
      PERAS=CAS*MAS*100/DEN
      PERSB=CSB*MSB*100/DEN
      TIME=TIME+DELT
  500 CONTINUE
      TC=TIME-10
      WRITE(6,550) TC,PERCU,PERBI,PERAS,PERSB,NBI,NBI2,NSB,NSB2
  550 FORMAT(F6.0,F7.3,F7.4,2F7.3,4E11.3)
  600 CONTINUE
      ALOSS=MASS-V*DEN
      WRITE(6,*)ALOSS
      STOP
      END
*END

*GO
```

APPENDIX 5

The following is a list of the sources of the equipment and materials which were used in this study and mentioned in Chapter Four :

Induction Furnace	: 'Tocco' by Inductotherm Inc., Rancocas, N.J. supplied Deltec Systems Inc., Primrose, PA. (bankrupt).
Power Supply	: Reliance Electrical, Cleveland, Ohio, supplied by Deltec Systems Inc.
Vacuum Chamber	: Deltec Systems Inc.
Pumping System	: Deltec Systems Inc.
Crucibles	
a) Hycor	: Engineering Ceramics, Gilliberts, Ill.
b) Tercod	: Ferro Electric, Buffalo, N.Y.
Cathode Copper	: Canadian Copper Refineries, Montréal, Qué.
Blister Copper	: INCO Metals Ltd., Sudbury, Ont.
White Metal	: INCO Metals Ltd., Sudbury, Ont.
Bismuth	: Anachemia, Montréal, Qué.
Antimony	: Anachemia, Montréal, Qué.
Arsenic	: Anachemia, Montréal, Qué.
Mc Leod Gauge	: Fischer Scientific Co., Montréal, Qué.
'DIP TIP' Pt/Pt-13 % Rh Thermocouple	: Leeds and Northrup, Elliport, PA.

Digital Potentiometer :
John Fluke Mfg. Co. Inc., Mississauga, Ont.

Graphite : Union Carbide Ltd., Lachine, Qué.

Argon : Welding Products Ltd., Montréal, Qué.

Lanthanum : (As Lanthanum Chloride)
Fischer Scientific Co., Montréal, Qué.

Nitric Acid : Fischer Scientific Co., Momtréal, Qué.

Atomic Adsorption Standards :
Fischer Scientific Co., Montréal, Qué.

Perkin Elmer Flame Atomic Absorption Spectrometer :
Perkin Elmer, Norwalk, Conn.

Pye Unicam Flame Atomic Absorption Spectrometer :
Pye Unicam Ltd. Cambridge, England.